2006

Action of Tyrosyl DNA Phosphodiesterase on 3'-Phosphoglycolate Terminated DNA Strand Breaks

Haritha Tatavarthi
Virginia Commonwealth University

ACTION OF TYROSYL DNA PHOSPHODIESTERASE ON 3'-PHOSPHO GLYCOLATE TERMINATED DNA STRAND BREAKS

A thesis submitted in partial fulfillment of the requirements for the Master Degree of Science at Virginia Commonwealth University.

by

HARITHA TATAVARTHI
M.S. RAMAIAH COLLEGE OF PHARMACY, INDIA, 2000

Director: LAWRENCE F. POVIRK
PROFESSOR, DEPARTMENT OF PHARMACOLOGY AND TOXICOLOGY

Virginia Commonwealth University
Richmond, Virginia
May 2006

Table of Contents

List of Figures

List of Abbreviations

Ab	antibody
ADP	adenosine diphosphate
AP	abasic, apyrimidinic, apurinic
° A	angstrom
APE	AP endonuclease
AT	ataxia telangiectasia
ATM	ataxia telangiectasia mutated
ATP	adenosine triphosphate
ATR	ataxia telangiectasia related
bleo	bleomycin
bp	base pair
BSA	bovine serum albumin
° C	degree centigrade
cDNA	complementary DNA
CHO	Chinese hamster ovary
cs	catalytic subunit
C-T	carboxy terminal
DMSO	dimethyl sulfoxide
DNA	deoxyribonucleic acid
DNA-PK	DNA dependent protein kinase

DNA pol	DNA polymerase
DNase	deoxyribonuclease
dNTP	deoxynucleotide triphosphate
ds	double stranded
DSBs	double strand breaks
DTT	dithiothreitol
E.coli	*Escherichia coli*
EDTA	disodium ethylenediaminetetraacetate
EJ	end joining
EMSA	electro mobility shift assay
FCS	fetal calf serum
Fmol	femtomole
HPLC	high pressure liquid chromatography
HRR	homologous recombination repair
IC50	dose at which drug produces fifty percent inhibition
IP	immunoprecipitation
IR	ionizing radiation
Kb	kilobyte
KCl	potassium chloride
kDa	kilo Dalton
ko	knock out
Mg^{+2}	magnesium
Mn^{+2}	manganese

mol	mole
µg	microgram
µl	microlitre
µM	micromolar
MilliQ	deionized, distilled
mL	milliliter
mM	millimolar
Mr	molecular weight
NAD	nicotinamide adenosine syndrome
NBS	nijmegan breakage syndrome
ng	nanogram
nm	nanometer
nM	nanomolar
N-T	amino terminal
OH	hydroxyl
%	percentage
PAGE	polyacrylamide gel electrophoresis
PARP	poly ADP-ribose polymerase
PCR	polymerase chain reaction
PBS	phosphate buffered saline
PG	phosphor glycolate
PI	phosphatidyl inositol
PIK	phosphatidyl inositol kinase

PLD	phospholipase D
PNKP	polynucleotide kinase phosphatase
PO_4	phosphate
REC	recombination
RNA	ribonucleic acid
rpm	rotations per minute
RPMI	Rosewell Park Institute medium
Sc	*Saccharomyces cerevisiae*
Scid	severe combined immunodeficient
SDS	sodium dodecyl sulfate
NaCl	sodium chloride
ss	single strand
SV 40	simian virus 40
TBE	Tris HCl/Borate/ EDTA
TBS	Tris buffered saline
Tdp1	Tyrosyl DNA phosphodiesterase
TEA	triethylamine
TEMED	N,N,N',N'-tetramethylethylene
Tris	tris(hydroxymethyl)aminomethane
UV	ultra violet
V(D)J	variable, (diversity), joining
WB	western blot
WS	werner syndrome

WRN	Werner syndrome protein
wt	wild type
XRCC	X-Ray cross complementation
xrs	X-Ray sensitive

Abstract

ACTION OF TYROSYL DNA PHOSPHODIESTERASE ON 3'-PHOSPHOGLYCOLATE TERMINATED DNA STRAND BREAKS

Haritha Tatavarthi, MS

A thesis submitted in partial fulfillment of the requirements for the Masters Degree of Science at Virginia Commonwealth University.

Virginia Commonwealth University, 2006

Major Director: Lawrence F. Povirk, Ph. D.
Professor, Department of Pharmacology and Toxicology

Free radical-mediated DNA double strand breaks (DSBs) are induced either directly by ionizing radiation or by certain chemicals like bleomycin. These breaks are terminated by 3'-PG ($PO_4CH_2COO^-$) or 3'-phosphate groups formed as a result of fragmentation of deoxyribose.

To study the nature of repair of these 3'-blocked breaks, we constructed substrates mimicking free-radical induced DSBs. Human and yeast tyrosyl DNA-phosphodiesterase (Tdp1) efficiently processed substrates with 3'-PGs, in either the presence or absence of magnesium, to give a 3'-phosphate. Gel filtration chromatography and western blotting confirmed that the putative enzyme in human extracts that efficiently processed PG was indeed tyrosyl DNA-phosphodiesterase. When recombinant hTdp1 was purified using HiTrap nickel chelating columns and its PG processing activity compared to that of partially purified native enzyme (from lymphoblastoid whole-cell extracts using Sephacryl S-300 gel filtration columns), we found that the recombinant enzyme had

lesser 3'-PG removal activity than the partially purified native enzyme. On cloning recombinant FLAG-tagged hTdp1 into human expression vectors, we observed that the FLAG epitope tag did not show any evidence of affecting the specificity of the enzyme. Due to the many differences between bacterial and human cells, we cloned recombinant FLAG-tagged hTdp1 into U-87 cells (adenovirus infected glioma cell) and this recombinant enzyme showed the same specificity toward PG substrates as when prepared from bacteria. End-processing assays using the NHEJ proteins- Ku, DNA-PK and XRCC4/Ligase IV- alone or in combination showed an inhibition of hTdp1 activity on 3'-overhangs. In nuclear extracts, hTdp1 association with XRCC1, a single-strand repair protein, showed to increase the PG-processing activity of Tdp1 up to 4 times. Whole-cell extracts containing mutant Tdp1 derived from patients suffering from spinocerebellar axonal neuropathy (SCAN1) were found to be deficient in PG-processing. Addition of JRL1 whole-cell extract (SCAN1 extract containing mutant Tdp1) to purified FLAG-tagged hTdp1 showed to decrease the phosphotyrosyl processing and increase the PG-processing of FLAG-tagged hTdp1 suggesting that there must be other factors in the extract that affect the enzyme activity.

Experiments carried out to check for the presence of Tdp1 in mitochondrial extracts obtained fromGM1310 normal human fibroblasts as well as in SCAN1 (JRL) mitochondrial extracts, showed that mitochondrial extracts contained Tdp1 at a concentration comparable to whole-cell extracts. Our results also showed that mitochondrial extracts from the SCAN1 cell-line, JRL3 (containing mutant Tdp1), lacked detectable Tdp1 activity suggesting that all PG-processing activity in mitochondria may be attributable to Tdp1.

Introduction

The field of cancer research is ever expanding and seems to be of pivotal importance because man has known cancer ever since the dawn of civilization. With increased life span of individuals, the likelihood of surviving to an age of high susceptibility to cancer is ever increasing, and statistically at least one in three people develop cancer. One in four men and one in five women die from it. The field of molecular biology has opened doors to genetic analysis of normal and tumor cells and allowed us to delve into previously unapproachable questions about the molecular mechanisms behind the development of cancer. It is these developments as well as the quest for finding a cause and cure for the disease that has given cancer research so much importance and attention.

Somatic mutations are the most common cause of development of cancer. Alterations as small as single base substitutions in specific genes can cause dramatic increases in the incidence of certain malignancies, for example colon cancer (Vogelstein and Kinzler, 1993). However it is known that cancer is a multi-step process involving an array of genetic alterations that come together to cause disruption of various cellular functions, ultimately leading to the development of cancer. With as many as 10,000 DNA lesions occurring in a metabolically active mammalian cell per day, highly discriminatory and efficient DNA repair mechanisms have developed for its preservation (Lindahl, 1993). One of the most detrimental types of DNA damage is DNA double strand breaks (DSBs) because they can directly disrupt the normal cellular function and survival. Endogenous sources of DNA DSBs include disruption of DNA replication, as well as free

radicals from oxidative metabolism (Giloni et al., 1981, Hutchinson, 1985). Among DNA damaging agents, the most significant source of DSBs is ionizing radiation (IR) such as gamma, neutron, alpha, proton and X-radiation. DSBs of similar structure are produced by radiomimetics such as bleomycin, neocarzinostatin, calicheamicin and esperamicin. Bleomycin and enediyne antibiotics are called radiomimetic because their effects on cells are similar to those caused by radiation. The formation of ionizing radiation-induced DSB occurs mostly through excitation of a water molecule followed by its ionization into hydrogen and hydroxyl radicals in a process also known as radiolysis of water.

1) excitation via IR: $H_2O \rightarrow H_2O^*$
2) ionization: $H_2O^* \rightarrow e + H^+ + OH^\bullet$ where *e* is high speed, high-energy electron which will interact with other atoms or electrons to produce more radicals.

These hydroxyl free radicals are the most reactive ones among IR-induced free radicals, and since the lifetime of the radicals is about 10^{-5} seconds, they will not diffuse very far from the site of formation. The hydroxyl free radicals are concentrated alongside the track of the IR beam and will target any substance nearby. They can also react with DNA molecules in close proximity targeting mainly DNA bases and sugar moieties.

Most of the free radical mediated DNA damage (~80%) occurs at the double bonds of bases resulting in either 6-hydrothymine, 5-hydroxy-5, 6-dihydrothymine, 5-hydroxymethyluracil, 5-hydroxycytosine, 4,6-diamino-5-formamidopyrimidine, 8-hydroxyadenine, 2,6-diamino-4-hydroxy-5-formamidopyrimidine, thymine glycol, or

8-oxoguanine (Dizdaroglu et al., 1986). These lesions do not produce the lethality caused by IR and can be easily repaired by base excision repair (BER). Although 8-oxoguanine is a mutagenic lesion where addition of O on position 8 of the guanine can mispair with A resulting in transversion, it is not considered the main cause of lethality observed from exposure to IR. The rest of the damage caused by IR-induced hydroxyl radicals (~20%) is on the sugar moieties through the abstraction of hydrogen atoms from C1′ to C5′ of the deoxyribose. Hydrogen abstraction of hydrogen atoms from these five sites of deoxyribose is a random process and leads to five possible sugar radicals, but the main attack which produces strand breaks is on the C4′ site of the deoxyribose. This is followed by some rearrangements that result in 3′-phosphoglycolate and release of base propenal. Thus, the formation of multiple SSBs concentrated within close proximity of IR tract results in 25-50 DSBs per 1 gray (Gy) of X-ray irradiation in a single diploid mammalian cell, which ultimately contributes to the lethality of IR (Erixon et al., 1995).

Also, similar to IR-induced DSBs, initial attack by radiomimetics such as bleomycin cause oxidation of C4′ of the deoxyribose of the first C following a G (Povirk, 1996). This leads to a strand break or apyrimidine (AP) site. Bleomycin is known to be semi-sequence specific and its reactivation can lead to another attack in the opposite strand producing a strand break or an abasic site. All breaks are blocked by a 3′-PG and are associated with base propenal formation.

Consequences of DSBs

The presence of DSBs in a cell can be devastating for its survival if they are left unrepaired, because many critical cellular functions such as replication and transcription depend on the integrity of DNA. These unrepaired DSBs can result in chromosome breaks leading to the loss of genetic material during cell division and can severely increase the chance for oncogenic transformation or cell death (Bryant et al., 1985). Autosomal recessive diseases such as ataxia-telangiectasia (A-T) and Nijmegen breakage syndrome are caused by the inherent inability to protect the genome against occurrences of DSBs, and patients with these diseases exhibit hypersensitivity to radiation, increased oncogenic transformation, and genomic instability (Varon et al., 1998 and Waldmann et al., 1983). Thus, the DNA DSB is thought to be the single most destructive DNA lesion.

There are other consequences to DSBs when they are inaccurately repaired. Such consequences are deletions, frame shift or point mutations in addition to various chromosomal abnormalities that may arise from misjoining of DSBs (Obe et al., 1992). Chromosomal abnormalities including inversions, reciprocal translocations, acentric, dicentric, ring chromosomes and other complex rearrangements have been determined to promote global genomic instability and oncogenic transformation in mammalian cells (Lengauer et al., 1998 and Wang et al., 1997). Consequently, mammalian cells have acquired an ability to accurately repair DSBs through a complex network of recognition and repair proteins.

DSB detection and signaling

Mammalian cells possess intrinsic cell-cycle signaling pathways that monitor and respond to DNA DSBs because of the devastating consequences they bring. Until now, most *in vitro* experiments regarding DSB repair have utilized naked DNA. However, in eukaryotic cells, DNA normally exists in a compacted chromatin structure where DNA is wrapped around two histone tetramers, H2A, H2B, H3 AND H4, into nucleosome complexes (Laskey et al., 1980). It has been shown that when cells are irradiated with IR, one of the histone subunits H2AX is immediately phosphorylated on a highly conserved serine residue in the C-terminus (Mannironi et al., 1989). Also, the location of phosphorylated H2AX was consistently coincident with the location of DSBs (Ohya et al., 2002 and Rogaku et al., 1998). This phosphorylation is also known to induce 'opening' of the compact chromatin structure to presumably allow easier access of DSB repair machinery to the breakage site (Downs et al., 2000). Recently, ataxia-telangiectasia mutated (ATM) protein has been found to catalyze this critical phosphorylation (Burma et al., 2001). ATM is the protein product of the gene mutated in the human genetic disorder ataxia-telangiectasia, and patients who suffer from this disease exhibit neuronal degeneration, immunodeficiency, sterility, genomic instability, radiation hypersensitivity and predisposition to carcinogenesis. Usually, A-T patients develop lymphoma, breast carcinoma, or leukemia during their lifetimes. These life-threatening consequences of A-T are not coincidental because of the role ATM plays in not only detecting DSBs (Anderson et al., 1993) but also in relaying this information to other cell regulatory proteins such as p53, hCHK1 and hCHK2 in order to arrest cell cycle progression at G1/S, G2/M and intra S check points (Falck et al., 2001, Lohman et al., 2001 and Pierce

et al., 2001). ATM, which belongs to the serine/threonine kinases of the phosphotidylinositol 3-kinase (PI3K) family, is thought to be one of 'guardians of genome' because of its important role in preventing progression of the cell cycle until completion of DSB repair (Kim et al., 1999 and Bannister et al., 1993). Another serine/threonine kinase belonging to PI3K family that may signal presence of DSB is DNA-dependent protein kinase (DNA-PK), which is the gene mutated in severe combined immune deficiency (SCID) in mice (Williams et al., 2001). In contrast to ATM, which induces cell cycle arrest, DNA-PK may be more heavily involved in signaling detection of DSBs to p53 dependent-apoptotic machinery through differential phosphorylation of p53 (Wang et al., 1997).

DSB repair pathways

DNA DSBs can be repaired through two distinct pathways: Homologous recombination (HR) and Non-homologous end joining (NHEJ). The cell seems to choose between these two pathways to repair the lesion and the choice primarily depends on which phase of the cell cycle it is currently in. If the cell is in between late S and G2 phase where an intact replicate sequence is available, then HR seems to be the predominant mode of repair. If the cell is in G0/G1 to early S phase, NHEJ appears to be the dominant mode of repair. Yet DNA repair is not exclusive to one repair pathway. Also, the reason NHEJ is considered to be the major pathway of DSB repair lies in the fact that most cells in an adult organism are not continuously dividing. It is possible that HR may be more important in stem cells that are actively dividing in the lining of the gut, mouth, esophagus, epidermal layer of skin, and blood forming tissues, in addition to cells

with the potential to divide which include hepatocytes, fibroblasts, glandular epithelial cells and endothelial cells.

Homologous Recombination Repair Pathway (HRR)

HRR is the predominant mode of repair in lower organisms and represents an accurate, high fidelity pathway with no sequence loss or addition. This pathway makes use of extensive homologies between the damaged strand and an intact homologous strand, replacing lost nucleotides at the break site with the help of sequence information from the undamaged strand. In HR, DSBs are introduced as an initial event followed by resection of the DNA ends in the 5′→3′ direction. Single stranded DNA thus derived then invades the homologous strand and DNA polymerase, which makes use of the information from the intact DNA, fills in the gaps. Following sister-chromatid pairing and strand invasion of DNA overhangs, HRR can go in either of two directions. Noncrossing-over, resulting from disengagement of Holliday junction (a point of strand crossover) followed by DNA pairing and gap filling in the damaged homologue, appears to be strongly favored during HRR in mammalian cells. This is quite different from the classical microbial pathway, in which the Holliday junctions are resolved by endonucleolytic cleavage, with an equal probability of yielding either a crossover or a non-crossover event. Holliday junctions are cleaved by resolvases to yield two intact DNA strands after ligation. The yeast *S. cerevisiae* provides an excellent model for understanding the biochemistry and genetics of HR. In *S. cerevisiae*, the RAD52 epistasis group of genes comprising RAD50-55 and RAD57 (Game, 1993), RAD59 (Bai et al., 1996), XRS2 (Ivanov et al., 1992) and the MRE11/RAD58 genes carries out HR

(Baumann and West, 1998). After DSB induction, Rad52 binds to the broken DNA ends in order to protect them from exonucleolytic degradation. Resection of the DNA from 5′→3′ is possibly through the coordination of the Rad50/Mre11/Xrs2 (Xrs2 is the yeast homologue of human NBS) complex. Evidence suggests that the MRN complex functions in NHEJ as well. The Rad50 binds to DNA in an ATP-dependent manner (Raymond et al., 1993). The Mre11 protein has an exonuclease function that is active in the 3′→ 5′ direction on the ss- and ds-DNA with a preference for recessed 3′ ends (Shinohara et al., 1992). It also has an endonuclease function critical in meiosis. Next in HR, Rad51 polymerizes on ss and ds-DNA forming filaments and mediates strand invasion in the 3′→ 5′ direction (Sung et al., 1994). The human Rad51 protein is also homologous to the *E.coli* RecA protein. Strand exchange is stimulated by the addition of RPA (Sugiyama et al., 1997).

BRCA1 and BRCA2 are two breast cancer susceptibility genes recently shown to be linked with DNA repair by virtue of their BRCT domains, which are a common feature of DNA repair proteins (Callebaut et al., 1997). Both proteins interact with Rad51 and co-localize to nuclear foci in response to DNA damage in mitotic cells (Scully et al., 1997). Recently, it was demonstrated that BRCA2 interacts with RAD51 and RPA at the site of DSB and helps load RAD51 onto DNA or to organize RAD51 filaments (Yang et al., 2002). Disruption of BRCA2 gene by targeted truncation in mice makes cells from them sensitive to UV light and methyl methane sulfonate. The cells arrest in G1 and G2/M phases and increased levels of p53 and p21 accompany this arrest (Patel et al., 1998). Mouse fibroblasts with BRCA1-/- and BRCA2-/- status develop spontaneous chromosomal aberrations, providing further evidence for the role of these proteins in

HRR (Patel et al., 1998). Altogether, BRCA1 and BRCA2 are believed to be important at early points of HRR and perhaps coordinate repair with other cellular processes.

Attempts to assess the biological consequences of defects in specific HRR factors have been hampered by the embryonic lethality of many mouse knockouts targeting genes involved in HRR. RAD54 knockout mice are viable, and embryonic fibroblasts of HRR-defective RAD54 knockout mice are radiosensitive (Essers et al., 1997, 2000). RAD54 deficiency does not confer radiosensitivity in otherwise normal adult mice, but futher enhances the radiosensitivity of NHEJ-deficient Scid mice (with a mutation in DNA-PKcs). These results suggest that HRR may be a more important repair component in embryonic cells than in normal adult somatic cells. Studies of both knockout mice and repair-deficient cultured cells suggest that disruption of any factor involved in HRR results in chromosomal instability and (for those defects that are not lethal) cancer predisposition (Thompson and Schild, 2001; van Gent et al., 2001).

Non-Homologous End-Joining Pathway

This is the second major pathway of DSB repair and is the predominant mechanism of repair in mammalian somatic cells. The term "non-homologous" is used to indicate the fact that this pathway does not require extensive homologies between two DNA strands to be recombined (Roth et al., 1985), although micro homologies of as little as 1-5 base pairs are often used (Labhart, 1999; Critchlow and Jackson, 1998). A deficiency in this pathway leads to a myriad of consequences like radio-sensitization, increased susceptibility to development of cancer and a variety of immunodeficiency syndromes, most if not all of which are due to the defect in the repair of DSBs. Over

more than a decade, genetic and biochemical approaches have now identified the major proteins that play a crucial role in this repair process. NHEJ involves a DNA-binding heterodimer of Ku70 and Ku80 proteins, which associates with the catalytic subunit of DNA-dependent protein kinase (DNA-PKcs) to form DNA-PK holoenzyme. Additional factors include DNA ligase IV, its cofactor XRCC4 and probably DNA polymerase λ and/or human polynucleotide kinase/phosphatase or hPNKP (Critchlow and Jackson, 1998; Jackson and Jeggo, 1995; Chu, 1997). Ku was first identified as an autoantigen for a number of autoimmune diseases in 1981, but Rathmell et al linked it to NHEJ when they observed that Ku complementation conferred X-ray resistance to X-ray sensitive hamster cell line, *xrs5*. Subsequently, several X-ray cross complementation (XRCC) genes were identified by virtue of their ability to correct radiation hypersensitivity in rodent cell lines. They are *XRCC4, XRCC5, XRCC6* and *XRCC7* encoding the proteins XRCC4, Ku86, Ku70 and DNA-PKcs respectively. With these discoveries, a host of other genes that are now known to be integral players in recognition, signaling, and repair of DSBs have begun to emerge. And the list is increasing at an extraordinary pace implicating additional factors such as hMre11, hRad50, Nbs1, APE1, Artemis and Werner, as well as many additional proteins involved in downstream signaling.

Structural and biochemical properties of end-joining proteins

Ku Heterodimer

As subunits of DNA-dependent protein kinase, Ku70 and Ku86 are proteins with molecular weights of 70 and 86 kDa respectively. This Ku heterodimer forms a close-fitting asymmetrical ring that threads onto a free end of DNA as a "nut on a bolt" (Walker

et al., 2001). Also, using nitrocellulose filter-binding assay, its affinity toward dsDNA has been determined to be much higher than toward ssDNA (Walker et al., 2001). The dissociation constant of Ku towards ds DNA is in the range of 1-2 nM while that for single-stranded DNA is about 300nM (Tuteja and Tuteja, et al., 1994). Later studies showed that Ku can also bind to gapped and nicked DNA as well as to DNA hairpins such as those generated during V(D)J recombination (Blier et al., 1993; Falzon et al., 1993). Although Ku tends to cling to the DNA end, it can translocate into the interior, allowing multiple Ku heterodimers to load onto longer DNA molecules (Mimori et al., 1986; Yaneva et al., 1997). The end-bound Ku occupies approximately 16-18bp, as indicated by X-ray crystallography, DNase footprinting (Lee et al., 2004) and ultraviolet crosslinking (Walker et al., 2001). The primary function of Ku70/86 in NHEJ, which is alignment of two DSB ends for subsequent repair processes to ensue, has been suggested from their ability to self-associate. In order to bind to DNA, both subunits of Ku should be present and interact with each other (Griffith et al., 1992). Also, in a DNA sequence-independent manner, the self-association of Ku molecules that form either DNA loops (intramolecular interaction) or DNA intermolecular bridges has been observed through atomic force microscopy (Cary et al., 1997). In addition to acting as a DSB alignment factor, Ku recruits DNA-PKcs molecules to DSB ends and forms a stable complex while stimulating its kinase activities (Dvir et al., 1992; Gottlieb and Jackson, 1993). It is also known to stimulate the catalytic activities of DNA ligase IV (Cary et al., 1997). A search for homology between the cDNAs of the 2 subunits of Ku led to the identification of leucine zipper motifs (Wu and Lieber, 1996) which suggested a role for Ku in regulation of transcription and ATP binding domains in both Ku70 and Ku80 which were thought to

be essential for ATPase function of Ku (Cao et al., 1994). In addition to the ATPase, Ku was reported to unwind duplex DNA and was thus classified as human DNA helicase II (Tuteja et al., 1994). It unwinds DNA duplexes in a 3′→ 5′ direction on the bound strand. The ATPase function is attributed to both the subunits whereas the helicase is entirely a function of Ku70 (Ochem et al., 1997).

DNA-PKcs

DNA-dependent protein kinase catalytic subunit (DNA-PKcs) is the largest component of the DNA-PK holoenzyme. It is a ~460 kDa serine/threonine kinase that belongs to the subgroup of PIK-related kinases within the phosphatidylinositol (PI)-3 kinase superfamily (Hartley et al., 1995). All the members of this subgroup have a 3′ conserved kinase domain similar to the lipid kinases, but in addition also have another conserved domain 3′ to the kinase domain. DNA-PK was purified from Hela nuclear extracts as a protein that was able to phosphorylate DNA binding proteins like p53, SV40 large T antigen and Ku (Carter et al., 1990; Jackson et al., 1990; Lees-Miller et al., 1990). Monoclonal antibodies against the 460 kDa kinase specifically inhibited the kinase activity from the cell extracts. Immunodepletion of the protein also abolished the kinase activity (Carter et al., 1990). Two smaller polypeptides were also isolated with the 460 kDa DNA-PK and sequence analysis revealed that they were in fact the 2 subunits of Ku that co-purified with DNA-PK (Lees-Miller et al., 1990). Subsequent studies showed that DNA-PK binds to and is activated by binding to dsDNA ends (Gottlieb and Jackson, 1993). They also showed that when Ku was mixed with the 460 kDa protein fractions, it stimulated the kinase activity of those fractions. Pre-incubating cell extracts with anti-Ku antibodies abolished the kinase activity. All these observations suggested that Ku was a

component of DNA-PK and was required for dsDNA dependent stimulation of DNA-PK. However, this is not true in its entirety because it was later shown that DNA-PK is not activated by many substrates that are efficiently bound by Ku like hairpins, nicks (Smider et al., 1994) and cis-platin cross-linked DNA (Turchi et al., 2000). Furthermore, DNA-PKcs can be activated in the absence of Ku as long as the concentration of DNA ends is sufficiently high and ionic strength sufficiently low to support DNA-PKcs binding to the DNA ends (Hammarsten and Chu, 1998). This suggested that DNA-PKcs was activated by its direct interaction with dsDNA and that Ku was needed just to stabilize this binding. An electron crystallography study revealed that the DNA-PKcs structure contains and open channel, and an enclosed cavity with three openings large enough to allow the binding of a single-stranded DNA (Leuther et al., 1999). The results from ultraviolet crosslinking studies suggest that, when a DNA-PKcs molecule binds a DNA terminus, it displaces Ku approximately10 bp interior away from the terminus (Yoo and Dynan, 1999). Formation of the DNA-PK holoenzyme complex (Ku and DNA-PKcs) on a DNA end results in the activation of its kinase activity (Smith and Jackson, 1999). Studies with various oligomeric substrates suggest that activation involves insertion of a few bases of the single strands into defined channels (Hammarsten and Chu, 1998). Activation is relatively insensitive to structural modifications in these single strands, suggesting that even severely damaged termini could still activate DNA-PK (Weinfeld et al., 1997; Martensson and Hammarsten, 2002).

Activated DNA-PK phosphorylates a variety of DNA-binding proteins (Anderson and Lees-Miller, 1992), including several with known or putative roles in end-joining such as Ku (Lees-Miller et al., 1990), XRCC4 (Leber et al., 1998), Werner (Yannone et

al., 2001) and the Artemis nuclease (Ma et al., 2002). Activated DNA-PK also phosphorylates itself, resulting in its dissociation from DNA (Chan and Lees-Miller, 1996). Pharmacological inhibitors of PI-3 kinase family can also regulate DNA-PK activity. Wortmanin, a sterol-like fungal metabolite, is one such potent and selective inhibitor of mammalian PI-3 kinases (Ui et al., 1995; Powis et al., 1994). A detailed kinetic analysis of wortmanin mediated DNA-PK inhibition showed that wortmanin inhibits DNA-PK in a non-competitive manner with a *Ki* of 120nM (Izzard et al., 1999). The compound forms a covalent bond with the kinase domain of DNA-PKcs *in vivo* and *in vitro* and this binding is not dependent on presence of Ku (Izzard et al., 1999). LY294002 is another potent inhibitor of DNA-PK and other PI-3 kinases (Rosenzweig et al., 1997) LY294002 also sensitizes human tumor cells to IR at the same concentration required to inhibit DNA-PK activity.

XRCC4/ DNA Ligase IV

The XRCC4 gene was originally isolated by complementation of radiosensitivity, V(D)J recombination deficiency and DSB repair deficiency of the radiosensitive CHO derivative XR-1 (Li et al., 1995). As revealed by X-ray crystallography, XRCC4 consists of a globular head plus a long α-helical tail. In the crystal, four XRCC4 monomers form a dumbbell shaped homotetramer with two globular heads at each end and the ends linked by the four interacting tails (Junop et al., 2000). In cells, DNA ligase IV is present in a tight complex with XRCC4 and the complex can withstand buffer conditions of 2 M NaCl or 7 M urea (Lee et al., 2000). Ligase IV is not detectable in cells lacking XRCC4, but XRCC4 is stable by itself (Bryans et al., 1999). Ligase IV binds to XRCC4 at a site near the middle of the α-helical tail. A unique characteristic of DNA ligase IV is a large

C-terminal region containing tandem repeats of BRCT domain, a motif commonly found in proteins involved in DNA repair and DNA damage signaling, which is also responsible for interacting with XRCC4 (Sibanda et al., 2001). In addition, it is the only DNA ligase that is able to maintain its catalytic activity in low magnesium concentration such as in 1 mM. The role of XRCC4/DNA ligase IV in NHEJ has been extensively investigated through its interaction with other proteins of the NHEJ machinery. Electrophoretic mobility shift assay and immune-precipitation show that Ku physically interacts with the complex and recruits it to DNA (McElhinny et al., 2000). The interaction of XRCC4/ligase IV with DNA is stabilized only in the presence of Ku, but DNA is not required for the interaction of Ku with the complex. Chen et al., in 2002, found that under their experimental conditions, Ku actually inhibits intramolecular ligation by XRCC4/ligase IV suggesting that this complex is rather complex. XRCC4 also interacts with DNA-PKcs and is an effective substrate for phosphorylation by DNA-PKcs, but the relevance of this phosphorylation to NHEJ is still unclear. Phosphorylation occurs on serine and threonine residues in the carboxy-terminal of the protein (Leber et al., 1998).

Oxidative Stress and DSBs

Oxidative stress plays a major role in aging and in many human diseases, including cancer and various neurological disorders (Lu et al., 2004). The primary known targets of oxidative damage are cell membranes and DNA. Ionizing radiation, radiomimetic drugs, and to some extent, all free radical based genotoxins induce DNA DSBs either by base release or oxidative fragmentation of DNA sugars (Inamdar et al., 2002). In particular, oxidation of the C-4′ position results in breaks with 5′-P and 3′-PG

termini. Repair of such breaks requires the conversion of these modified 3′ termini to 3′ hydroxyls, so that DNA polymerases can replace the missing nucleotide and DNA ligase can seal the nick. At single-strand breaks in double-stranded DNA, conversion of both 3′-P and 3′PG termini to 3′-hydroxyl termini were found to be catalyzed by the human basic endonuclease, Ape1 (Suh et al., 1997). However, 3′-PG termini in single-stranded segments of DNA, such as 3′ overhangs of DNA DSBs, are completely refractory to Ape1 (Chaudhry et al., 1999). The human polynucleotide kinase/phosphatase PNKP, which removes 3′-P from single-stranded 3′ termini, also has no detectable effect on 3′-PGs (Jilani et al., 1999; Karimi-Busheri et al., 1999) and this is similar to reports for rat PNKP (Habraken and Verly, 1988). The susceptibility of 3′-PGs to *E. coli* exonuclease I (Sandigursky and Franklin, 1993) raised the possibility that PGs on 3′ overhangs might be removed by a mammalian 3′→ 5′ exonuclease. However, DNase III, which is the dominant 3′→ 5′ exonuclease in mammalian cell extracts, has no detectable effect on any 3′-PG substrates (Inamdar et al., 2002). The Wrn1 and Mre11 3′→ 5′ exonucleases are also unlikely candidates to these enzymes (Kamath-Leob et al., 1998; Huang et al., 2002). Nevertheless, it was shown that *Xenopus*, human and hamster whole cell extracts possess potent activity for processing of PGs on single-stranded 3′overhangs of DSBs, as well as from simple single-stranded oligomers (Chen et al., 2001).

Tyrosyl DNA phosphodiesterase

Topoisomerases are essential ubiquitous cellular enzymes required to control the superhelical tension and DNA entanglement associated with DNA replication, recombination, transcription and chromosome segregation (Connelly and Leach, 2004). In

eukaryotes, topoisomerase I transiently breaks one strand of DNA, forming a covalent linkage between the side chain of its active site tyrosine and a 3′ P of DNA, subsequently reversing it to re-ligate the DNA. Although this activity is essential for survival, topoisomerase I can be toxic. When the enzyme cleaves DNA at or near a variety of DNA lesions, the re-ligation step is hindered and topoisomearse I remains on the DNA as a covalent 'cleavable complex'. The initial DNA lesion is thereby transformed unto a single-strand break that is encumbered with a protein adduct. Cleavable complex formation is also induced by chemotherapeutic agents, such as captothecin (CPT), that specifically inhibit topoisomerase I re-ligation. An encounter with a replication fork converts the cleavable complex into a potentially lethal DSB. Tyrosyl DNA phosphodiesterase 1 (Tdp1) was first isolated from *Sacchromyces cerevisiae* as an enzymatic activity that precisely cleaves this tyrosyl-phosphodiester bond linking tyrosine of topoisomerase I to a 3′ DNA end (Yang et al., 1996). Subsequently the *S.cerevisiae* gene for Tdp1 was cloned and characterized, and orthologs were identified in other eukaryotic but not prokaryotic species.

Previous experiments in yeast presented two lines of evidence showing that Tdp1 is a repair protein that only acts after the occurrence of a DSB. First, biochemical studies with highly purified Tdp1 showed that the enzyme is most active on substrates that mimic DNA that has a topoisomerase I-linked DSB and is less active on a substrate that resembles an unprocessed cleavable complex. Second, an analysis of the phenotype of single and double mutants shows that the *in vivo* repair of topoisomerase I lesions by Tdp1 depend on the function of the *RAD52* gene, which is known to be vital for DSB repair. Taken together, these results for the first time placed *tdp1* in a *RAD52*-dependent

DSB repair pathway. Surprisingly, a *S.cerevisiae* strain containing a null mutation in the *tdp1* gene is no more sensitive to CPT killing than the wild-type strain. However, when the *tdp1* null mutation of S. cerevisiae was added to a *rad9* mutation there was a 10-fold increase in the lethal effects of CPT, suggesting that there are other, Tdp1-independent, pathways of repair. The *RAD9* gene is vital for the function of a DNA damage checkpoint. Since it is also critical for DNA damage-induced expression and the post-translational modification of several genes, it is possible that an important component of the Tdp1-independent pathway might be limiting in a *rad9* strain. Subsequent genetic studies in yeast have revealed at least two other separate pathways that can contribute to the repair of topoisomerase I-DNA covalent complexes. These include the structure-specific endonucleases Rad1/Rad10 and Mus81/Mms4. Deletion of the *MUS81* confers sensitivity to CPT apparently through a pathway parallel to Tdp1 and Rad1 as the triple mutant *tdp1 rad1 mus81* is more sensitive than the double-mutant *tdp1 rad1*. Experiments using a genome wide screen to detect all non-essential genes that are important for protection from growth inhibition or killing produced by continuous exposure to CPT helped identify two further pathways involved in repairing the Top1-DNA complex, one involving Slx4 which acts in a parallel pathway to Tdp1 and Rad1/Rad10, and Sae2 which appears to act by stimulating the endonulcease activity of Mre11.

Evidence for a 3′-P intermediate in 3′-PG removal in human cell extracts suggested possible involvement of hTdp1, and indeed, both hTdp1 and yTdp1 were found to catalyze similar glycolate removal from a single-stranded oligomer as well as from a single strand overhang of a DSB (Inamdar et al., 2002). Yeast and human Tdp1 differ

from other activities for processing blocked 3′ ends in that they leave behind a 3′-P rather than a 3′-hydroxyl. The 3′-P can then be removed by PNKP (Jilani et al., 1999; Karimi-Busheri et al., 1999).

The exact step of NHEJ at which Tdp1 acts is yet unknown. Kinetic studies show that at least in extracts, much of the PG removal from 3′ overhangs occurs within the first few minutes, suggesting that it does not require the formation of the full repair complex (Inamdar et al., 2002). Indeed, the kinetic data suggest that as the ends become sequestered by DNA-PK, PG-removal is dramatically suppressed, raising the possibility that there maybe additional 3′-PG processing enzymes that act in context of the repair complex.

Tdp1 is a member of the phospholipase D superfamily

The members of the PLD superfamily comprise a highly diverse group of proteins that include plant, mammalian and bacterial PLDs, bacterial phosphatidyl-serine and cardiolipin synthases, a bacterial toxin, several pox-virus envelope proteins, and some bacterial nucleases.

Recent database searches revealed a full-length human cDNA encoding a 608-aa Tdp1 ortholog (68.5 kDa) located on chromosome 14. Predicted Tdp1 orthologs are present in a number of other eukaryotic organisms. The homology between the Tdp1 orthologs from different species extends from approximately amino acid 150 of the human protein to the C terminus. The N-terminal regions of the Tdp1 orthologs are poorly conserved and vary substantially in length. Among the regions that are best conserved are amino acids 262-289 and 492-522 of the human protein. A sequence alignment of these conserved regions with motifs 3 and 4 of representative members of

each class within the PLD superfamily reveals a high degree of similarity. Importantly, motifs 3 and 4 encompass the highly conserved HKD sequence identified as a hallmark of the PLD superfamily. In both Tdp1 and the members of the PLD superfamily, the conserved histidines, lysines, and aspartic acidss that form the HKD motif, surround the active site pocket. However, a conserved aspartate, positioned a long way from the active site and important for protein folding and stability, is present only in the PLD superfamily members and not Tdp1. Furthermore, the remainder of the human Tdp1 protein sequence cannot be reasonably aligned with any of the other PLD family members. Based on these findings, it was indicated that the Tdp1 orthologs represent a distinct class within the PLD superfamily.

As a member of the PLD superfamily, human Tdp1 is predicted to require a combination of two histidines (H263 and H493) and two lysines (K265 and K495) for catalytic activity. Biochemical experiments and the crystal structure of human Tdp1 confirm this prediction and demonstrate that the reaction proceeds through an intermediate in which the active site H263 is covalently bound through a phosphoamide bond to the 3′ end of the DNA moiety of the substrate. In the second step of the reaction, hydrolysis of the covalent intermediate yields the DNA product and frees the enzyme.

Substrate specificity of Tdp1

Role of Tdp1 in SSB repair

DNA SSB repair is critical for the survival and genetic stability of mammalian cells. SSBs can arise either directly (e.g., from attack of deoxyribose by free radicals such as ROS) or indirectly (via enzymatic cleavage of the phosphodiester backbone, e.g., as

normal intermediates of DNA BER). SSB repair can be divided into four basic steps, beginning with DNA damage binding. The second step in SSB repair is DNA end processing followed by DNA gap filling. In the final step, the integrity of the phosphodiester backbone is restored by DNA ligation.

In yeast, Tdp1 has been implicated in the repair of topoisomerase I-DNA adducts via the DSB repair pathway, although it is also clear that additional Tdp1-independent repair pathways can also correct topoisomerase I-mediated lesions. However, the role of Tdp1 in mammalian cells is not well understood. Its role in SSB repair is controversial. Early papers have proposed that Tdp1 participates in SSB repair. In humans, a mutation that inactivates Tdp1 *in vitro* is associated with inherited Spinocerebellar ataxia with axonal neuropathy or SCAN1. This result was initially surprising since DSBs form as a result of DNA replication in yeast and the inability to repair topoisomerase I-DNA adducts should not preferentially affect non-dividing neuronal cells. This observation therefore led to the proposition that Tdp1 acts via a SS repair pathway since SSBs can result from the collision of transcription complexes with abortive topoisomerase I-DNA adducts. A variety of recent observations have also been used to argue that SSB repair pathways are the preferred routes for repairing topoisomerase I-cleavage complexes in mammalian cells. First, cells containing inactive SSB repair proteins and XRCC1 are hypersensitive to CPT. In addition, yeast two-hybrid experiments revealed that Tdp1 associates with the SSB repair machinery by direct interaction with DNA ligase IIIα, a partner of XRCC1, a scaffold for repair proteins involved in SSB repair in higher eukaryotes. This might account for the observation that Tdp1 co-immunoprecipitates with XRCC1. Based on this result, it has been proposed that XRCC1 DNA repair complexes

contain enzymes required to excise the topoisomerase I-DNA adduct (Tdp1), process the DNA strand (PNKP), replace the missing DNA segment (β-polymerase), and seal the DNA in the absence of a DSB (ligase III). Therefore, one would expect the nicked or tailed substrate (mimicking a gapped DNA duplex) to be good substrates for Tdp1.

Recently, Raymond et al. (2005) presented results showing that Tdp1 does not have a kinetic or binding preference for single strand DNA over blunt end duplex DNA. The paper suggested that both single strand and double stranded blunt DNA substrates have significantly higher specificity constants (k_{cat}/K_M) over nicked or tailed substrates. It was also shown that Tdp1 binds single stranded and double blunt stranded substrates with significantly higher affinity (lower K_D) than with nicked or tailed substrates. Because single stranded DNA is not expected to be a common substrate *in vivo*, the authors proposed that double stranded blunt DNA is the natural substrate *in vivo*. If this is the case, these studies clearly suggest that Tdp1 acts after the topoisomerase I-mediated damage is converted to a DSB.

Proposed mechanism of action of Tdp1

SCAN1

The association of human genetic disorders with defects in the DNA damage response is well established. Most of the major DNA repair pathways are represented by diseases in which that pathway is absent or impaired. Hereditary ataxia comprises a clinically and genetically heterogeneous group of diseases that include disorders in DNA repair, such as AT, XP and Cockayne syndrome. In contrast to the isolated forms of hereditary ataxia, disorders of DNA repair typically cause additional symptoms, such as mental retardation, photosensitivity, immunodeficiency and neoplasia. A homozygous

recessive mutation in the human *TDP1* gene (A1478G) that results in the substitution of H493 with an arginine residue was found to be responsible for the human hereditary disorder SCAN1. The ataxia first becomes noticeable in the teenage years and apparently results from an effect on non-dividing terminally differentiated neuronal cells. SCAN1 is characterized by peripheral axonal motor and sensory neuropathy, distal muscular atrophy, and steppage gait. The association of a DNA repair protein with SCAN1 is striking, in that this is a neuro-degenerative disease that lacks any obvious extraneurological features such as genetic instability or cancer.

The A1478G mutation was originally proposed to be a loss of function mutation but a recent paper (Interthal et al., 2005) has suggested that the H493R mutation reduces the activity of the enzyme only ~25-fold based on the rate of product formation by the purified enzyme. This small amount of residual activity maybe sufficient to provide most of the repair capacity required throughout the life of an individual and thus explains the late onset of the disease in SCAN1 individuals. Alternatively, similar to yeast, there maybe a functional overlap of other repair systems so that, in the absence of sufficient Tdp1 activity, other pathways capable of repairing topoisomerase-I DNA covalent complexes fulfill the needs of the organism.

It is not known yet whether a SSB repair process or a DSB repair process is defective in SCAN1.Quantitative γ-H2AX immunostaining and neutral comet assays to examine whether the breaks that accumulate in SCAN1 cells are SSBs or DSBs, were carried out. Neither assay revealed a measurable difference between the level of DSBs in non-replicating normal and SCAN1 cells. Consequently, it was assumed that since both assays can detect as little as 1-2 Gy equivalents of DSBs, more than 98% of the breaks

that accumulate in non-replicating SCAN1 cells are SSBs. But at the same time, there have been suggestions of XRCC1 involvement in DSB repair pathway. A protein partner of XRCC1, PARP-1, binds both SSBs and DSBs, and in NHEJ defective background, the additional disruption of PARP-1 results in embryonic lethality. This has raised the possibility that PARP-1 fulfills a back up role during DSB repair, by binding and recruiting XRCC1 and other SSB repair proteins to DSBs that are not repaired by classical NHEJ.

It remains unclear why neurons are specifically affected by the Tdp1 defect in SCAN1 individuals. One possibility is that the elevated oxidative stress in post-mitotic neurons creates a particularly high level of SSBs. In addition, the limited regenerative capacity of the nervous system might render this tissue particularly susceptible to cell loss. Another possibility might be that unrepaired SSBs can be processed by HR, in proliferating cells, even in the absence of Tdp1, once they have been converted to DSBs during DNA replication, as in budding yeast. Terminally differentiated neurons have an enhanced need for Tdp1-mediated repair or are hypersensitive to the effects of persistent topoisomerase I-DNA covalent complexes, perhaps because alternative pathways may be attenuated in differentiated neurons. Interestingly, CPT was shown to induce apoptotic cell death in post-mitotic cortical neurons, indicating an important replication-independent role for topoisomearse I in this cell type.

Other roles of Tdp1

Tdp1 may also have multiple roles in the cell. For example in Drosophila, Tdp1 has been shown to be essential for the formation of epithelial polarity and for neuronal development during embryogenesis, and it has been proposed that Tdp1 is involved in the

localization of membrane proteins (Dunlop et al., 2004). Although no substrate or mechanism has been proposed to support this function, Tdp1 is a member of the PLD superfamily of enzymes (Interthal et al., 2001) and other members of this superfamily participate in membrane vesicle trafficking by hydrolyzing phosphatidylcholine to generate phosphatidic acid (Hughes et al., 2004; Humeau et al., 2001). These results emphasize the importance of understanding the *in vitro* binding properties and catalytic mechanism of Tdp1 to better understand its biological role(s).

Materials and Methods

Polyacrylamide gel electrophoresis

For denaturing gels, 8 M urea solution containing 20:1 acrylamide: bisacrylamide solution was prepared. Urea was allowed to dissolve at low heat and the mixture was then allowed to cool to room temperature. Polymerization was initiated by addition of 0.075% (w/v) ammonium persulfate and further accelerated with 0.03%(v/v) TEMED (N', N', N', N'-tetra methylethylene). The gel was allowed to set for ~ 1hour after which samples were loaded onto the gel and electrophoresed at a constant power of 40 to 50 watts depending on the size of the gel for 3 to 6 hours respectively. For end-processing assays, the gel was frozen and exposed on PhosphorImager screens for 1-2 days at -20° C. Phosphor images were analyzed and bands were quantified using ImageQuant software (Molecular Dynamics). For labeling of oligonucleotides with ^{32}P, the gel was exposed to X-ray film for approximately 30 seconds to 1 minute. The film was transilluminated against white light and the bands on the film were lined up with the gel. The part of the gel corresponding to the bands was cut and placed in 6 mL of 0.3 M sodium acetate/ 1 mM EDTA and allowed to elute at room temperature over night. On the second day, the elute was removed, divided into 1 mL eppendorf tubes and vacuum dried until all the liquid evaporated and left behind a white residue. The residue was dissolved in 800 µL of deionized water and mixed with 800 µL of 0.2 M triethylamine. The oligonucleotides were then subjected to high-pressure liquid chromatography (HPLC).

High-pressure liquid chromatography (HPLC)

DNA oligonucleotides were purified by the use of reverse phase high pressure liquid chromatography (HPLC). Reverse phase means that the gradient starts with a more aqueous mobile phase and progresses to a more hydrophobic mobile phase. Chromatography was carried out using a Rainin 5 μM Microsorb C_{18} column and 2 buffers, buffer A (5 % acetonitrile, 0.1 M triethylammonium acetate pH 7) and buffer B (50% acetonitrile, 0.1 M triethylammonium acetate pH 7). Glacial acetic acid was used to adjust the pH of the buffers while the use of NaOH was prohibited to avoid salt build up in the column. DNA interacts with column via the triethylamine present in the buffer. The negative charges of the DNA phosphate backbone are attracted to positively charged amine groups. Furthermore, the ethylene groups of triethylamine mediate interactions with the carbon chains. This DNA-triethylamine- C_{18} column interaction is hindered as the acetonitrile concentration is increased through a computer-controlled gradient directly competing for triethylamine until the DNA is eluted. First, the column was flushed with buffer B for 10 min to expel any residues from previous use. Then, the column was flushed with buffer A for 10 min. Next, the linear gradient was activated which mainly functions to increase the mobile phase acetonitrile percentage from 5% to 30% over 60 min by controlling the buffer flow from buffer A and B. the DNA oligo sample dissolved in 0.1 M triethylamine to a volume of 800 μL was injected into the sample loading port. With a flow-rate of 1 mL/min, the content of the effluent was monitered by a photomultiplier-tube detector and was recorded on the polygraph. After 20 to 30 min, the oligonucleotides eluted and the elute was vacuum dried for approximately 4 to 6 hours.

After the oligo was completely dried, it was resuspended in TE buffer (10 mM Tris-HCl pH 8, 0.1 mM EDTA).

Whole-cell extract preparation from human lymphoblastoid cells (GM0058B)

The procedure described by West and Baumann, 1998, PNAS was used. Cell lines were purchased from NIGMS Human Genetic Mutant Cell Repsotiory (Camden, NJ). GM0058B was a normal transformed cell line from a young 26-year old Caucasian. Cells were cultured in suspension in Rosewell Park institute medium (RPMI 1640) with 10% fetal calf serum (FCS) and allowed to grow to a density of 8 x 10^5 cells/ml before harvesting. They were then washed once in RPMI 1640 containing 10% FCS and once in ice-cold phosphate buffered saline (PBS) before transporting to the laboratory for extract preparation. Cells were received re-suspended in 200 ml of RPMI 1640. A sterile centrifuge bottle was weighed and the cells were transferred to the bottle and spun down at 1200 rpm for 10 minutes in the SS34 rotor. The cell pellet was re-suspended in 200 ml of ice-cold PBS and washed two times. PBS was then discarded and the cells were washed with hypotonic lysis buffer containing 10 mM Tris-HCl, ph 8.0/ 1 mM EDTA/ 5 mM DTT. A 2 ml pellet was obtained at the end of the final wash, which was the re-suspended in 2 volumes (4 ml) of hypotonic lysis buffer again. Cells were allowed to swell for about 20 minutes on ice after which they were transferred to a 7 ml tissue homogenizer and cells were lysed with 20 stokes of pestle "A". The following protease inhibitors were added in appropriate concentrations-phenylmethylsulfonyl fluoride, 0.17 mg/ml; aprotinin, 0.01 trypsin inhibitors units/ ml; leupeptin, 1 μg/ml; pepstatin, 1 μg/ml and chymostatin 1 μg/ml. The homogenizer with the lysed cells was put on ice for 20

minutes. After 20 minutes, the lysate was transferred to a 50 ml centrifuge tube and 0.5 volumes (3 ml) of high salt buffer (50 mM Tris-HCl, pH 7.5/ 1 M KCl/ 2 mM EDTA/ 2 mM DTT) was added. The total 9 ml volume was then subjected to high-speed centrifugation. A Beckman SW 50.1 rotor with six-buckets was used. The initial weight of the buckets was noted down. The extract was divided into equal volumes and transferred to Beckman centrifuge tubes. The buckets were weighed again after placing the tubes in them. The weight of each bucket was balanced against each other to within 0.001 g. the buckets were then transferred to a Beckman ultracentrifuge, which was pre-cooled to 4°C before putting the buckets in. the extract was then centrifuged for 3 hours at 42000 rpm. After 3 hours, the SW 50.1 rotor was removed and the contents showed three distinct layers; a top layer of cellular fat, the second layer of clear supernatant and the third layer of cell debris. The clear supernatant was carefully aspirated out using a 20 G hypodermic needle and a 3 ml syringe. The extract was then transferred to a pre-treated dialysis tubing of M.W. exclusion range between 6000-8000 Dalton and dialyzed for 3 hours in a buffer containing 20 mM Tris-HCl, pH 8.0/ 0.1 M potassium acetate/ 20% (v/v) glycerol/ 0.5 mM EDTA/ 1 mM DTT. The dialyzed extract was then divided into 50 and 100 µl aliquots and transferred to cryo-freeze vials, flash frozen and stored at -70°C until further use. Protein concentration of the extract was determined using the Lowry protein assay. For each batch of extract, an ~ 10-12 mg/ml protein concentration was obtained.

Purification of DNA from non-competent cells using QIAamp DNA Minikit

6 ml LB medium (10 g/L tryptone, 5 g/L yeast extract, 5 g/L NaCl, 1N NaOH, 1M $MgSO_4$ and 1% glucose) containing 25 mg/ml ampicillin with plasmid containing *E.coli* bacterial colony was incubated overnight at 37°C. Bacteria were then pelleted by centrifugation for 10 minutes at 8000 rpm. The bacterial pellet was resuspended in 180 µl ATL buffer to which 20 µl Proteinase K was mixed by vortexing. The mixture was incubated at 56°C in a shaking water bath for 2 hours or until the tissue is completely lysed. The microcentrifuge tube was briefly centrifuged to remove drops from the inside of the lid. 4 µl of 100 mg/ml Rnase A was added and the mixture was mixed by pulse-vortexing for 15 seconds and then incubated for 2 minutes at room temperature. The tube was centrifuged briefly to remove drops and 200 µl buffer AL was added to the sample. The tube was again pulse-vortexed for 15 seconds and incubated for 10 minutes at 70°C. 200 µl of 96-100 % ethanol was added and mixed by pulse-vortexing for 15 seconds. Once again the tube was briefly centrifuged to remove drops. Next, the mixture (including precipitate) was carefully applied to the QIAamp spin column in a collection tube (2 ml) without wetting the rim. The cap was closed and the tube was centrifuged at 8000 rpm for 1 minute. The spin column was placed in a clean collection tube and the tube containing the filtrate was discarded. The spin column was carefully opened and 500 µl of buffer AW1 was added without wetting the rim. . The cap was closed and the tube was centrifuged at 8000 rpm for 1 minute. The spin column was placed in a clean collection tube and the tube containing the filtrate was discarded. 500 µl of buffer AW2 was then added to the spin column without wetting the rim and centrifuged at 14000 rpm for 3 minutes. The spin column was placed in a new 2 ml collection tube and centrifuged at 14000 rpm for 1 minute. Once again the spin column was placed in a clean collection

tube and 200 µl buffer AE was added to the tube which was then incubated at room temperature for 5 minutes and centrifuged at 8000 rpm for 1 minute. The latter elution step was repeated 3 times and finally the purified DNA was stored at in buffer AE at -20°C.

Transfer of pure DNA into XL1-Blue competent cells

Plasmid pHN1910, encoding an amino-terminal histidine-tagged version of the hTdp1 protein sequence, was transformed into competent cells. XL1-Blue competent cells are usually the strain of choice for preparation of high-quality plasmid DNA. For our transfer experiment, 30 µl cells were thawed on ice. 1 µl of DNA purified from non-competent cells was directly pipetted into the competent cells and mixed by tapping gently. The vial was incubated on ice for 5 minutes and then incubated for exactly 30 seconds in a 42°C water bath without mixing or shaking. The vial was removed from the bath and placed on ice. To this mixture, 250 µl of pre-warmed SOC medium (2% tryptone, 0.5% yeast extract, 10 mM NaCl, 2.5 mM KCl, 10 mM $MgCl_2$, 10 mM $MgSO_4$ and 20 mM glucose) was added. SOC is a rich medium and therefore sterile technique was practiced to avoid contamination. The vial was placed in a microcentrifuge rack on its side and secured with tape to avoid loss of the vial. The vial was then incubated at 37°C for exactly 1 hour in a shaking water bath set at 225 rpm. After incubation, 200 µl of the mixture from the vial was spread onto an agar plate pre-treated with 25 mg/ml ampicillin. In order to obtain well-spaced colonies, 1 µl of the mixture was diluted 1:100 with LB medium and then spread on another ampicillin pre-treated agar plate. The plates were inverted and incubated at 37°C overnight. The next day a single colony was selected

and inoculated into 6 ml LB medium and grown overnight at 37 °C. The overnight culture should turn turbid. 1 ml of this overnight culture was then added into I L LB medium (1:1000 dilution), which was pre-treated with 25 mg/ml ampicillin, and grown with vigorous shaking at 37 °C for at least 6 hours. Once turbidity starts to show, an aliquot was removed and the optical density (OD) checked at 600 nm, using LB (with no cells but antibiotic) as a blank. Once the required OD of 0.8- 1.0 has been reached, IPTG (isopropyl-β-D-thiogalactopyranoside) was added to a final concentration of 1 mM. IPTG is a non-metabolisable artificial inducer of the *lac* operon. As a *lac* operon inducer, IPTG has been successfully used to increase the production of recombinant proteins produced in *E. coli*. The culture was allowed to shake vigorously at 37 °C for at least 2 hours. Cells were then pelleted by centrifugation at 4000 x g for 20 minutes at 4 °C and resuspended in buffer containing 20 mM sodium phosphate, pH 7.4. The cell suspension was then sonicated in order to lyse the cells and this suspension was used for purification of recombinant enzyme.

Recombinant hTdp1 was purified using HiTrap Nickel Chelating columns.

HiTrap Chelating, when charged with Ni^{+2} ions, will selectively bind proteins if complex-forming amino acid residues, in particular histidine, are exposed on the surface of proteins, e.g. poly-histidine tagged recombinant proteins. Proteins can be purified directly from bacterial lysates and are recovered from the matrix under mild elution conditions, using imidazole, which preserve antigenicity and functionality of the protein. The properties of the matrix give the opportunity to perform a complete purification in just 10-15 minutes maintaining high selectivity and binding capacity. No special equipment is

required, just a syringe is enough to perform purification. A HiTrap Chelating HP 1 ml column was used for our purification procedure. Prior to use, the column was pre-washed with 5 ml of distilled water using a syringe. For charging with ion, the column was then loaded with 0.5 ml of 0.1 M $NiSO_4$ in distilled water. The column was then washed a second time with 5 ml distilled water to remove any unbound metal ions. Once the sonicated cell suspension containing the recombinant protein was loaded, the columns was washed with 5 ml binding buffer containing 0.02 M sodium phosphate, 0.5 M NaCl and 5 mM imidazole, pH 7.4. Recombinant enzyme was eluted using 5 ml of elution buffer containing 0.02 M sodium phosphate, 0.5 M NaCl and 0.5 M imidazole, pH 7.4. The eluted protein was stored at 4°C.

Cloning of *Tdp1* gene into pFLAG-CMV2 human expression vector

pFLAG-CMV2 human expression vector consists of a FLAG epitope tag that provides a method to localize gene products in living cells, identify associated proteins, track the movement of tagged proteins within a cell, and characterize new genes without creating protein-specific antibodies. Previously, the full length coding sequence of human *Tdp1* was PCR-amplified and cloned into the BamHI sites of the pET-15b expression vector[40], which adds a His-tag and a thrombin cleavage site to the N-terminus of Tdp1 and then transformed into *E.coli.* This pET-Tdp1 plasmid was cut with BsrGI restriction enzyme; the gap filled in and then again cut with BamHI restriction enzyme to release the *Tdp1* gene. The gene was then cloned within the Bgl II and EcoRV sites of the pFLAG-CMV2 vector and the ends ligated with the help of ligase at 16°C for 16 hours. A 0.8% agarose gel was run to check for correct ligation.

Transient Transfection of FLAG-Tdp1 and Untagged-Tdp1 into 293B embryonic kidney cells

Cells were seeded in 10 ml D-MEM/F-12 media from Life Technologies in 150mm dishes until 80% confluence was reached on the day of transfection. Cells were incubated under normal growth conditions (37°C and 5% CO_2). On the day of transfection, a total of 25 µg DNA (FLAG-tagged Tdp1 or Untagged-Tdp1) for 5 plates (5 µg/ plate), dissolved in TE buffer, was diluted with cell growth medium (D-MEM/F-12) containing no serum, proteins, or antibiotics to a total volume of 750 µl. The solution was mixed and spun down for a few seconds to remove drops from the top of the tube. 150 µl of SuperFect Transfection Reagent, purchased from Qiagen, was added to the DNA solution and mixed by pipetting up and down 5 times, or by vortexing for 10seconds. The samples were incubated for 5-10 minutes at room temperature to allow transfection-complex formation. While the complex formation was taking place, the growth medium from the 150 mm dishes was gently aspirated and the cells were washed once with 10 ml PBS. 7.5ml of D-MEM/F-12 medium containing serum and antibiotics was added to the reaction tube containing the transfection complexes, mixed by pipetting up and down twice, and immediately transferred to the cells in the 150 mm dishes. Cells were incubated with the transfection complexes for 2-3 hours on a rotating platform under their normal growth conditions. At the end of the incubation time, the medium containing the remaining complexes was removed by gentle aspiration and fresh cell growth medium containing serum and antibiotics was then added to the dishes and cells incubated for 48-72 hours before purification of Tdp1.

Purification of recombinant Tdp1 protein by Pull-down with Flag Beads and elution with Flag Peptide (by detergent)

Extracts were prepared by first washing recombinant Tdp1 transfected 293B cells from five 150 mm plates, with ice-cold PBS extensively. 4 ml of lysis buffer (10 mM Hepes, 60 mM KCl, 1 mM EDTA, 0.5% NP-40, 0.5 mM PMSF, 0.5 mM DTT, 110 mM $NaNO_4$, 0.5 µg/ml leupeptin, 0.5 µg/ml pepstatin) was added and cells were lysed on ice for 10 minutes. Lysed cells were spun at 2000 rpm for 5 minutes and the pellet containing nuclei was saved. The supernatant was re-spun for 10 minutes at 14000 rpm. After centrifugation, 4 ml TE (10 mM Tris-HCl, 0.1 mM EDTA; pH 8.0) containing protease inhibitors (PMSF, leupeptin, aprotinin, pepstatin) and 80-120 µl of Flag beads (washed with PBS) were added to the supernatant and the reaction incubated at 4°C on a rotating platform for 3 hours. The reaction was spun at 5000 rpm for 6 minutes. The beads were subjected to different washes containing 1X TE alone or 1X TE and 0.15 M NaCl or 0.5 M NaCl or 1 M NaCl or 0.5 M LiCl or a combination of 1X TE, 0.15 M NaCl and 1% Triton or 1X TX, 1 M NaCl and 1% Triton or 1X TX, 0.5 M LiCl and 1% Triton. Beads washed twice with 1 ml 1X TE containing protease inhibitors followed by washing twice with 1 ml TE containing PMSF only were subjected to western blot analyses to look for the co-precipitation of either XRCC1 or Ku with Tdp1. Beads subjected to washes with different salt concentrations followed by washing twice with 1 ml 1X TE containing PMSF were subjected to western blot analyses to look for presence of purified Tdp1 alone. After washing, 200 µl TE containing PMSF, 8 µl Flag peptide (Sigma, stock no.-F3290, concentration-4 mg) and 1 µl 100 µM DTT were added to the beads and

incubated on a shaker at 1200 rpm overnight at 4°C. The reaction was spun at 5000 rpm for 6 minutes and 20% v/v of glycerol was added to the supernatant. Purified Flag-tagged Tdp1 was then stored at -20°C.

Purification of recombinant Tdp1 protein by Pull-down with Flag Beads and elution with Flag Peptide (by dounce homogenization)

Extracts were prepared by washing recombinant Tdp1 transfected 293B cells from five 150 mm plates, with ice-cold PBS three times and once in ice-cold hypotonic lysis buffer containing 10 mM Tris-HCl; pH 8.0, 1 mM EDTA and 5 mM DTT. Cells were resuspended in 2 volume of hypotonic lysis buffer for 20 minutes at 0°C. Cells were then lysed by dounce homogenization (~ 20 strokes with a pestle). To the lysed cells, protease inhibitors (PMSF, leupeptin, aprotinin, pepstatin) were added and incubated for 20 minutes on ice, following which high salt buffer containing 50 mM Tris-HCl; pH 7.5, 1 M KCl, 2 mM EDTA and 2 mM DTT was added. The extract was centrifuged for 1 hour at 15000 rpm and the supernatant was dialyzed over night against E buffer (20 mM Tris-HCl; pH 8.0, 0.1 M KOAc, 20% vol/vol glycerol, 0.5 mM EDTA and 1 mM DTT). The next day, 4 ml TE (10 mM Tris-HCl, 0.1 mM EDTA; pH 8.0) containing protease inhibitors (PMSF, leupeptin, aprotinin, pepstatin) and 80-120 µl of Flag beads (washed with PBS) were added to the supernatant and the reaction incubated at 4°C on a rotating platform for 3 hours. The reaction was spun at 5000 rpm for 6 minutes. The beads were washed twice with 1 ml TE containing protease inhibitors and twice with 1 ml TE containing PMSF only. After washing, 200 µl TE containing PMSF, 8 µl Flag peptide and 1 µl 100 µM DTT were added to the beads and incubated on a shaker at 1200 rpm

overnight at 4°C. The reaction was spun at 5000 rpm for 6 minutes and 20% v/v of glycerol was added to the supernatant. Purified Flag-tagged Tdp1 was then stored at -20°C.

Whole-cell extract preparation from lymphoblastoid cells obtained from SCAN1 patients (JRL1, JRL3, JRL4), from unaffected relatives (JRL2, JRL5) and from known heterozygous carriers (JRL6, JRL7).

The various cell-lines were obtained from Dr. James Lupski, Baylor University. Whole-cell extracts were prepared by growing cells in suspension culture using RPMI 1640 medium containing 10% FCS until a cell density of 2.5 to 5.0 x 10^5 cells/ml was reached. After extensive washing with PBS, the cells were incubated in 2 volume (pellet volume) hypotonic buffer (10mM Tris-HCl (pH 7.0), 1mM EDTA, 5mM DTT) for 20 minutes at 0°C to induce cell swelling. The cells were subjected to mechanical shearing by the use of a Dounce homogenizer. After 10-20 strokes, protease inhibitors (PMSF, leupeptin, pepstatin) were added and incubated for 20 minutes on ice. 0.5 volume high salt buffer (50mM Tris-HCl (pH 7.5), 1M KCl, 2mM EDTA, 2mM DTT) was added and centrifuged for 1 hour at 15000rpm. The supernatant was subjected to overnight dialysis at 4°C with E-buffer (20mM Tris-HCl (pH 8.0), 0.1M KOAc, 20% v/v glycerol, 0.5mM EDTA, 1mM DTT). Following dialysis, the extract was aliquoted and fast-frozen using liquid nitrogen to be stored at -70°C.

Gel Filtration Chromatography and end-processing assays with GM00558B fractions

Gel filtration was performed using a pre-packed 1.6 cm x 60 cm (190 ml bed volume) Sephacryl S-300 column (Pharmacia). The column was set up in the cold room and pre-washed with 2 column volumes (120 ml) of end-joining buffer (50 mM triethanolamine HCl/ 60 mM KOAc/ 0.5 mM magnesium acetate/ 2 mM ATP/ 1 mM DTT/ 100 μg/ml BSA). Glycerol was omitted from the end-joining buffer in order to reduce column flow pressure and facilitate column flow. The column was connected to a peristaltic pump whose rate was set such that 1 ml fractions were collected every seven minutes. Degassed and filtered buffer was pumped through the column. Prior to loading the extract, a standard curve was obtained using molecular weight markers (Bio-Rad) ranging from 1.7 kDa to 650,000 kDa. Five peaks corresponding to five different color-coded markers were recorded. Next, the column was again washed with 1 column volume of end-joining buffer before loading the extract. 1 ml of undiluted human lymphoblastoid cell extract (10 mg/ml) was thawed at 37°C for 5 minutes followed by microcentrifugation at 10,000 rpm for 5 minutes to remove any debris in the extract. Debris-free extract was then loaded onto the column and elution buffer containing 20 mM Tris-HCl, pH 7.5/ 0.1 M KOAc/ 0.5 mM EDTA/ 1 mM DTT, 2 mM ATP/ and 100 μg/ml BSA was applied with a peristaltic pump at 0.14 ml/min. A_{280} was recorded and 2 ml fractions were collected overnight and stored at 4°C.

End-processing assays with the fractions (10 μl) showing peak-enzyme activities were performed using 6 μl of each fraction in buffer containing 20 mM triethanolamine-HCl, pH 7.5/ 60 mM KOAc/ 0.5 mM magnesium acetate/ 2 mM ATP/ 1 mM DTT/ 100 μg/ml BSA and 20% (v/v) glycerol. The reaction buffer contained 0.5 mM EDTA, and therefore the magnesium acetate concentration in the reactions was adjusted so that the

final free Mg^{+2} concentration would be 0.5 mM. In some experiments Mg^{+2} was completely eliminated and instead, various concentrations of EDTA were used. 20 fmol of 3′-PG ss-14 mer or 3′-phosphotyrosine ss-18 were used for the reactions. Following incubation at 37°C for 2 hours, the oligomeric substrate was diluted with one volume of formamide containing 40 mM EDTA and electrophoresed on 20% denaturing polyacrylamide-sequencing gels. Phosphorimages were analyzed with ImageQuant 3.3 (molecular dynamics).

End-processing assays of a double-stranded substrate with a 3'-PG overhang by Ku, DNA-PK and XRCC4-ligase IV.

A double-stranded substrate with a 3'-PG overhang was pre-incubated with various dilutions of recombinant Ku or Ku-DNA-PK complex for 5 minutes at 25 °C to allow binding to the open end of the substrate followed by incubation with a 1:512 dilution (0.098 ng) of hTdp1 (diluted using Pouliot dilution buffer containing 50 mM Tris-HCl, pH 8.0/ 5 mM DTT/ 100 mM NaCl/ 5 mM EDTA/ 10% glycerol/ 500 μg/ml BSA) for 10 minutes at 37 °C to allow PG-processing. If XRCC4-ligase IV was to be added, it was added after pre-incubation with the Ku-DNA-PK complex and before addition of Tdp1 (and pre-incubated for 5 minutes at 25°C). End-processing assays of the double-stranded substrate with a 3'-PG overhang by Ku were carried out in Kedar buffer containing 20 mM triethanolamine-HCl, pH 7.5/ 60 mM KOAc/ 0.5 mM magnesium acetate/ 2 mM ATP/ 1 mM DTT/ 100 μg/ml BSA and 20% (v/v) glycerol. 3 M sodium acetate and 1 mg/ml tRNA were added to final concentrations and samples were then subjected to phenol/chloroform extraction. After extraction of Ku, samples were

dissolved in 1X TE. NEB buffer 4 and 40 µg/ml PNKP were added and samples incubated for 1 hour at 37 °C. Mg^{+2} was not added separately as it was already present in the reaction buffer. *AvaI* was added and samples were incubated for 3 hours at 37 °C to yield a 15-mer with the 3'-OH. The samples were then electrophoresed on 20% denaturing polyacrylamide-sequencing gels. Phosphorimages were analyzed with ImageQuant 3.3 (molecular dynamics).

. End-processing assays consisting of DNA-PK alone, Ku-DNA-PK complex and Ku-DNA-PK-XRCC4/ligaseIV complex were carried out in Ramsden buffer containing 25 mM Tris-HCl, pH 7.5/ 50 µg/ml BSA/ 45 mM KCl/ 105 mM NaCl/ 0.05% Triton X-100/ 0.1 mM EDTA/ 2 mM DTT. If the Ramsden buffer was used, 0.2µl of a mixture of 100µM ATP and 5 mM $MgCl_2$ was added as required along with the hTdp1. For experiments conducted without ATP, $MgCl_2$ was also not added. Following boiling of the samples at 90°C for 2 minutes, the substrate was incubated with 1 µl of 1000 units/ mL alkaline phosphatase (CIP) for 1 hour at 37°C for removal of 3'-terminal phosphate group. The samples were again heated at 90°C for 5 minutes and then incubated with 1 µl *Taq*$^{\alpha}$*I* (20,000 units/ml) for 3 hours at 65°C to yield a 15-mer with the 3'-OH. The samples were then electrophoresed on 20% denaturing polyacrylamide-sequencing gels. Phosphorimages were analyzed with ImageQuant 3.3 (molecular dynamics).

Western Blotting

10% SDS-polyacrylamide gels were used for western blotting. A large and a small glass plate were cleaned with 70% ethanol and dried with kim-wipes and aligned in a gel caster. Resolving gel (20ml) was prepared with 8.8 mL milliQ water/ 4.2 mL1.5 M

Tris-HCl, pH 8.8/ 6.6 mL 30% acrylamide/ 166 µL 10% SDS/ 166 µL 10% ammonium persulfate and 67 µL TEMED. Stacking gel (3 mL) was prepared with 2.1 mL milliQ water/ 0.5 mL 30% acrylamide/ 0.38 mL 1 M Tris-HCl, pH 6.8/ 30 µL 10% SDS/ 30 µL 10% ammonium persulfate and 3 µL TEMED. 10 µl aliquots of whole-cell extracts or purified Tdp1 were mixed with 2 µl 5X sample buffer containing 1 M Tris, pH 6.8/ 5 % glycerol/ 10% SDS/ 5 % β-mercaptoethanol/ 2% bromophenyl blue, denatured by boiling for 5 minutes and electrophoresed on the 10% SDS-polyacrylamide gel in running buffer containing 25 mM Tris base/ 250 mM glycine and 0.1 % SDS. Electrophoresis was carried out at 100V for the first 8 minutes followed by 200V for the next 40 minutes. The gel was removed and the stacking gel cut off. The resolving gel was then put into transfer buffer containing 25 mM tris base/ 192 mM glycine and 20% methanol. The 'transfer sandwich' was assembled from the black side of the cassette to the white side with sponge, Whatman filter paper, the gel followed by nitrocellulose membrane followed again by Whatman filter paper and finally by another sponge. The sandwich was put into the transfer box, black side to back. A spacer pack frozen at -20°C was also put into the transfer box. Transfer buffer was poured in and the transfer was carried out at 100V for ~2 hours. Following transfer, the nitrocellulose membrane was stained with Ponceau S stain to check for completion of transfer. The dye was rinsed off with distilled water and the membrane was transferred into blotto solution made up of 10 mM Tris, pH 7.4, NaCl and 5% non-fat dry milk. The membrane was blocked in blotto overnight at 4°C with continuous rocking. Next day, the respective primary antibodies were mixed in fresh blotto (Table 1). Incubation with primary antibody was carried out at room temperature for ~2 hours with continuous rocking. The primary antibodies were washed off twice

using 20 mL Blotto wash containing 0.05% Nonidet P-40 and 1X PBS. Each wash was carried out for 15 minutes. The membrane was then incubated with the required secondary antibody for 1 hour at room temperature. The blot was then subjected to two washes, each for 15 minutes, with 20 mL Tris-Buffered Saline (TBS)-Tween 20. For chemi-luminescence, 500 µl of each of the two super signal solutions (Pierce, Rockford, IL) were mixed and the blot was exposed to the solution for about 1 minute followed by autoradiography.

TABLE 1.

PRIMARY ANTIBODY	DILUTION USED	VOLUMES FOR INCUBATION	SECONDARY ANTIBODY	DILUTION USED	VOLUMES FOR INCUBATION
Rabbit anti-hTdp1 (Abcam Inc.; Cat No.- ab4166)	1:1000	10 µl in 10 mL	Goat anti-rabbit	1:10,000	1 µl in 10 mL
Mouse Anti-FLAG (Sigma; Cat No.- F-3165)	1:2000	5 µl in 10 mL	Anti-mouse	1:5000	2 µl in 10 mL
Rabbit anti-Ku 70 (Serotec Inc.; Cat No.- AHP316)	1:2000	5 µl in 10 mL	Goat anti-rabbit	1:10,000	1 µl in 10 mL
Mouse Anti-XRCC1 (NeoMarkers; Cat No.- MS-434-P1)	1:1000	10 µl in 10 mL	Anti-mouse	1:5000	2 µl in 10 mL
Rabbit anti-XRCC4 (GeneTex, Inc.; Cat No.- GTX12069)	1:1000	10 µl in 10 mL	Goat anti-rabbit	1:10,000	1 µl in 10 mL

Results

Tyrosyl-DNA phosphodiesterase (Tdp1) is capable of removing glycolate from 3′-PG overhangs.

Tdp1 is the only enzyme known so far to convert any 3′-blocked termini to 3′-phosphates. The first report of an activity that cleaves a 3′-tyrosyl-phosphodiester bond was reported in 1996. Using column chromatography, Yang et al partially purified this activity from crude extracts of budding yeast *S. cerevisiae* as a ~55 kDa enzyme independent of any cofactor requirement to function. The enzyme specifically cleaved the phosphodiester bond that connected the 3′-end of DNA to a tyrosine in the active site of topoisomerase I enzyme, thus liberating a 3′-phosphate ended DNA molecule (Yang et al., 1996). Such linkages are formed as intermediates during DNA relaxation by topoisomerase I, and in DNA cleavage and reunion by various recombinases. These intermediates can become trapped if the process is interrupted, *e.g*., by a topisomerase inhibitor or by collision with a replication fork. The hypersensitivity of *tdp1* mutant yeast to topoisomerase I-mediated DNA damage (Pouliot et al., 1999) suggests a critical role for scTdp1 in repair of such lesions. Later, a gene (*TDP1*) encoding this enzyme was identified in yeast, which was conserved in eukaryotes. Analysis of single and double mutants of *TDP1* and *RAD52* suggests that both belong to the same epistasis group while *TDP1* and *RAD9* belong to different groups (Pouliot et al., 2001). A human homologue with similar 3′-phosphotyrosyl- processing activity, hTdp1, was cloned by homology to scTdp1 and was eventually shown to have some homology to the phospholipase D (PLD) superfamily of phosphodisterases (Interthal et al., 2001). Yeast and human Tdp1 differ from other activities for processing blocked 3′ ends in that they leave a 3′-phosphate

Figure 1: 3'-PG (·) and 3'-phosphotyrosine (*p-Tyr*) substrates.

The 3'-PG oligomers were prepared by bleomycin treatment of partial duplexes**.**
* indicate the site of the ^{32}P label. The plasmid substrate is 5.5kb in length.

Figure 1

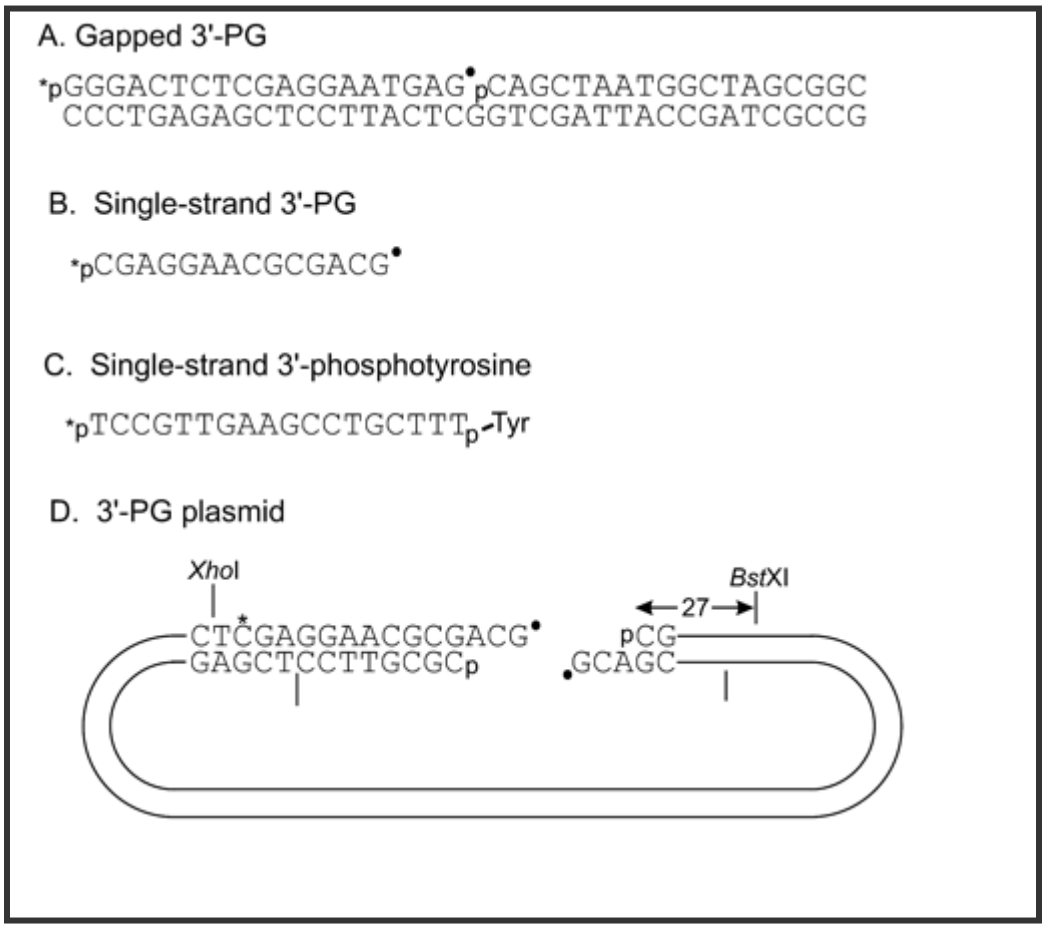
A. Gapped 3'-PG
*pGGGACTCTCGAGGAATGAG•pCAGCTAATGGCTAGCGGC
CCCTGAGAGCTCCTTACTCGGTCGATTACCGATCGCCG
B. Single-strand 3'-PG
*pCGAGGAACGCGACG•
C. Single-strand 3'-phosphotyrosine
*pTCCGTTGAAGCCTGCTTTp-Tyr
D. 3'-PG plasmid
XhoI
BstXI
27
CTCGAGGAACGCGACG•
GAGCTCCTTGCGCp
pCG
•GCAGC

Figure 2: Conversion of 3'-phosphotyrosine termini to 3'-phosphate termini by native hTdp1.

20fmol of 3'-phosphotyrosine 18-mer was treated with 6µl Sephacryl fractions 20-40 from human whole-cell extracts in Kedar buffer containing 20 mM triethanolamine-HCl, pH 7.5/ 60 mM KOAc/ 5 mM EDTA/ 2 mM ATP/ 1 mM DTT/ 100 µg/ml BSA and 20% (v/v) glycerol. Samples were incubated for 2 hours at 37°C and conversion to 3'-phosphate was assessed by denaturing gel electrophoresis. Fractions 27-30 showed 100% conversion to 3'-phosphate.

Figure 2

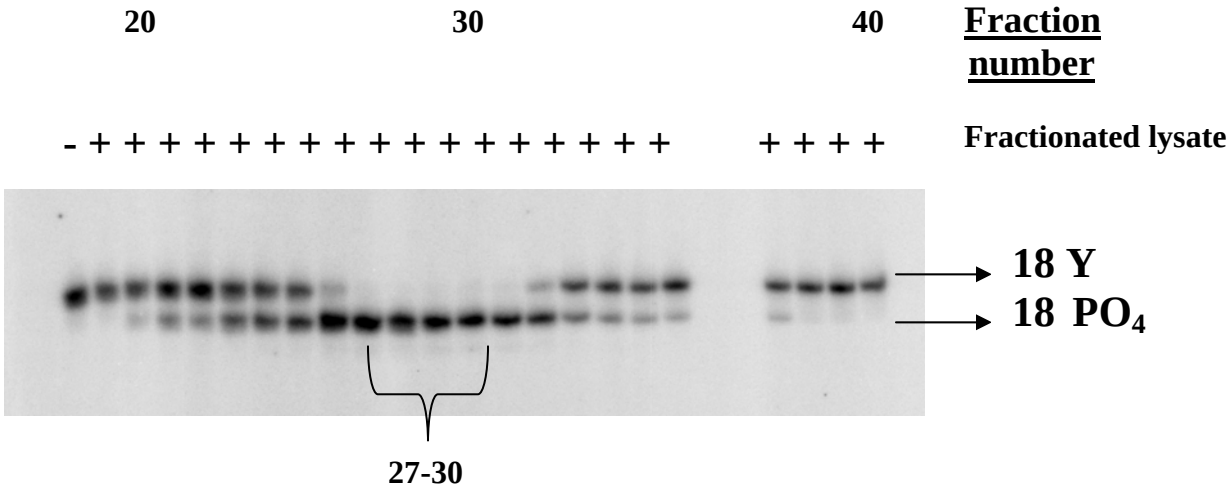
20
30
40
Fraction number
- +
Fractionated lysate
18 Y
18 PO4
27-30

rather than a 3′-hydroxyl. To determine whether the activity for removal of glycolate from single-stranded 3′-PG termini in human cell extracts might be hTdp1, we fractionated extracts by gel filteration chromatography on Sephacryl S-300 (Inamdar et al., 2002). A prominent peak of glycolate-removing activity was found to colelute with hTdp1 protein as detected with hTdp1 antiserum at a position approximately midway between the 44- and 158-kDa markers. In the presence of EDTA, this fraction was found to catalyze the 3′-PG-to-3′-phosphate conversion with no detectable formation of 3′-hydroxyl (Figure 3).

No evidence of multiple forms of the enzyme separable by the sephacryl column

Previously in our laboratory, titration of the activity in the peak fraction showed that it processed a 3′-phosphotyrosine oligomer 8-fold more efficiently than a plasmid containing PG-terminated 3′-overhang (Figure 4), consistent with its identification as hTdp1 (Inamdar et al., 2002). However, the peak of PG-processing activity seemed to be slightly shifted from the peak of hTdp1 as detected with an antibody, raising the possibility of multiple forms with differing PG-processing efficiencies. To determine whether this difference in processing efficiencies was due to the presence of different splice forms of hTdp1, we duplicated the above experiment and four fractions showing peak activity were chosen. The plasmid containing the 3′-PG terminated single-strand overhang was replaced by a 3′-PG containing 14-mer. Titration experiments using each of the 4 fractions showed that hTdp1 processed the 3′-phosphotyrosine containing 18-mer 10-fold more efficiently than the 3′-PG containing 14-mer (Figure 5). Since the Sephacryl S-300 column separates different fractions based on size, we conclude that there was no evidence of splice variants or other multiple forms of the enzyme.

Figure 3: Conversion of 3'-PG termini to 3'-phosphate termini by native hTdp1.

20 fmol of 3'-PG 14-mer was treated with 6µl Sephacryl fractions 24-35 in Kedar buffer containing 20 mM triethanolamine-HCl, pH 7.5/ 60 mM KOAc/ 5 mM EDTA/ 2 mM ATP/ 1 mM DTT/ 100 µg/ml BSA and 20% (v/v) glycerol. Samples (a total volume of 10 µl) were incubated for 2 hours at 37°C and conversion to 3'-phosphate was assessed by denaturing gel electrophoresis.

Figure 3

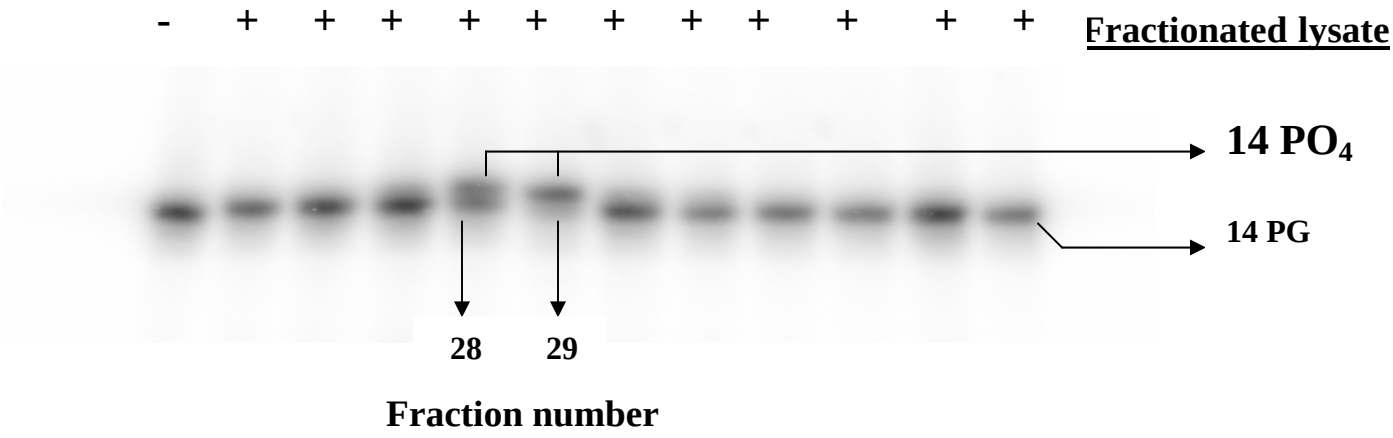

Figure 4: Relative efficiency of native end-processing activities

A 3'-phosphotyrosine 18-mer (▲) or a plasmid with a PG-terminated 3'-overhang (●) was treated with 4 µl of undiluted, followed by 1 µl of seven 1:4 dilutions of sephacryl fraction 30 from human whole-cell extracts. Each substrate was incubated at 37 ºC for 2 hours in Kedar buffer containing 5 mM EDTA and no Mg^{2+} (see Fig. 2). Conversion to 3'-phosphate was assessed by denaturing gel electrophoresis and quantified using ImageQuant software. The difference in relative end-processing efficiency was found to be approximately 8-fold.

Figure 4

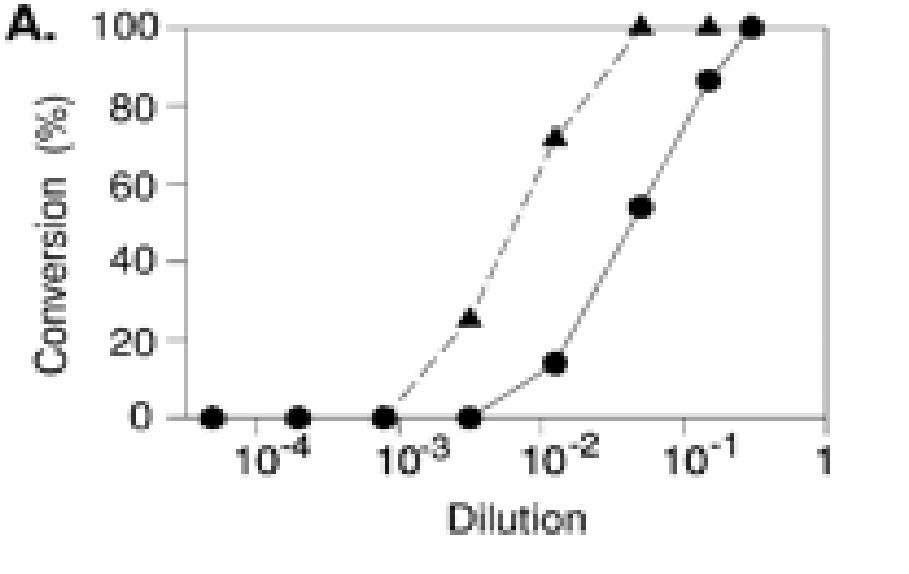

Figure 5: Relative efficiencies of native end-processing activities.

A 3'-phosphotyrosine 18-mer (○) or a 3'-PG 14-mer (●) was treated with 4 µl of undiluted, followed by 1 µl of seven 1:4 dilutions of sephacryl fractions 27-30. Each substrate was incubated at 37 ºC for 2 hours in Kedar buffer containing 5 mM EDTA and no Mg^{2+}. Conversion to 3'-phosphate was assessed by denaturing gel electrophoresis and quantified using ImageQuant software. The difference in end-processing efficiencies between the two substrates was found to be approximately 10-fold in each of the four fractions.

Figure 5

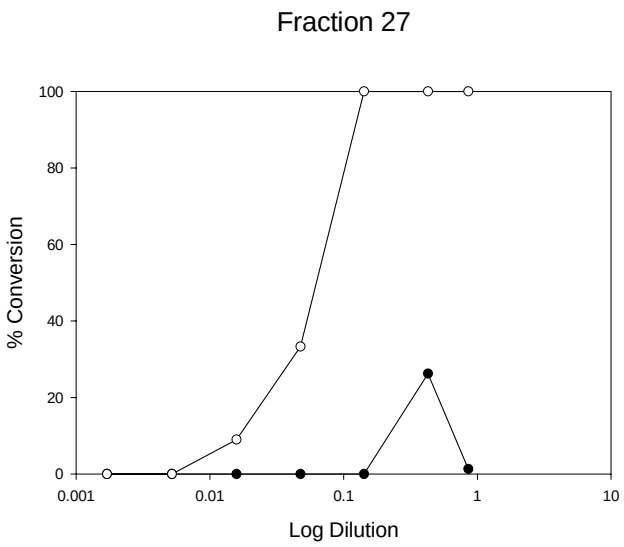
Fraction 27
% Conversion
Log Dilution
0
20
40
60
80
100
0.001
0.01
0.1
1
10


Fraction 28
% Conversion
Log Dilution
0
20
40
60
80
100
0.001
0.01
0.1
1
10

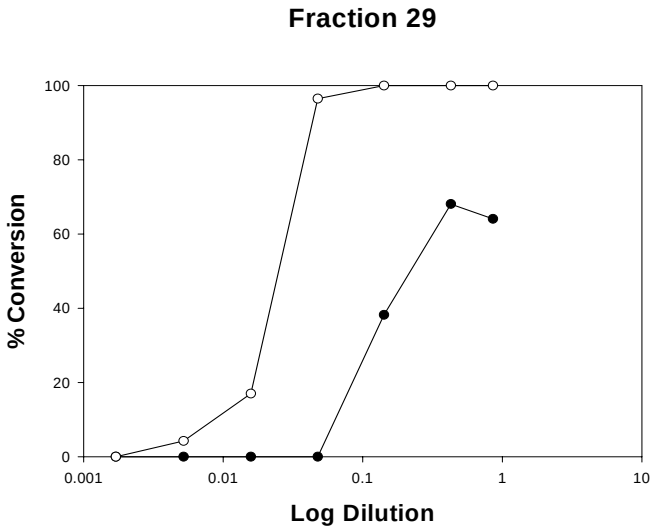
Fraction 29
% Conversion
Log Dilution
0
20
40
60
80
100
0.001
0.01
0.1
1
10

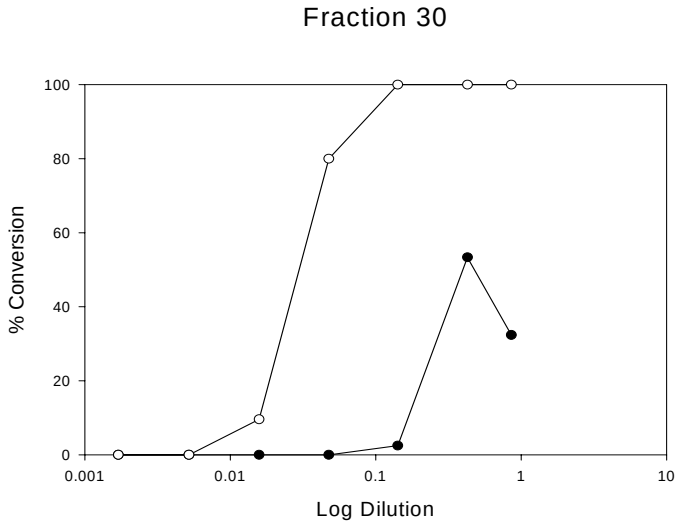
Fraction 30
% Conversion
Log Dilution
0
20
40
60
80
100
0.001
0.01
0.1
1
10

Processing efficiency of scTdp1 is affected by various factors

Previously, experiments using scTdp1 showed that, compared with its hydrolysis of a 3′-phosphotyrosine residue, scTdp1 or yTdp1 removed 3′-PG very inefficiently (Pouliot et al., 2002). When a mixture containing roughly equimolar amounts of an 18-mer containing 3′-phosphotyrosine and a 21-mer containing 3′-PG was incubated with scTdp1 at 30°C for 20 minutes in buffer without EDTA, the 21-mer terminating in 3′-PG required at least a 50-fold higher concentration of the enzyme to achieve a comparable initial rate and at least a 100-fold increase in concentration to achieve a 50% conversion rate. Based on these results, our laboratory decided to compare the processing efficiencies of an 18-mer containing 3′-terminal phosphotyrosine with a 14-mer containing a terminal 3′-PG and a 19-mer containing a 3′-PG. In comparison to the experimental conditions used by Pouliot et al., we incubated the substrates with the recombinant scTdp1 for 2 hours at 37°C in buffer containing EDTA (as was carried out by our laboratory with hTdp1). The results showed that under these conditions, the difference between the processing efficiencies of the 18-mer with 3′-phosphotyrosine and the 3′-PG containing substrates was lesser (~ 10-fold) and both the 14-mer and the 19-mer containing terminal 3′-PG achieved 50% conversion of the substrate with approximately the same concentration of the enzyme suggesting that the size of the substrate did not affect the processing efficiency of recombinant yeast Tdp1 (Figure 6a). We next conducted two sets of experiments in which one set containing a mixture of the 18-mer with phosphotyrosine, 14-mer with 3′-PG and the 19-mer with 3′-PG was incubated with scTdp1 for 20 minutes at 30°C, heated for 1 minute at 90°C, treated with 20 ng hPNKP, again incubated for 1 hour at 37°C and electrophoresed on a denaturing polyacrylamide

gel. hPNKP, a Mg^{+2} dependent enzyme, was added for conversion of 3′-phosphate to 3′-OH which separates much better from 3′-PG on sequencing gels . The second set consisted of a mixture of another 19-mer with terminal 3′-PG and scTdp1 supplemented with 20 ng hPNKP that was incubated for 20 minutes at 30°C, heated for 1 minute at 90°C and then electrophoresed on a denaturing polyacrylamide gel. Both the sets of reactions were carried out in buffer containing a final concentration of 0.5 mM $MgCl_2$ and without EDTA. Our results showed that under these different conditions, the 18-mer with terminal 3′-phosphotyrosine was processed ~20-fold more efficiently than the 14-mer containing terminal 3′-PG (when compared to the ~ 10-fold difference in our previous experiment). Also, there was at least an 8-fold difference in the processing efficiencies between the 14-mer and 19-mer 3′-PG substrates making the processing difference between the 3′-tyrosine substrate and 3′-PG containing 19-mer ~100-fold (Figure 6b). All these data suggested that the relative efficiency of the yeast enzyme was affected by different experimental conditions such as temperature and time of incubation. It was shown previously that both human and yeast recombinant enzymes converted 3′-PG termini to 3′-phosphate termini in either the presence or absence of Mg^{+2} (Inamdar et al., 2002). However, omitting EDTA from the buffer and adding Mg^{+2} in our experiments was also found to affect the activity of scTdp1. The combination of buffer, temperature and oligo length effects can explain the apparent disparity between our results (Inamdar et al., 2002) and results from Pouliot et al. (2002).

Recombinant human Tdp1 shows relatively lower 3′-PG removal activity than partially purified native hTdp1

Figure 6: Relative end-processing efficiencies of recombinant scTdp1.

6a- 28, 7, 1.75, 0.44, 0.11, 0.027, 0.0068 or 0.0017 ng of recombinant yeast Tdp1 was incubated with 3'-phosphotyrosine 18-mer (■) or a 3'-PG 14-mer (▲) or a 3'-PG 19-mer (♦) in end-joining Kedar buffer containing EDTA for 2 hours at 37 °C. Conversion to 3'-phosphate was analyzed by PAGE and results were quantified using ImageQuant software.

6b- 28, 7, 1.75, 0.44, 0.11, 0.027, 0.0068 or 0.0017 ng of recombinant yeast Tdp1 was treated with 3'-phosphotyrosine 18-mer (○) or a 3'-PG 14-mer (●) or a 3'-PG 19-mer (▲), incubated at 30 °C for 20 mins in Kedar buffer and heated at 90°C for 1 min. 20 ng of human PNKP was added and samples were incubated at 37°C for 1 hour and analyzed by gel electrophoresis. A second 19-mer with 3'-PG (Δ) was treated with both yeast Tdp1 and hPNKP together and incubated at 30 °C for 20 mins before being analyzed. EDTA was not present; instead a final concentration of 0.5 mM $MgCl_2$ was added to the buffer.

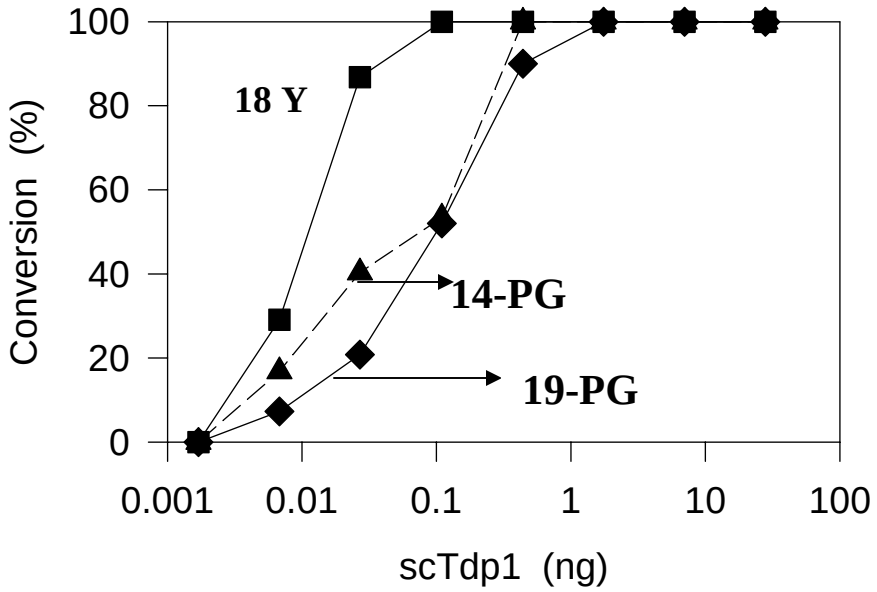

Figure 6a

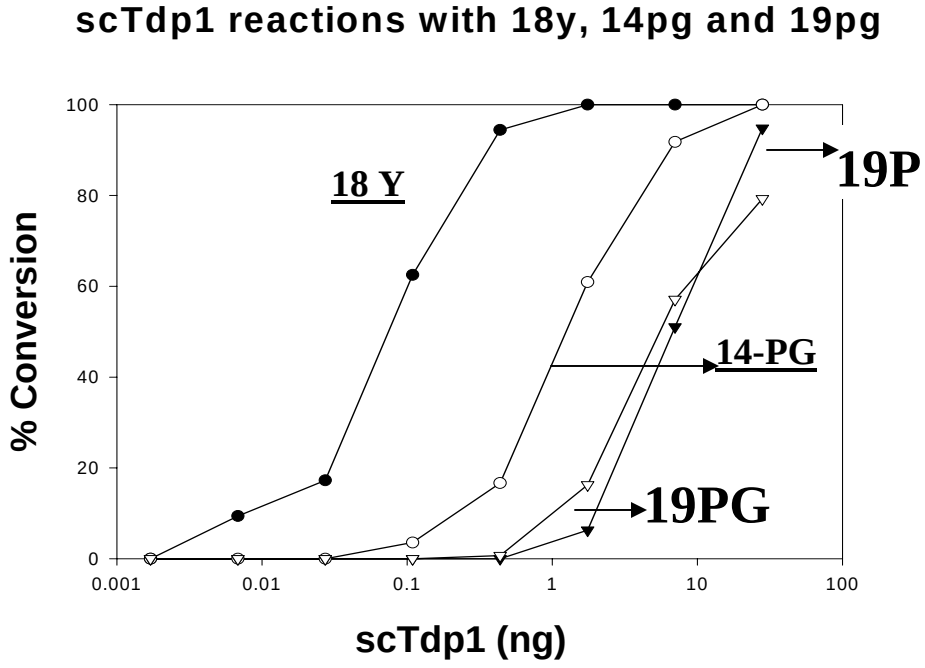

Figure 6b

Previously, experiments conducted to determine the efficiency of the processing of 3′-PG termini by hTdp1 using a 3′-phosphotyrosine DNA oligomer and a DSB substrate with a PG-terminated 3′-overhang treated with various concentrations of the recombinant His-tagged hTdp1, grown in *E.coli*, showed that the 3′-PG substrate required an ~80-fold greater concentration of recombinant hTdp1 for half-maximal conversion than did the 3′-phosphotyrosine oligomer, more than would have been expected based on the activities in fractionated extracts (Inamdar et al., 2002). This difference in relative preference for 3′ phosphotyrosine over 3′-PG substrates, 80-fold for purified recombinant hTdp1 *versus* 10-fold for native activity in extracts, raised the question of whether most of the native PG-processing activity might be attributable to some functionally similar but distinct enzyme. While this possibility has not been completely eliminated, it seems unlikely, as such an enzyme would have to precisely co-elute with hTdp1 from the Sephacryl S-300 column and would also have to cross-react with antibody against the recombinant hTdp1 to explain immunodepletion data observed previously (Inamdar et al., 2002). To determine whether this difference in processing efficiencies was due to degradation of the enzyme (provided by Dr. Jeff Pouliot, NIMH) during its shipping and/or its freezing and thawing, we purified recombinant hTdp1 in our laboratory using Amersham Hi-Trap nickel chelating columns and repeated the experiment. Our results still showed a 100-fold difference in the processing activities (Figure 7) suggesting that the different substrate preferences may likely be attributable to other factors such as the presence of the histidine tag, interactions with other proteins in the fractionated extract that may enhance activity or differences in post-translational modification in human *versus* bacterial cells.

Figure 7: Relative end-processing efficiency of recombinant hTdp1

A 3'-phosphotyrosine 18-mer (○) or a 3'-PG 14-mer (●) was treated with 4 µl of undiluted, followed by 1 µl of six 1:4 dilutions of recombinant His-tagged hTdp1, purified from *E.coli*. Each substrate was incubated at 37 ºC for 2 hours in Kedar buffer containing 5 mM EDTA and no Mg^{2+}. Conversion to 3'-phosphate was assessed by denaturing gel electrophoresis and quantified using ImageQuant software. The relative end-processing efficiency was found to be approximately 100-fold.

Figure 7

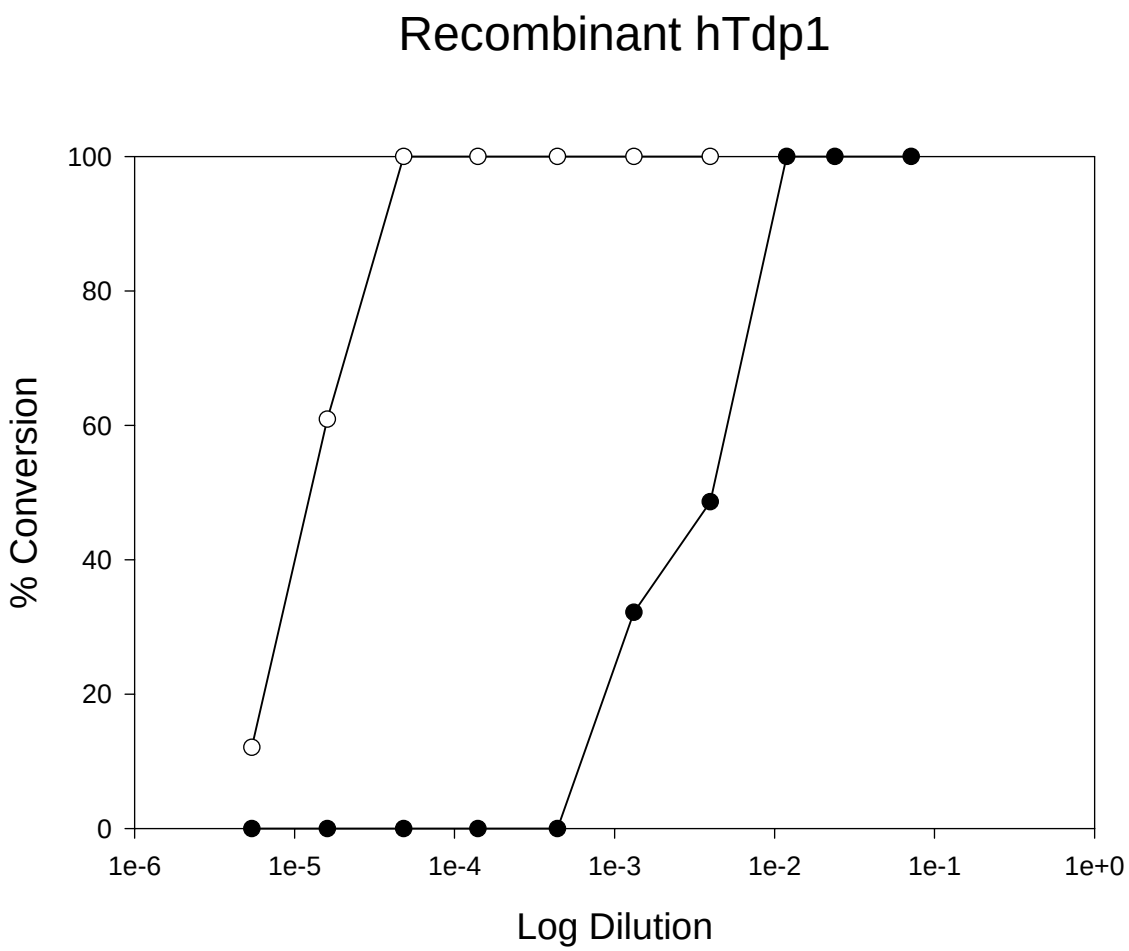
Recombinant hTdp1
% Conversion
100
80
60
40
20
0
1e-6
1e-5
1e-4
1e-3
1e-2
1e-1
1e+0
Log Dilution

No evidence of the Flag peptide having any effect on the specificity of the enzyme

To assure that hTdp1 has normal post-translational modification and also to avoid any inactivation due to exposure of the enzyme to the nickel column (as was seen with PNKP; M.Weinfeld, personal communication), our laboratory cloned the *Tdp1* gene into the human expression vector, pFLAG-CMV2 (Figure 9). The pFLAG-CMV2 vector consists of a FLAG epitope tag that provides a method to localize gene products in living cells, identify associated proteins, track the movement of tagged proteins within a cell and characterize new genes without creating protein-specific antibodies. Untagged Tdp1 was cloned into pCMV-M human expression vector and used as a negative control for our experiment. The pFLAG-CMV2 vector containing the cloned *Tdp1* gene was transfected into 293B embryonic kidney cells, and overexpressed hTdp1 protein was purified using FLAG beads and eluted with FLAG peptide (Figures 11a and b). Untagged-Tdp1 was also cloned into pCMV-Tag1 human expression vector (Figure 10), transfected, purified and used as a negative control for our experiment. We carried out a western blot analysis that showed a high and approximately equal expression of Tdp1 in whole cell extracts from cells with both FLAG-tagged Tdp1 and Untagged-Tdp1. We also observed recovery of FLAG-tagged hTdp1 and no recovery of Untagged-hTdp1 after purification with FLAG beads suggesting that only the tagged protein was bound to and eluted from the beads as expected (Figure 11c). When the processing efficiencies of whole cell extracts containing either FLAG-tagged Tdp1 or Untagged-Tdp1 were compared, we observed about the same 100-fold difference in processing efficiencies for 3'-PG and 3'-phosphotyrosine oligomers as with recombinant hTdp1 purified from Hi-

Figure 8: The pET-15b *E.coli* vector; the source for His-tagged *Tdp1* gene.

Figure 8

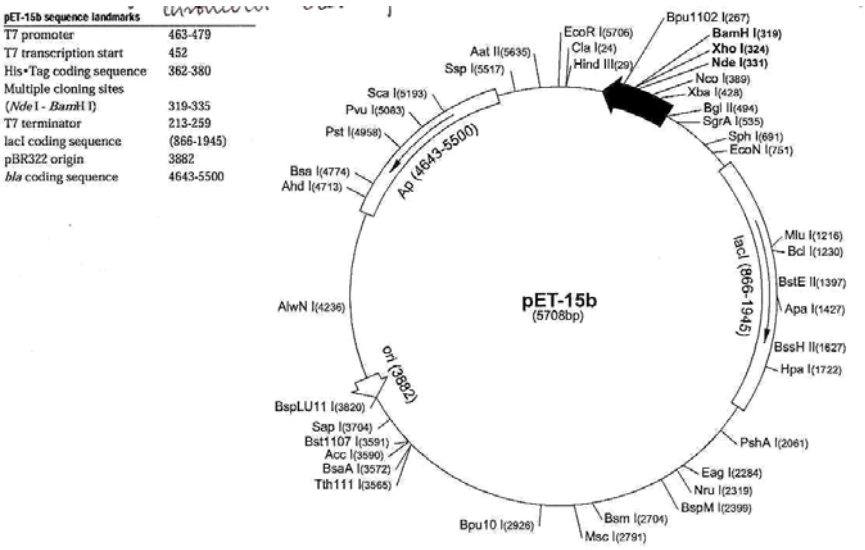
pET-15b sequence landmarks
T7 promoter 463-479
T7 transcription start 452
His•Tag coding sequence 362-380
Multiple cloning sites
(NdeI - BamH I) 319-335
T7 terminator 213-259
lacI coding sequence (866-1945)
pBR322 origin 3882
bla coding sequence 4643-5500
pET-15b
(5708bp)
Bpu1102 I(267)
BamH I(319)
Xho I(324)
Nde I(331)
Nco I(389)
Xba I(428)
Bgl II(494)
SgrA I(535)
Sph I(691)
EcoN I(751)
Mlu I(1216)
Bcl I(1230)
BstE II(1397)
Apa I(1427)
BssH II(1627)
Hpa I(1722)
PshA I(2061)
Eag I(2284)
Nru I(2319)
BspM I(2399)
Bsm I(2704)
Msc I(2791)
Bpu10 I(2926)
BspLU11 I(3820)
Sap I(3704)
Bst1107 I(3591)
Acc I(3590)
BsaA I(3572)
Tth111 I(3565)
AlwN I(4236)
Bsa I(4774)
Ahd I(4713)
Pst I(4958)
Pvu I(5083)
Sca I(5193)
Ssp I(5517)
Aat II(5635)
EcoR I(5706)
Cla I(24)
Hind III(29)
lacI (866-1945)
Ap (4643-5500)
ori (3882)

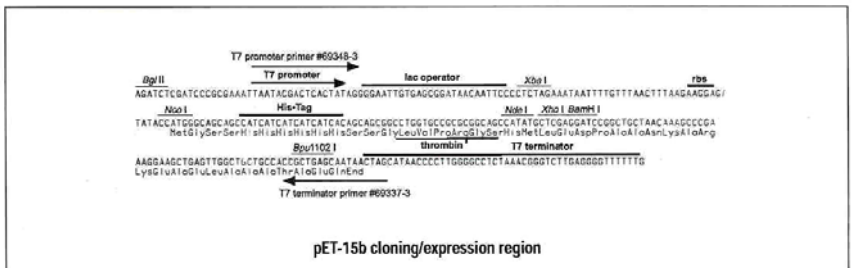
T7 promoter primer #69348-3
T7 promoter
lac operator
rbs
Bgl II
Xba I
Nco I
His-Tag
Nde I
Xho I
BamH I
thrombin
T7 terminator
Bpu1102 I
T7 terminator primer #69337-3
pET-15b cloning/expression region

Figure 9a: The pFLAG-CMV2 human expression vector used for cloning *Tdp1* gene.

Figure 9b: Protocol for cloning.
Tdp1 insert was excised from pET 15-Tdp1 as a Bam HI-BsrGI fragment, filled in with BsrGI and cloned into the BglII and EcoRV sites of the vector to give rise to a plasmid encoding FLAG-tagged Tdp1, designated as pCMV-FLAG-Tdp1.

Figure 9a

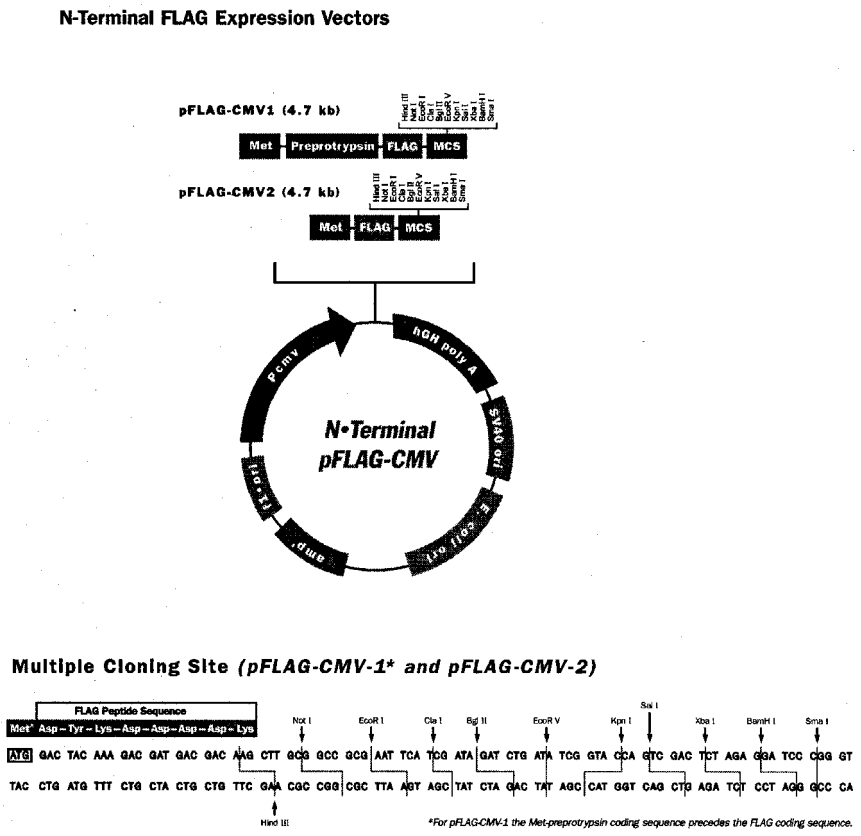
N-Terminal FLAG Expression Vectors
pFLAG-CMV1 (4.7 kb)
Met
Preprotrypsin
FLAG
MCS
pFLAG-CMV2 (4.7 kb)
Met
FLAG
MCS
hGH poly A
SV40 ori
f1 ori
Amp
N•Terminal
pFLAG-CMV
Multiple Cloning Site (pFLAG-CMV-1* and pFLAG-CMV-2)
FLAG Peptide Sequence
Met* Asp – Tyr – Lys – Asp – Asp – Asp – Asp – Lys
Not I
EcoR I
Cla I
Bgl II
EcoR V
Kpn I
Sal I
Xba I
BamH I
Sma I
ATG GAC TAC AAA GAC GAT GAC GAC AAG CTT GCG GCC GCG AAT TCA TCG ATA GAT CTG ATA TCG GTA CCA GTC GAC TCT AGA GGA TCC CGG GT
TAC CTG ATG TTT CTG CTA CTG CTG TTC GAA CGC CGG CGC TTA AGT AGC TAT CTA GAC TAT AGC CAT GGT CAG CTG AGA TCT CCT AGG GCC CA
Hind III
*For pFLAG-CMV-1 the Met-preprotrypsin coding sequence precedes the FLAG coding sequence.

Figure 9b

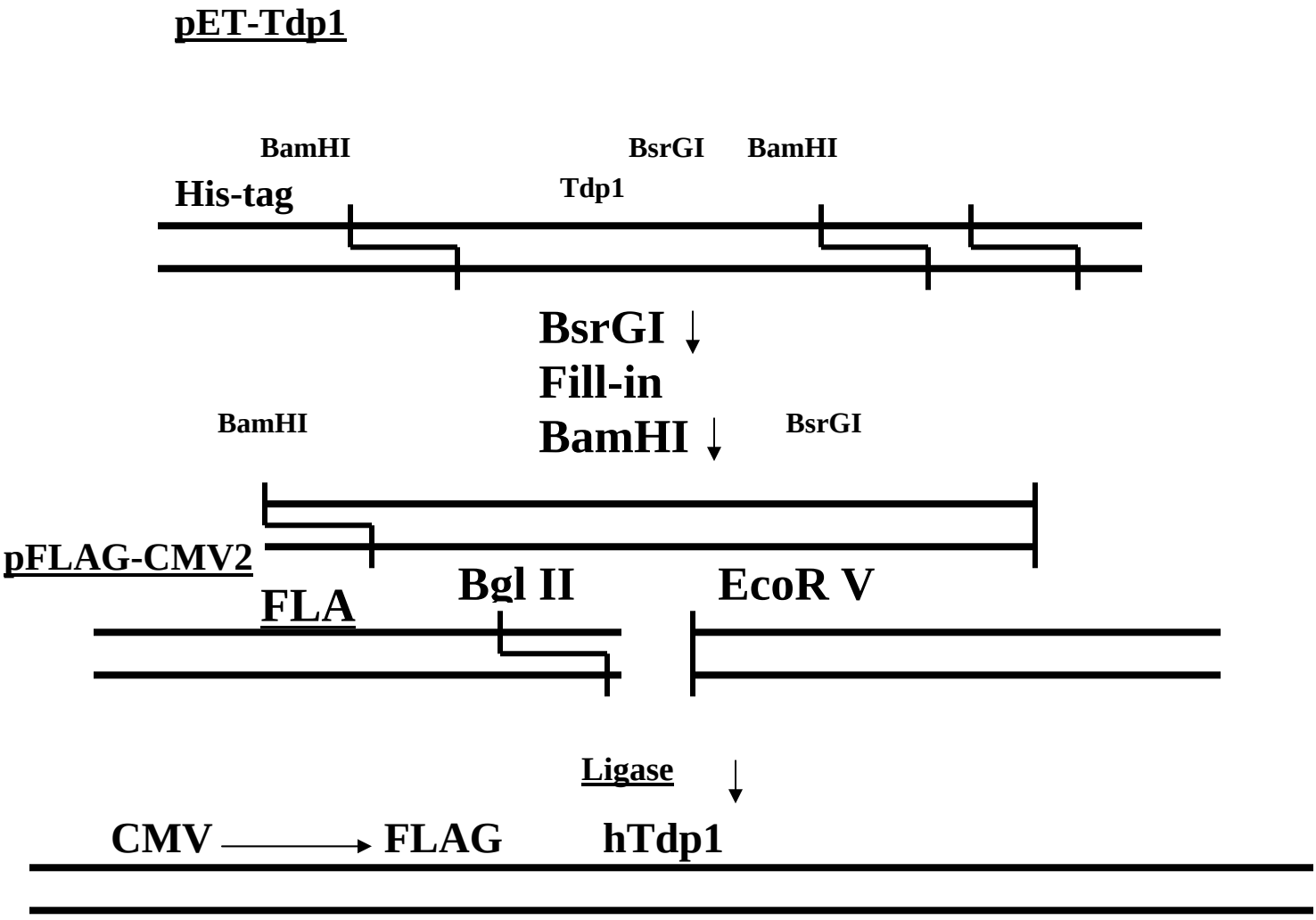
pET-Tdp1
BamHI
BsrGI
BamHI
His-tag
Tdp1
BsrGI ↓
Fill-in
BamHI ↓
BamHI
BsrGI
pFLAG-CMV2
FLA
Bgl II
EcoR V
Ligase ↓
CMV
FLAG
hTdp1
pCMV-FLAG-hTdp1

Figure 10: The pCMV-Tag1 human expression vector used for cloning *Tdp1* gene.

Flag and c-myc epitopes were removed. Within the *Tdp1* insert a pyrimidine at –3 position to an ATG sequence was replaced with a purine to ensure normal translation. The product formed was untagged Tdp1 which was used as a negative control.

Figure 10

CMV promoter 1–602
multiple cloning site 1 651–692
FLAG tag 699–722
multiple cloning site 2 737–764
c-myc tag 762—791
SV40 polyA 852–1235
f1 origin 1373–1679
***bla* promoter** 1704–1828
SV40 promoter 1848–2186
neomycin/kanamycin resistance ORF 2221–3012
HSV-TK polyA 3013–3471
pUC origin 3600–4267

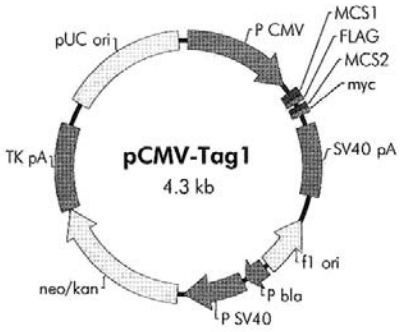

pCMV-Tag 1 Multiple Cloning Site Region
(sequence shown 620–840)

T3 promoter
A ATT AAC CCT CAC TAA AGG GAA CAA AAG CTG GAG CTC CAC CGC GGT GGC GGC CGC TCT A...
Sac I
Not I

FLAG tag
Bgl II
Srf I
BamH I
EcoR V
...GC CCG GGC GGA TCC ACC ATG GAT TAC AAG GAT GAC GAC GAT AAG ATC TGA TCA GAT...
M D Y K D D D D K I
KOZAK
STOP

myc tag
Hind III
Acc I/Sal I
Xho I
...ATC AAG CTT ATC GAT ACC GTC GAC CTC GAG CAG AAA CTC ATC TCT GAA GAG GAT CTG...
E Q K L I S E E D L

Kpn I
T7 promoter
...TAGGTACCAGGTAAGTGTACCCAATTCGCCCTATAGTGAGTCGTATTAC
STOP

Protein gel using silver staining

A protein gel was carried out to estimate the concentration of FLAG-hTdp1 purified by dounce homogenization and by using detergent from both pFLAG-Tdp1 transfected 293B human embryonic kidney cells and from adenovirus infected U-87 glioma cells. 30, 100, 300, 1000 or 3000 ng of BSA was loaded onto separate wells as controls.
11a: The last 4 wells contain 2 µl of FLAG-hTdp1 purified using detergent from U-87 cells, 5 µl and 2 µl of FLAG-hTdp1 purified using dounce homogenization from 293B cells and 2 µl of FLAG-hTdp1 purified using detergent from 293B cells respectively.
11b: The last 4 wells contain 2 µl of FLAG-hTdp1 from 293B cells, 4 µl of micro-dialyzed hTdp1, 4 µl each of 1st and 2nd hTdp1 elutions from U-87 cells. Each of these samples was purified using 0.5% NP-40.

Figure 11a

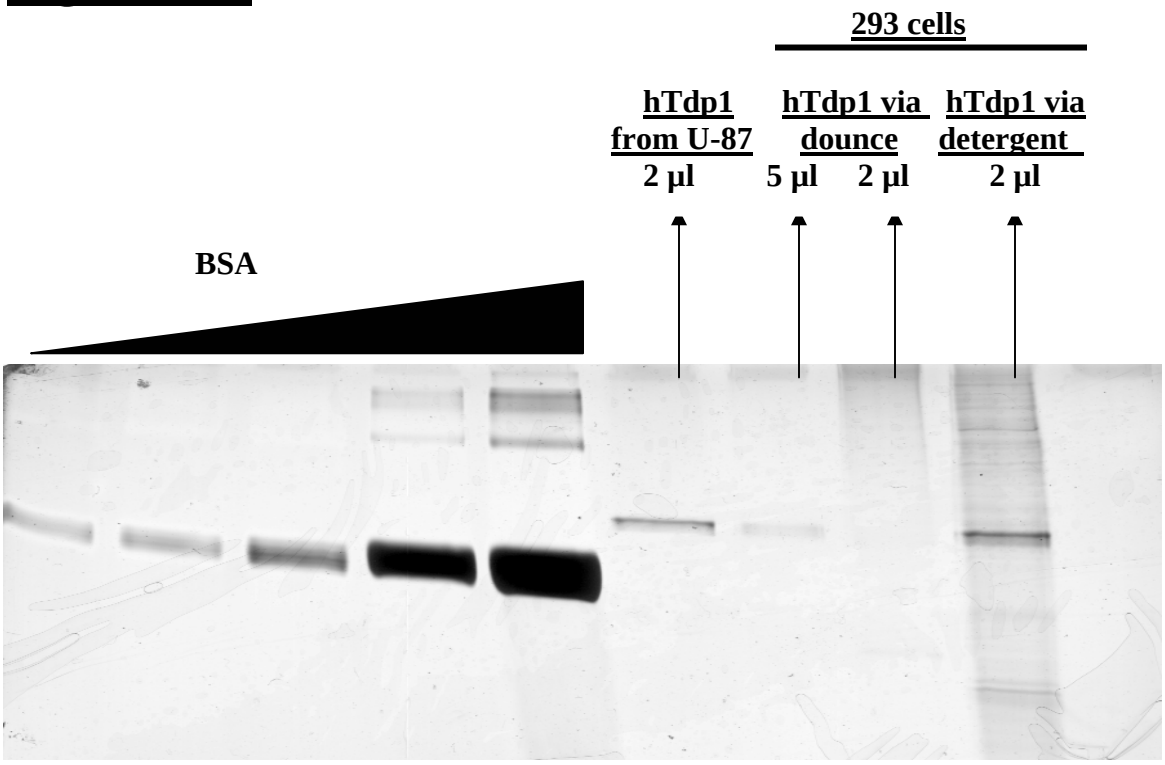

Figure 11b

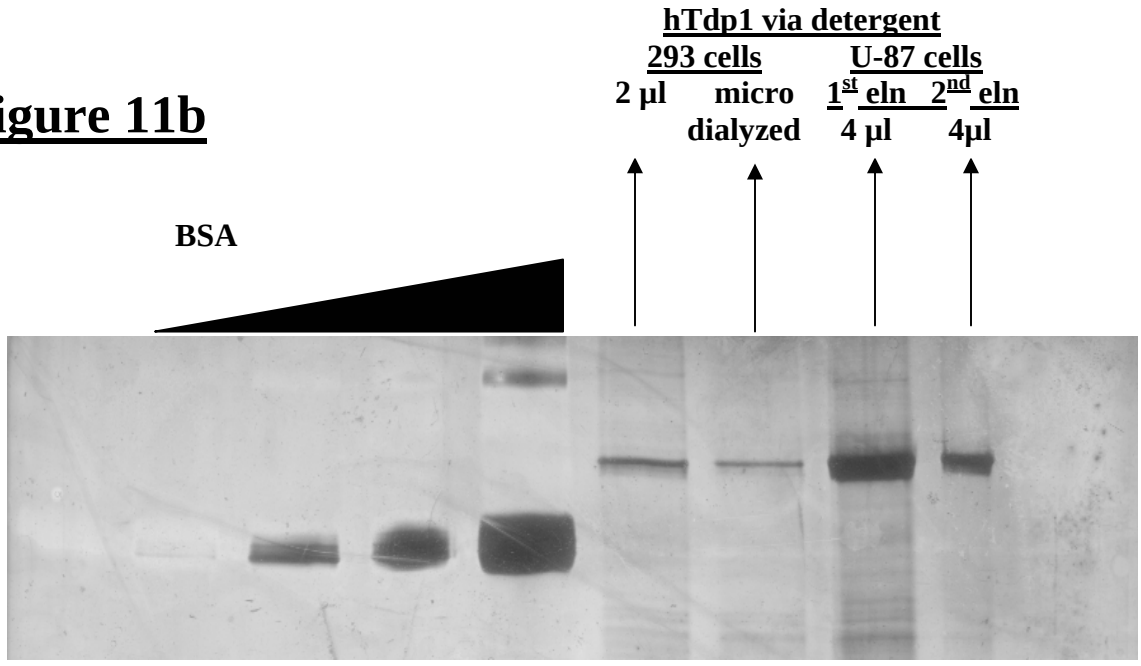

Figure 11c: Western Blot analysis of whole-cell and purified extracts

A western (using Mouse anti-FLAG antibody) was carried out with samples containing 0.2 µl and 1µl whole-cell extracts containing FLAG-tagged hTdp1, 0.2 µl whole-cell extract containing untagged hTdp1, 0.5 µl purified FLAG-hTdp1 and 0.5 µl untagged hTdp1. Equal concentration of hTdp1 was found in the whole-cell extracts containing FLAG-hTdp1 and untagged hTdp1. The sample containing purified FLAG-hTdp1 showed a band while the sample containing purified untagged hTdp1 did not show a band proving that only FLAG-hTdp1 was purified using FLAG beads and FLAG peptide.

Figure 11c

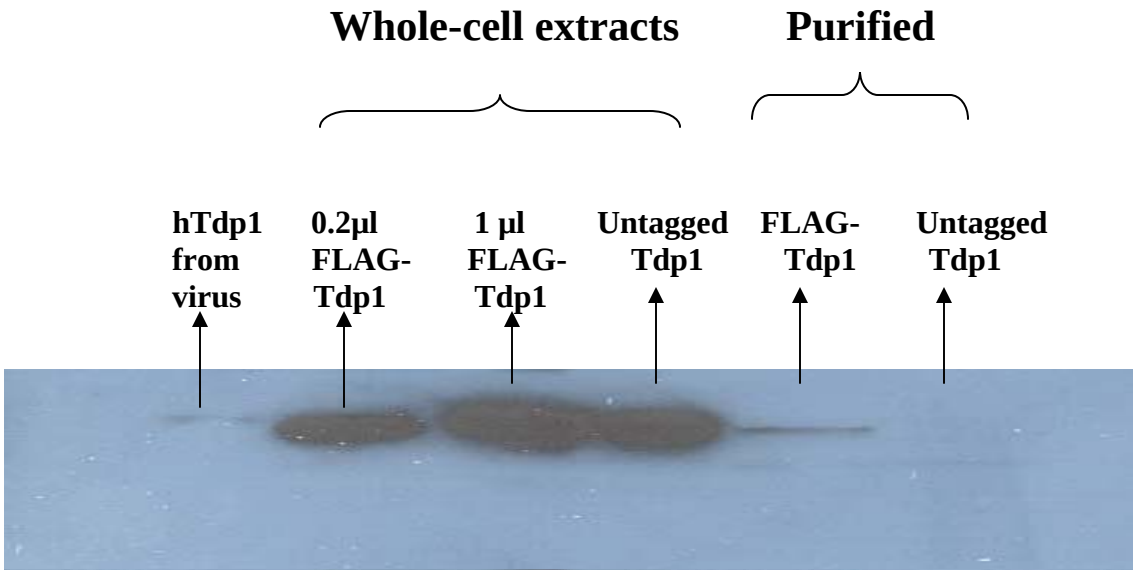
Whole-cell extracts
Purified
hTdp1 from virus
0.2µl FLAG-Tdp1
1 µl FLAG-Tdp1
Untagged Tdp1
FLAG-Tdp1
Untagged Tdp1

Trap nickel chelating columns, suggesting that the FLAG tag has no effect on the potency or specificity of the enzyme (Figure 12).

Better recovery of Tdp1 activity by NP-40 detergent lysis than by dounce homogenization

In our laboratory, pFLAG-Tdp1, along with Superfect transfection reagent, was transfected into 293B embryonic kidney cells. Following incubation for 3 days, the cells, instead of being dounced as per usual experimental procedure, were treated with lysis buffer containing Nonidet P-40 or NP-40 (a phenol-containing detergent) to lyse the cells and release their cytoplasmic contents. Protease inhibitors were added and FLAG-Tdp1 was adsorbed onto FLAG beads and eluted with FLAG peptide. A protein gel using silver staining was carried out to compare the protein content in the extracts purified using dounce homogenization *vs.* extracts purified using 0.5% NP-40 (Figures 11a and b). When we compared the processing efficiencies of FLAG-Tdp1 obtained using detergent with that of FLAG-Tdp1 obtained via dounce homogenization, we observed that while the former retained the 100-fold difference between phosphotyrosyl and PG-substrates as seen with recombinant Tdp1 purified using Hi-Trap Nickel chelating columns, the latter hardly showed any PG-processing even at undiluted concentrations. These results lead us to use NP-40 for cell lysis rather than dounce homogenization while purifying FLAG-Tdp1 (Figure 13).

Relative processing efficiency of FLAG-hTdp1 cloned into an adenovirus was ~100-fold

The many differences between bacterial and human cells lead us to clone human FLAG-Tdp1 into an adenovirus and purify it from transduced human cells using FLAG

Figure 12: Relative end-processing efficiencies of FLAG-hTdp1 and Untagged hTdp1

A 3'-phosphotyrosine 18-mer (○) or a 3'-PG 14-mer (●) was treated with 1 µl of undiluted or 1 µl of six 1:8 dilutions of extracts containing overexpressed FLAG-hTdp1 and Untagged hTdp1. Each 5µl reaction was incubated at 37 ºC for 2 hours in Kedar buffer containing 5 mM EDTA. Samples were boiled for 1 minute at 90 ºC. 20 mM Mg^{2+} and 20 ng hPNKP were added. Conversion to 3'-OH was assessed by denaturing gel electrophoresis and quantified using ImageQuant software. The difference in relative end-processing efficiencies was found to be approximately 100-fold.

Figure 12

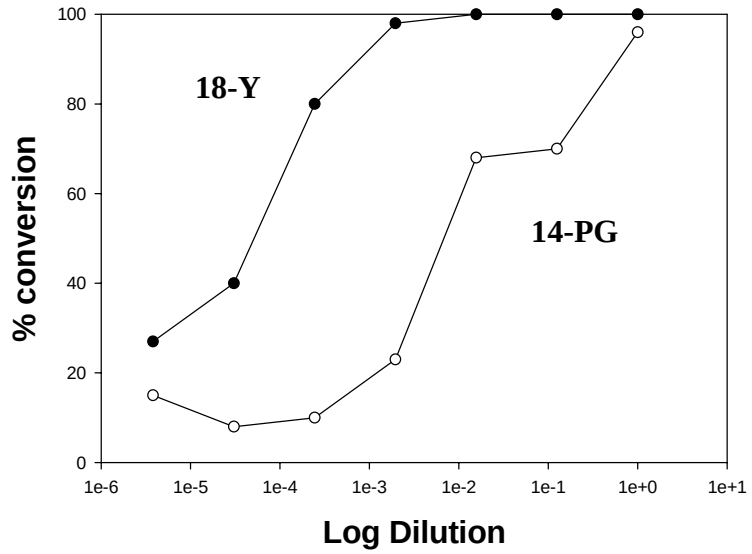

FLAG-Tdp1 extract

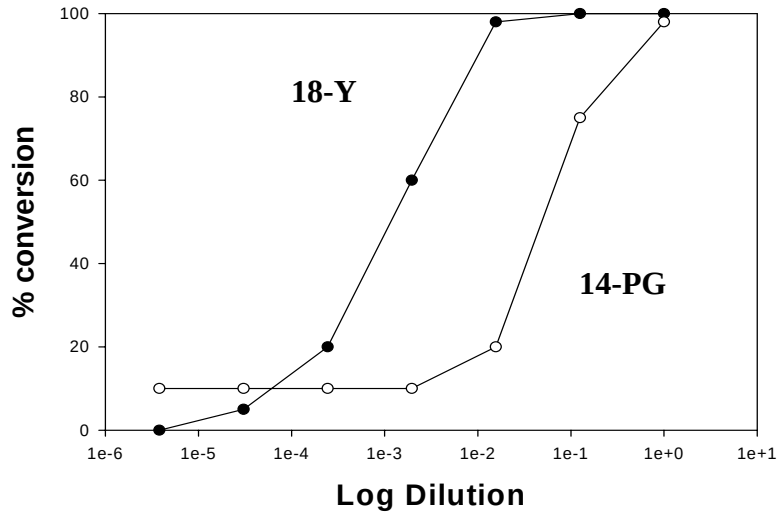

Untagged-Tdp1 extract

Figure 13: To compare the end-processing efficiencies of FLAG-hTdp1 purified via dounce homogenization *vs.* FLAG-hTdp1 purified using 0.5% NP-40

A 3'-phosphotyrosine 18-mer (○) or a 3'-PG 14-mer (●) was treated with 25, 3.125, 0.39, 0.048, 0.0061, 0.00077, 0.000095 or 0.0000012 ng of FLAG-hTdp1 purified using dounce homogenization OR 50, 6.25, 0.78, 0.098, 0.012, 0.0015 or 0.0002 ng of FLAG-hTdp1, purified using 0.5% NP-40. Each 5µl reaction was incubated at 37 ºC for 2 hours in Kedar buffer containing 5 mM EDTA. Samples were boiled for 1 minute at 90 ºC. A final concentration of 20 mM Mg^{2+} and 20 ng hPNKP were added. Conversion to 3'-OH was assessed by denaturing gel electrophoresis and quantified using ImageQuant software. Our results showed that the latter retained the 100-fold difference as seen with recombinant Tdp1 purified using Hi-Trap Nickel chelating columns, while the former hardly showed any PG-processing even at undiluted concentrations.

Figure 13

Via DOUNCE HOMEGENIZATION

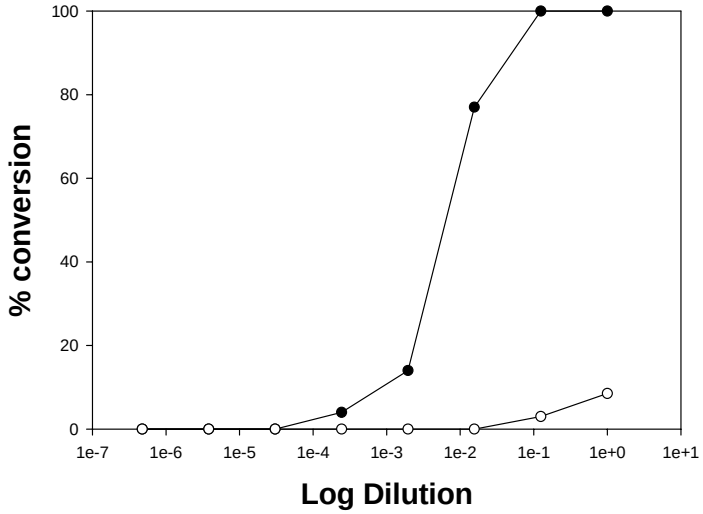

Via DETERGENT

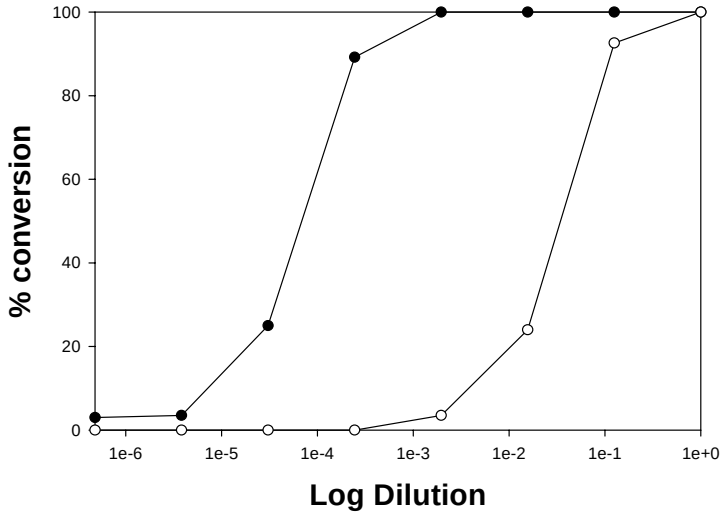

100-FOLD

beads and FLAG peptide. Once cloned, when the relative processing efficiency of FLAG-tagged Tdp1 from purified adenovirus infected U87 glioma cells was compared, we observed about the same 100-fold difference in processing efficiencies for 3'-PG and 3'-phosphotyrosine oligomers (Figures 14a and 14b) as with recombinant hTdp1 purified from bacteria using Hi-Trap nickel chelating columns, suggesting that if Tdp1 was post-translationally modified in mammalian cells, these modifications did not have any effect on the specificity of the enzyme.

Extracts of SCAN1 cells with mutant Tdp1 are deficient in PG-processing

A possible theory regarding patients suffering from spinocellebelar ataxia with axonal neuropathy is that oxidative stress coupled with hTdp1 deficiency results in persistent 3'-phosphoglycolates resulting in persistent DSBs and neuronal apoptosis. To examine the molecular basis of SCAN1, blood samples were collected from 7 related individuals of an affected Saudi Arabian family and Epstein-Barr virus transformed lymphoblastoid cell lines were established by Dr. James Lupski. Upon receiving these 7 cell lines, named JRL1-7 respectively, we prepared whole-cell extracts and tested dilutions of each extract for the processing of a 3'-phosphotyrosine containing 18-mer. We observed that while JRL-1 and JRL-3 extracts showed no conversion of 3'-phosphotyrosine to 3'-phosphate, undiluted JRL -5, 6 and 7 extracts catalyzed complete conversion (Figure 15a). JRL-4 extract showed an extremely low conversion when undiluted and no conversion with subsequent dilutions. These results suggested that JRL-1 and 3 extracts contained mutated hTdp1 while JRL-5, 6 and 7 extracts contained the wild-type hTdp1 and this was found to be in agreement with genetic and sequencing data; JRL-1,-3 and –4 are homozygous Tdp1 mutants, JRL-2 and –5 are normal while JRL-6

Figure 14a and 14b: Relative end-processing efficiency of FLAG-hTdp1 cloned into an adenovirus.

A 3'-phosphotyrosine 18-mer (○) or a 3'-PG 14-mer (●) was treated with 50, 6.25, 0.78, 0.098, 0.012, 0.0015 or 0.0002 ng of FLAG-hTdp1, purified from adenovirus infected U-87 glioma cells. Each 5µl reaction was incubated at 37 ºC for 2 hours in Kedar buffer containing 5 mM EDTA. Samples were boiled for 1 minute at 90 ºC. A final concentration of 20 mM Mg^{2+} and 20 ng hPNKP were added. Conversion to 3'-OH was assessed by denaturing gel electrophoresis and quantified using ImageQuant software. The difference in relative end-processing efficiencies was found to be approximately 100-fold.

Figure 14a

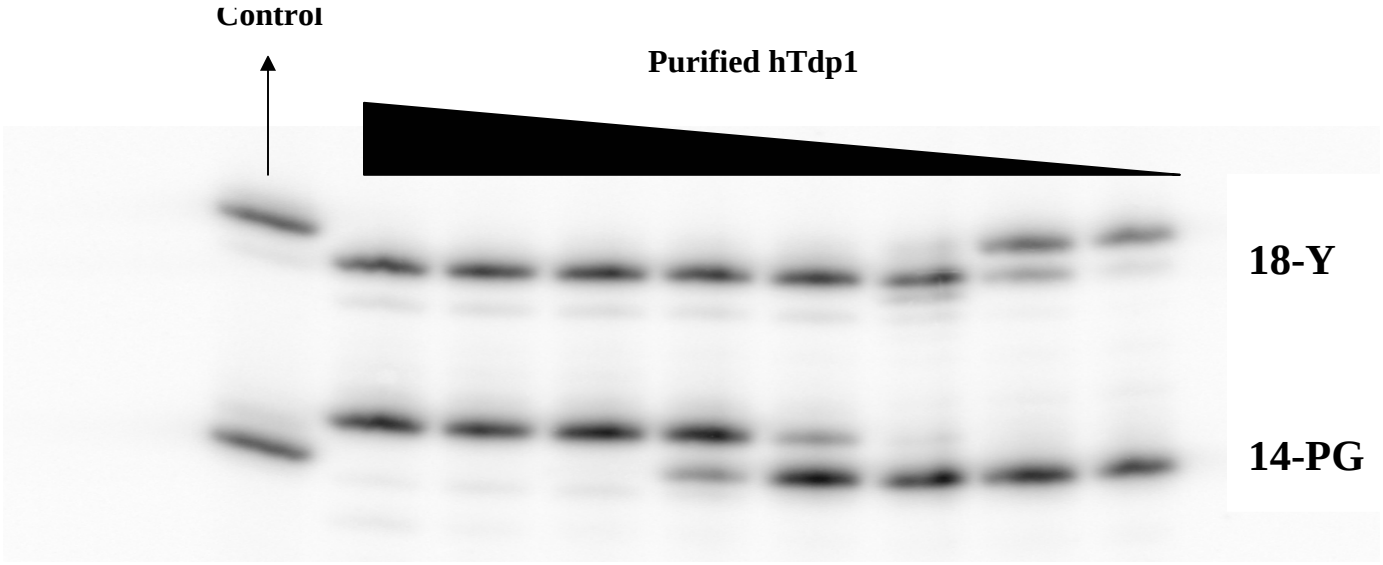

Figure 14b

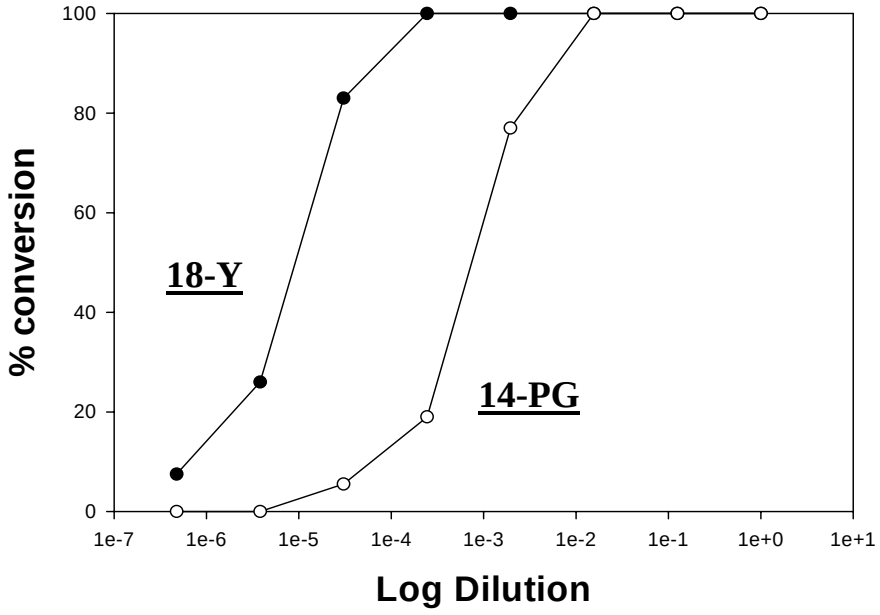

100-FOLD

and –7 are heterozygous carriers. To assess whether this mutation resulted in deficiency in 3'-PG processing, a 3'-PG containing14-mer was incubated with JRL-1, 5 and 6 extracts (Figure 15b). In JRL-1 whole-cell extract, PG processing was undetectable while partial conversion to 3'-phosphate was seen in JRL-5 and JRL-6. This suggests that most, if not all 3'-PG processing activity in extracts is attributable to Tdp1.

When the processing efficiencies of purified FLAG-tagged hTdp1 were compared in our previous experiments, we observed that the 3'-phosphotyrosyl-containing 18-mer was 100-fold more efficiently processed than the 3'-PG containing 14-mer. However, addition of whole-cell extracts from Tdp1-mutant, JRL-1, to purified FLAG-hTdp1 reduced the ratio of phosphotyrosyl to PG processing activities from 100:1 to 10:1. Our results showed that the 3'-phosphotyrosine processing efficiency decreased while the 3'-PG processing efficiency increased on addition of JRL-1 extract (Figure 15c). These results suggest that Tdp1 specificity is modulated by other factors in the whole-cell extract.

No evidence for the presence of other Mg^{+2} –dependent PG-processing enzymes

Since whole-cell extracts of Tdp1-mutant SCAN1 cells showed no detectable processing of 3'-PG-terminated oligomers, it was suggested that most, if not all, 3'-PG-processing is attributable to Tdp1. However, these assays were conducted in the presence of 5mM EDTA in the reaction buffer in order to inhibit nucleases that would otherwise interfere with the detection of PG-processing activity of Tdp1. Mg^{+2} acts as a co-factor for most nucleases. In the presence of this EDTA, any Mg^{+2} added would form a chelate complex rendering it inaccessible to enzymes and therefore, Mg^{+2} –dependent PG-processing enzymes, if present, would have been difficult to detect. In order to look for

Figure 15: Relative end-processing efficiencies of SCAN1 whole-cell extracts (JRL 1-7)

15a: An 18-mer containing 3'-phosphotyrosine was treated with 1 µl of undiluted, followed by 1 µl of two 1:8 dilutions of each of the seven JRL whole-cell extracts for 2 hours at 37° C in Kedar buffer with EDTA and samples were analyzed by polyacrylamide gel electrophoresis. JRL 2, 5, 6 and 7 showed presence of wild-type hTdp1 while JRL 1, 3 and 4 seemed to contain no 3'-phosphotyrosine processing activity, consistent with these cells harboring mutant hTdp1. JRL 4 also showed some residual activity.
15b: An 14-mer containing 3'-PG was treated with 1 µl of undiluted, followed by 1 µl of four 1:8 dilutions of JRL whole-cell extracts-1, 5, and 6- for 2 hours at 37° C in Kedar buffer with EDTA and samples were analyzed by PAGE. JRL 5 and JRL 6 showed a partial conversion to 3'-phosphate at undiluted concentration.

Figure 15a

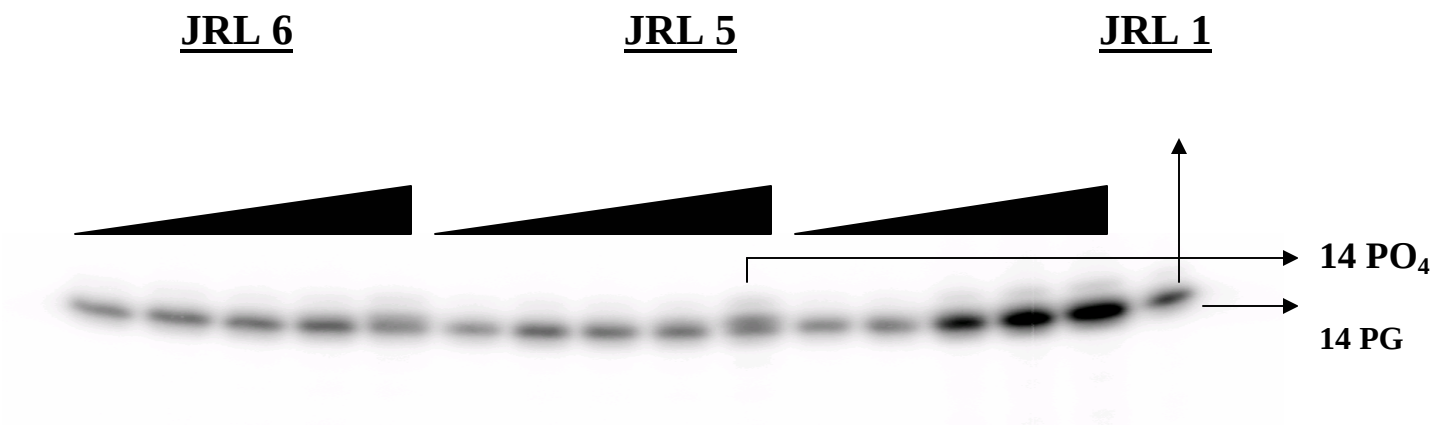

Figure 15b

Figure 15c. Effect of addition of JRL 1 whole-cell extract to purified FLAG-tagged hTdp1

An 18-mer containing 3'-phosphotyrosine or a 14-mer containing 3'-PG was treated with 50, 6.25, 0.78, 0.098, 0.012, 0.0015 or 0.0002 ng of FLAG-hTdp1, purified from adenovirus infected U-87 glioma cells. To another similar set, 1.8 µl of a 7mg/ml JRL 1 whole-cell extract (containing mutated hTdp1) was added along with the FLAG-hTdp1 and the substrate. Each set was incubated for 2 hours at 37° C in Kedar buffer with EDTA and no ATP. Samples were then analyzed by polyacrylamide gel electrophoresis. Our results showed that addition of JRL-1 whole-cell extract reduced the ratio of phosphotyrosyl to PG processing activities from 100:1 to 10:1 (also refer to Fig 14b). The 3'-phosphotyrosine processing efficiency decreased while the 3'-PG processing efficiency increased suggesting that Tdp1 specificity is modulated by other factors in the whole-cell extract.

Figure 15c

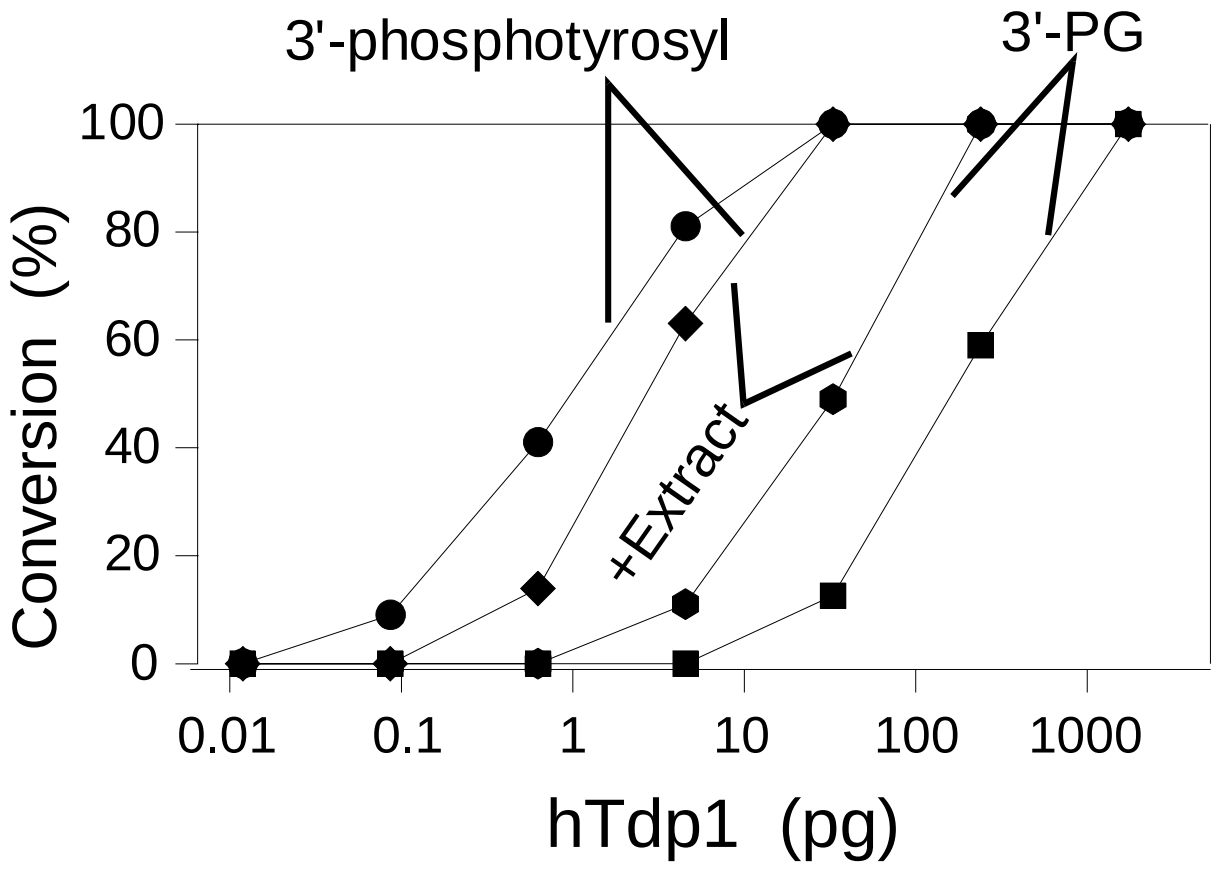
3'-phosphotyrosyl
3'-PG
+Extract
Conversion (%)
100
80
60
40
20
0
0.01
0.1
1
10
100
1000
hTdp1 (pg)

the presence of such enzymes, a phosphorothioate- substituted 3'-PG substrate that is nuclease-resistant was prepared in our laboratory. This thiolated oligo prevents 3'-> 5' exonucleases from degradaing the DNA end. The oligomer was incubated with different dilutions of JRL1 cells containing mutated Tdp1 in the presence of 100 mM Mg^{+2} and subsequently treated with PNKP. We did not observe any conversion of the 3'-phosphotyrosyl and 3'-PG substrates to 3'-OH, although at the highest concentration there was some loss of both substrates, probably due to degradation by nucleases present in extracts (Figure 16).

Processing of the single-strand PG terminated oligomer by human FLAG-Tdp1 is independent of cofactor requirement

Cheng et al. in 2002 proposed that Mn^{2+} has a stimulatory effect on Tdp1 activity. Experiments carried out in our laboratory showed that adding 5mM Mn^{2+} in our reaction buffer and then looking at the processing efficiency with which the 3'-PG containing 14-mer was processed, generated an approximately 8 % conversion of 3'-PG to 3'-phosphate only in the undiluted fraction (Figure 17). This is in agreement with Yang et al. (1996) who proposed that Tdp1 activity is independent of any co-factor requirement. According to them, there was no stimulation of Tdp1 activity when reactions were conducted in the presence of a simple buffer that was supplemented with 10mM Mg, Ca, Co, Cd and Zn.

Tdp1 associates with XRCC1

The *XRCC1* gene product is a scaffolding protein containing two BRCA1 carboxyl terminal (BRCT) domains, which are binding motifs for DNA repair and cell cycle check points (Huyton et al., 2000). XRCC1 is implicated in single strand break repair pathway (SSBR) (Thompson et al., 2000) and forms a mutimeric repair complex

Figure 16: No evidence for the presence of other Mg^{+2} –dependent PG-processing enzymes

A 3'-phosphotyrosine 18-mer or a phosphorothiaote-substituted 3'-PG 14-mer was treated with 1 µl of undiluted or 1 µl of seven 1:8 dilutions of JRL 1 whole-cell extract, containing mutant hTdp1. Each 5µl reaction was incubated at 37 ºC for 2 hours in buffer with 0.5 mM $MgCl_2$ without EDTA. Samples were boiled for 1 minute at 90 ºC. A final concentration of 20 mM Mg^{2+} and 20 ng hPNKP were added. Conversion to 3'-OH was assessed by denaturing gel electrophoresis and quantified using ImageQuant software. There was no conversion to the 3'-OH substrate.

Figure 16

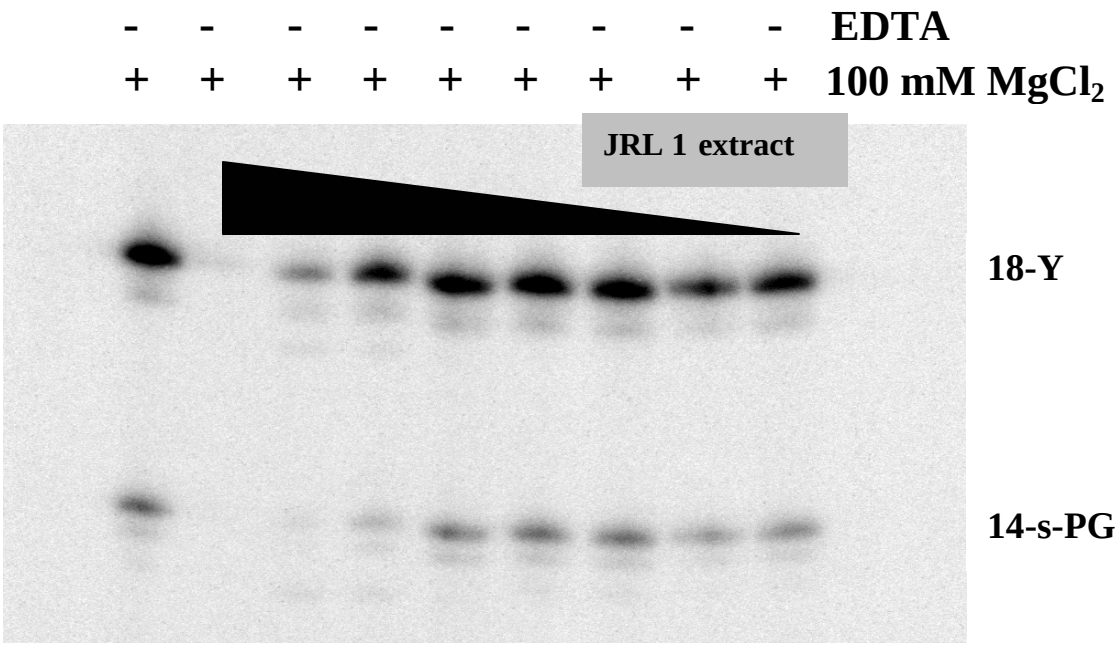

Figure 17: Effect of 5 mM Mn^{+2} on hTdp1 activity.

A 3'-PG 14-mer was treated with 50, 6.25, 0.78, 0.098, 0.012, 0.0015, 0.0002 or 0.000025 ng of FLAG-hTdp1, purified from adenovirus infected U-87 glioma cells. Each 5µl reaction was incubated in buffer containing 50 mM Tris-HCl, pH 8.5/100 mM NaCl/5 mM $MnCl_2$ /1 mM DTT/ 100 µg/ml BSA at 37 ºC for 15 minutes. Conversion to 3'-phosphate was assessed by denaturing gel electrophoresis and quantified using ImageQuant software. There was 8 % conversion to 3'-phosphate only in the undiluted fraction.

Figure 17

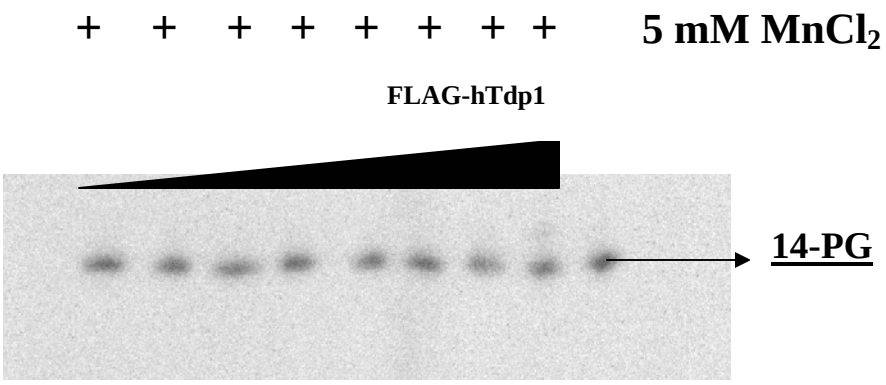

with several enzymes implicated in base excision and gap repair: DNA ligase III (Caldecott et al., 1994), PARP-1 (Caldecott et al., 1996), PARP-2 (Schreiber et al., 2002), DNA polymerase β (Kubota et al., 1996), PNKP (Whitehouse et al., 2001) and APE1 (Vidal et al., 2001). Because of this scaffolding property of XRCC1, its possible association with Tdp1 was tested (Plo et al., 2003). Results showed that Tdp1 co-immunoprecipitated with XRCC1 antibody and that this activity was inhibited in the presence of sodium vanadate, a reported inhibitor of Tdp1 (Davies et al., 2002). Western blot analysis also showed the presence of Tdp1 in XRCC1 immuno precipitates. Our laboratory carried out a western blot analysis using anti-XRCC1 antibody to determine whether we could detect complexes formed by Tdp1 in cells. We used samples containing whole cell-extracts, a 1X TE wash obtained during the elution of Tdp1 and immunoprecipitated FLAG-tagged Tdp1. Our results showed the presence of XRCC1 in both the whole-cell extract as well as in the sample containing immunoprecipitated Tdp1 while none was present in the wash suggesting that XRCC1 co-precipitates with Tdp1 and a wash with 1X TE does not eliminate their binding (Figure 18a).

XRCC1-complementation enhances Tdp1-activity

To determine whether XRCC1 influenced the repair of topoisomerase I covalent complexes, Plo and colleagues (2003), incubated a 3'-phosphotyrosine containing 14-mer with nuclear extracts obtained from XRCC1-deficient (EM9-V) and XRCC1-complemented (EM9-XH) cells. Nuclear extracts from XRCC1-deficient (EM9-V) cells showed reduced processing of the phosphotyrosine substrate to the 14-OH product when compared to nuclear extracts from XRCC1-complemented (EM9-XH) cells suggesting that XRCC1 complementation enhances Tdp1 and PNKP activities. When we tried to

Figure 18a: Tdp1 associates with XRCC1

A western (using Mouse anti-XRCC1 antibody) was carried out with samples containing 50 ng of XRCC1 as a control, 1 µl of whole-cell extract containing FLAG-tagged hTdp1, 10 µl of a TE wash of the whole-cell extract and 2 µl (100 ng) of IMMUNOPRECIPITATED FLAG-tagged hTdp1. Our results show the presence of XRCC1 in both the whole-cell extract as well as in the sample containing immunoprecipitated FLAG-tagged hTdp1 while none was present in the TE wash suggesting that XRCC1 co-precipitates with Tdp1 and a wash with 1X TE does not eliminate their binding.

Figure 18a

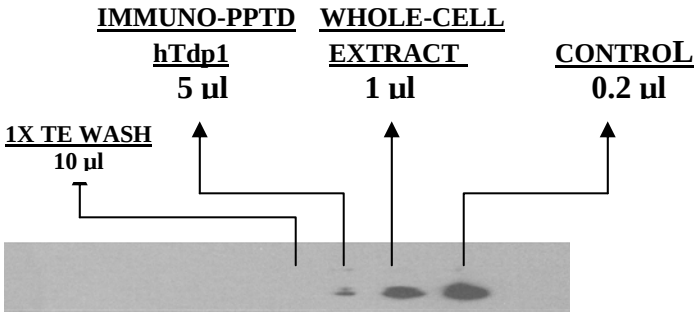
IMMUNO-PPTD
hTdp1
5 µl
WHOLE-CELL
EXTRACT
1 µl
CONTROL
0.2 µl
1X TE WASH
10 µl

duplicate these results in our laboratory by incubating 3'-PG containing 14-mer with pure FLAG-Tdp1 (washed 3 times with salt and then purified with FLAG beads) and different concentrations of XRCC1, we did not see any marked increase in Tdp1 activity. Yeast two-hybrid experiments revealed that Tdp1 associates with the single-strand break repair machinery by direct interaction with DNA ligase IIIα, a partner of XRCC1 (El-Khamisy et al., 2005). Since, during purification, we washed our extracts in buffer containing high concentrations of salt, we speculated that ligase III could have been washed away, thus removing the bridge required for XRCC1 and Tdp1 binding. In order to check for this possibility, we repeated the above experiment but this time used nuclear extracts derived from U-87 glioma cells (FLAG-hTdp1 virus-infected cells) instead of purified Tdp1. Our results indeed showed that with increasing concentrations of XRCC1, Tdp1 activity is increased (a maximum of ~4 times) before it reaches a plateau (Figures 18b and 18c).

We also carried out a western blot analysis to check for the presence of Ku in immunoprecipitated extracts. As shown in figure 18d, although a high concentration of Ku was seen in the control and the whole-cell extracts, there was no indication of co-precipitation of Ku with FLAG-hTdp1 during the latter's immunoprecipitation, even though the extracts were washed only with buffer containing1X TE and no salt.

Presence of Tdp1 protein in mitochondrial extracts

Human mitochondria contain approximately 5-10 copies per mitochondrion of a covalently closed duplex DNA genome (Moraes et al., 2001). Because mitochondrial DNA molecules are closed circular and therefore topologically constrained, there must be a mechanism to relieve the DNA strain that arises during replication. Zhang et al. (2001) reported the existence of a mitochondrial topoisomerase I gene *TOP1mt*, which is

Figures 18b and c: Effect of XRCC1 on FLAG-hTdp1 activity

A 3'-PG 14-mer (●) plus 15, 30, 45, 60 or 75 ng of recombinant XRCC1 was added to 1 µl of undiluted nuclear extracts derived from U-87 glioma cells infected with adenovirus expressing FLAG-hTdp1. Samples (total volume of 5 µl) were incubated for 15 minutes at 37 ºC in Kedar buffer, followed by boiling of samples at 90 ºC for 1 minute. A final concentration of 20 mM $MgCl_2$ and 20 ng of PNKP were added and incubation was continued for 1 hour. Conversion to 3'-OH was assessed by denaturing gel electrophoresis and quantified using ImageQuant software. Our results showed an increase in hTdp1 activity (upto 4X) with increasing concentrations of XRCC1.

Figure18b

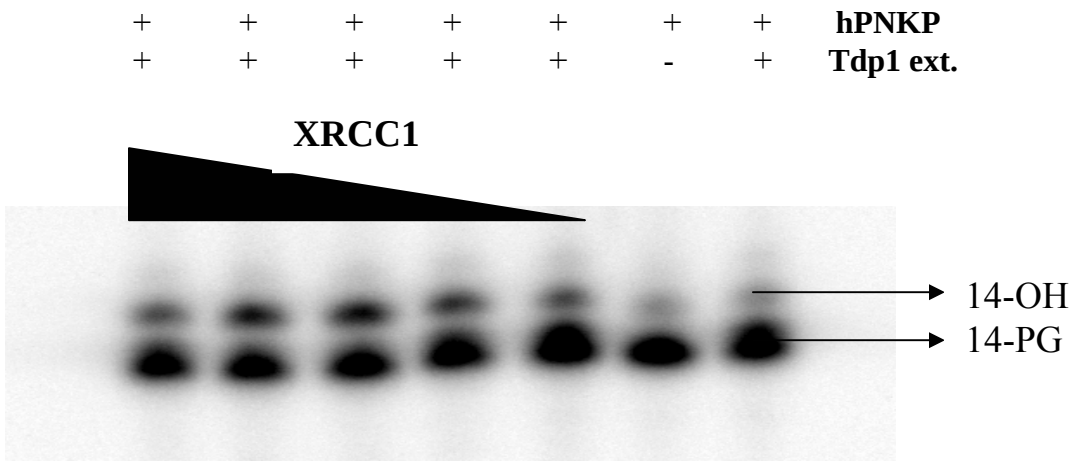

Figure 18c

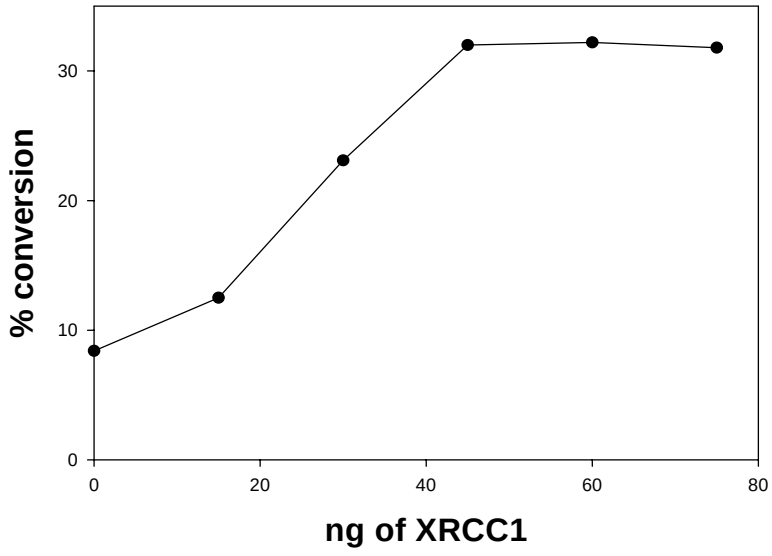

Figure 18d: A western blot analysis to check for the presence of Ku in immunoprecipitated hTdp1 extracts

A western (using Rabbit anti-Ku 70 antibody) was carried out with samples containing 120 ng Ku as a control, 1 µl of whole-cell extract containing FLAG-tagged hTdp1, 10 µl of a TE wash of the whole-cell extract and 5 µl (250 ng) of immunoprecipitated FLAG-tagged hTdp1. Although, a high concentration of Ku was seen in the control and the whole-cell extracts, there was no indication of co-precipitation of Ku with FLAG-hTdp1 during the latter's immunoprecipitation, even though the extracts were washed only with buffer containing1X TE and no salt.

Figure 18d

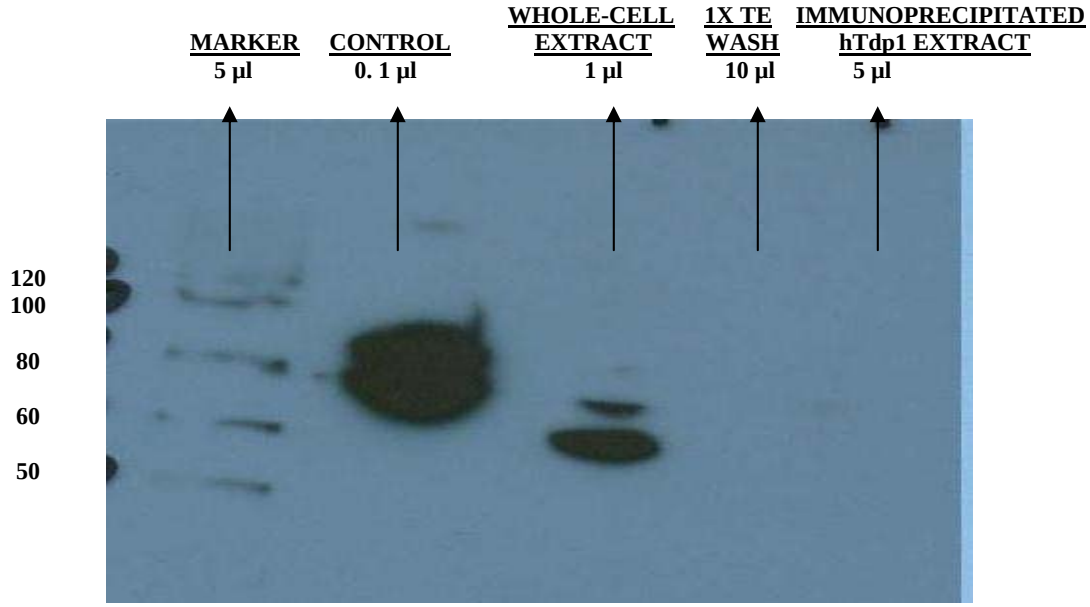
MARKER
5 µl
CONTROL
0. 1 µl
WHOLE-CELL EXTRACT
1 µl
1X TE WASH
10 µl
IMMUNOPRECIPITATED hTdp1 EXTRACT
5 µl
120
100
80
60
50

localized on human chromosome 8q24. They found a high degree of homology between top1mt and nuclear topo1 which was further demonstrated by the top1mt protein being sensitive to CPT treatment (Tua et al., 1997), thus generating DNA strand breaks by blocking the re-ligation of topo1-linked DNA breaks. The formation of the mitochondrial topo1-DNA covalent complex lead us to speculate the presence of Tdp1 within the mitochondria to repair topoI-linked breaks as well as DSBs with 3′-PG termini that might arise as a result of oxidative stress. Western blot analysis using samples containing Tdp1 purified from whole-cell extracts (as a control), mitochondrial extract (from GM1310 normal human fibroblasts; gift of Penelope Mason, National Institute of Aging), whole-cell and mitochondrial extracts from the SCAN 1 cell-lines JRL 5 (containing wild-type Tdp1) and JRL 3 (containing mutant Tdp1) using anti-Tdp1 antibody indeed showed presence of a high concentration of hTdp1 in the mitochondrial extract derived from the GM1310 cell-line (Figure 19). While the whole-cell extracts from both the SCAN1 cell-lines seemed to contain hTdp1, along with some quantity of degradation products, only the mitochondrial extracts from JRL 5 cells showed the presence of hTdp1.

Mitochondrial extracts show similar PG-processing efficiency as whole-cell extracts

We incubated serial 1:8 dilutions each of whole-cell extracts (without mitochondria) and mitochondrial extracts with an 18-mer containing 3'-phosphotyrosine for 15 minutes at 37°C and our results showed that there was no marked difference in the processing efficiencies between the extracts. When we carried out similar experiments using a 14-mer with 3'-PG, we found the same result, i.e., the difference in processing of the phosphotyrosine *vs.* PG oligomers was similar for both the whole-cell and

Figure 19: Western Blot analysis of whole-cell and mitochondrial extracts derived from GM1310 normal human fibroblasts and SCAN1 cells.

A western blot was carried out using 2 µl (100 ng) of FLAG-hTdp1, purified from adenovirus infected U-87 glioma cells, 2 µl of mitochondrial extract derived from GM1310 cell-line, 10 µl of whole-cell extracts as well as 5 µl of mitochondrial extracts from the SCAN1 cell-lines, JRL 3 (mutant hTdp1) and 5 (wild-type hTdp1) respectively. The blot showed a high concentration of hTdp1 protein in the mitochondrial extract derived from the GM1310 cell-line. While the whole-cell extracts from both the SCAN1 cell-lines seemed to contain hTdp1, along with some quantity of degradation products, only the mitochondrial extracts from JRL 5 cells showed the presence of hTdp1.

Figure 19

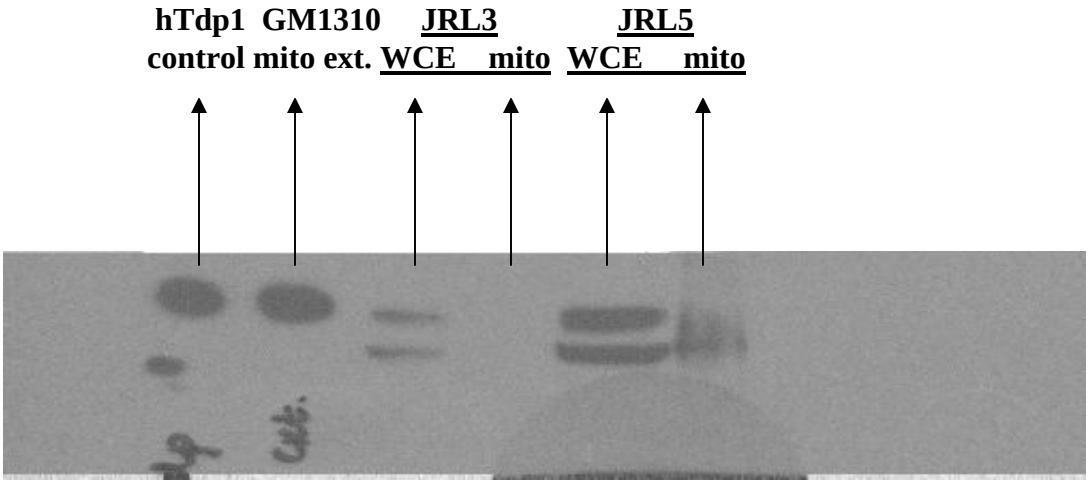
hTdp1 control
GM1310 mito ext.
JRL3 WCE
JRL3 mito
JRL5 WCE
JRL5 mito

Figure 20: Relative end-processing efficiencies of whole-cell *vs.* mitochondrial extracts derived from GM1310 normal human fibroblasts.

1 μl of undiluted or1 μl of five 1:8 dilutions of each of the whole-cell extracts and the mitochondrial extracts were incubated with 18-mer containing 3'-phosphotyrosine (●) or the 14-mer containing 3'-PG (○) for 15 minutes at 37° C in Kedar buffer containing 5 mM EDTA. Samples were boiled for 1 minute at 90 ºC. A final concentration of 20 mM Mg^{2+} and 20 ng hPNKP were added. Conversion to 3'-OH was assessed by denaturing gel electrophoresis and quantified using ImageQuant software. Both whole-cell extracts and mitochondrial extracts showed comparable phosphotyrosine and PG-processing activities.

Figure 20

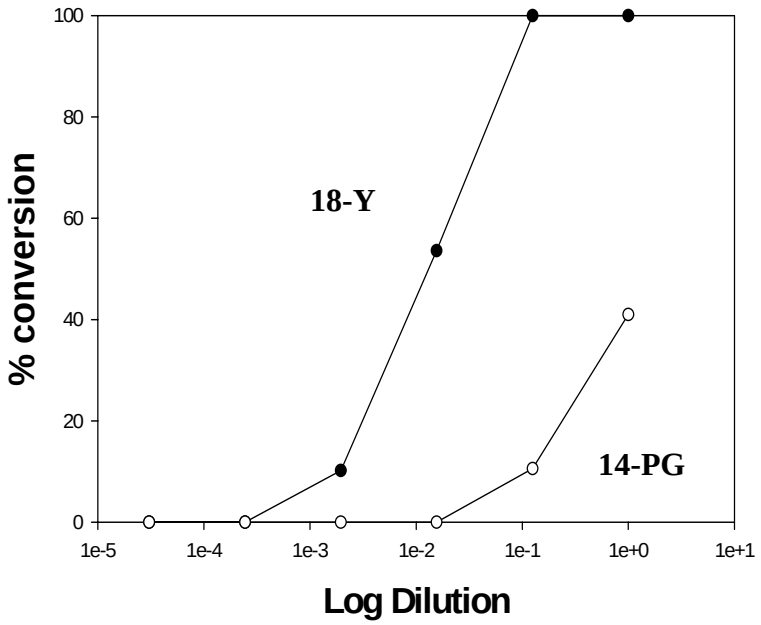

Whole-cell extracts (-mito)

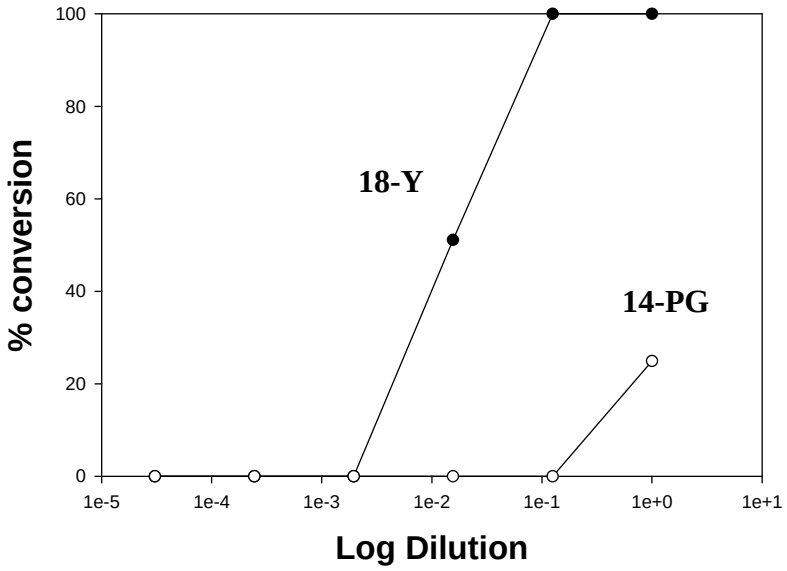

Mitochondrial extracts

mitochondrial extracts suggesting that the specificity of mitochondrial Tdp1 is very similar to the nuclear protein and that mitochondrial extracts contain Tdp1 at a concentration comparable to whole-cell extracts (Figure 20).

Processing efficiencies of JRL 5 (wild-type Tdp1) and JRL 3 (mutant Tdp1) mitochondrial extracts

Consistent with the above western blot analysis, when we compared the efficiency with which various 1:8 dilutions of the JRL 5 and the JRL 3 mitochondrial extracts process a 3'-phosphotyrosine containing 18-mer and a 3'-PG containing 14-mer, we found that while there was absolutely no conversion to 3'-OH with the JRL 3 mitochondrial extract, our results did show ~ 34% and ~ 15% conversion from 3'-phosphotyrosine to the 3'-OH product with the undiluted and the first 1:8 diluted JRL 5 mitochondrial extracts respectively adding further evidence that all PG-processing activity in mitochondria is attributable to hTdp1. Neither the JRL-3 nor the JRL-5 mitochondrial extract showed any activity with the 3'-PG containing oligomer (Figure 21), consistent with the low level of phosphotyrosyl processing seen in the JRL-5 extract and the relative inefficiency of Tdp1 in processing PG substrates.

Processing of a 3'-PG oligomer is partially inhibited by Ku

The Ku heterodimer, consisting of a tight complex of Ku70 and Ku80, forms a close-fitting asymmetrical ring that threads onto the free end of DNA as a nut in a bolt (Walker et al., 2001). Although Ku tends to cling to DNA ends, it can translocate to the interior of the DNA, thus allowing multiple Ku heterodimers to load onto longer DNA molecules (Yaneva et al., 1997). Ku purified from human placenta by MonoQ chromatography also showed the presence of substantial 3'-phosphotyrosine processing

Figure 21: Relative end-processing efficiencies of JRL 3 and 5 mitochondrial extracts

An 18-mer containing 3'-phosphotyrosine or a 14-mer containing 3'-PG was treated with 1 µl of undiluted or1 µl of seven 1:8 dilutions of each of the mitochondrial extracts derived from JRL 3 and 5 cell-lines for 15 minutes at 37° C in Kedar buffer containing 5 mM EDTA. Samples were boiled for 1 minute at 90 ºC. A final concentration of 20 mM Mg^{2+} and 20 ng hPNKP were added. Conversion to 3'-OH was assessed by denaturing gel electrophoresis and quantified using ImageQuant software. Our results showed ~ 34% and ~ 15% conversion from 3'-phosphotyrosine to the 3'-OH product with the undiluted and the first 1:8 diluted JRL 5 samples respectively and absolutely no conversion to 3'-OH with the JRL 3 mitochondrial extract.

Figure 21

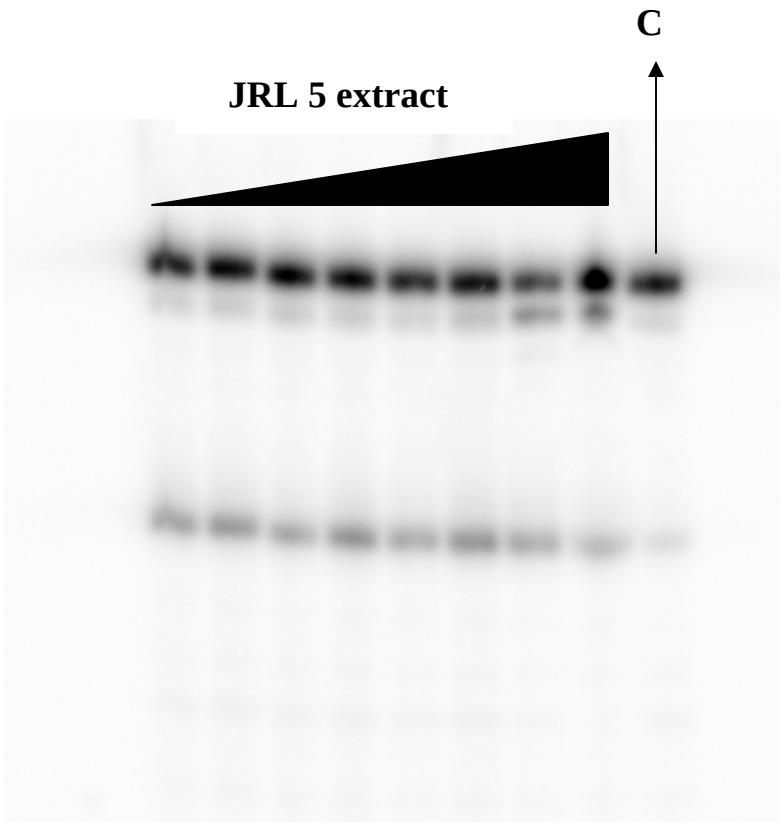

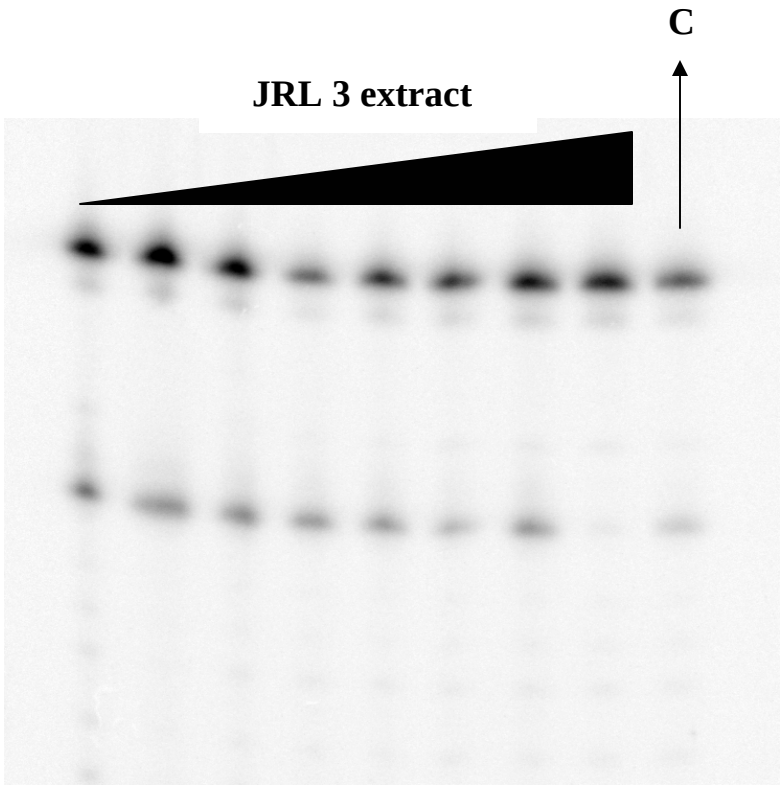

activity (Inamdar et al., 2002). This association of glycolate removing activity with human placental Ku raised the possibility that Ku may bind to Tdp1 and recruit it to the DNA ends. When we compared the efficiencies with which this purified Ku processes both a 3'-phosphotyrosine containing 18-mer and a 3'-PG containing 14-mer, we found that there was a 10-fold difference similar to that of human Tdp1 partially purified from lymphoblastoid while-cell extracts (figures 22a and 22b). Although Ku does not bind to single-stranded substrates, binding of Ku to Tdp1 could modify its specificity. To examine this possibility, hTdp1-catalyzed tyrosine and glycolate removal from the 18-mer with 3'-phosphotyrosine and the14-mer with 3'-PG respectively, was assayed in the presence and absence of 20 ng of recombinant Ku, which unlike the human placental Ku, was free of any PG-processing activity. As shown in figures 23a and 23b, the effect of recombinant Ku was inhibitory i.e., the presence of recombinant Ku decreased the susceptibility of both substrates to hTdp1-mediated processing (compare to Fig 14). However, phosphotyrosyl processing was inhibited more than the PG-processing, so that in the presence of Ku the ratio of processing efficiencies was reduced from 100-fold to 26-fold. This result suggests possible interaction between hTdp1 and Ku.

Processing of a double-stranded substrate with 3'-PG overhang is partially inhibited by Ku

Since Ku is part of the repair complex that repairs DSBs via the NHEJ pathway, we looked at the effect of Ku on hTdp1 activity using a double-stranded substrate with a 3'-PG-terminated 3' overhang. The substrate was pre-incubated with various dilutions of recombinant Ku for 5 minutes to allow binding to the open end of the substrate followed by incubation with hTdp1 for 10 minutes to allow PG-processing. Following boiling of

Figure 22a and b: Processing of a 3'-PG oligomer by Ku derived from placental tissue

A 3'-phosphotyrosine 18-mer (●) or a 3'-PG 14-mer (○) was treated with 170, 21.25, 2.65, 0.33, 0.042, 0.0052 or 0.00065 ng of Ku, purified from placental tissue by MonoQ chromatography. Each 5µl reaction was incubated at 37 ºC for 2 hours in Kedar buffer containing 5 mM EDTA. Samples were boiled for 1 minute at 90 ºC. 20 mM Mg^{2+} and 20 ng hPNKP were added. Conversion to 3'-OH was assessed by denaturing gel electrophoresis and quantified using ImageQuant software. The relative end-processing efficiencies was found to be approximately 10-fold.

Figure 22a

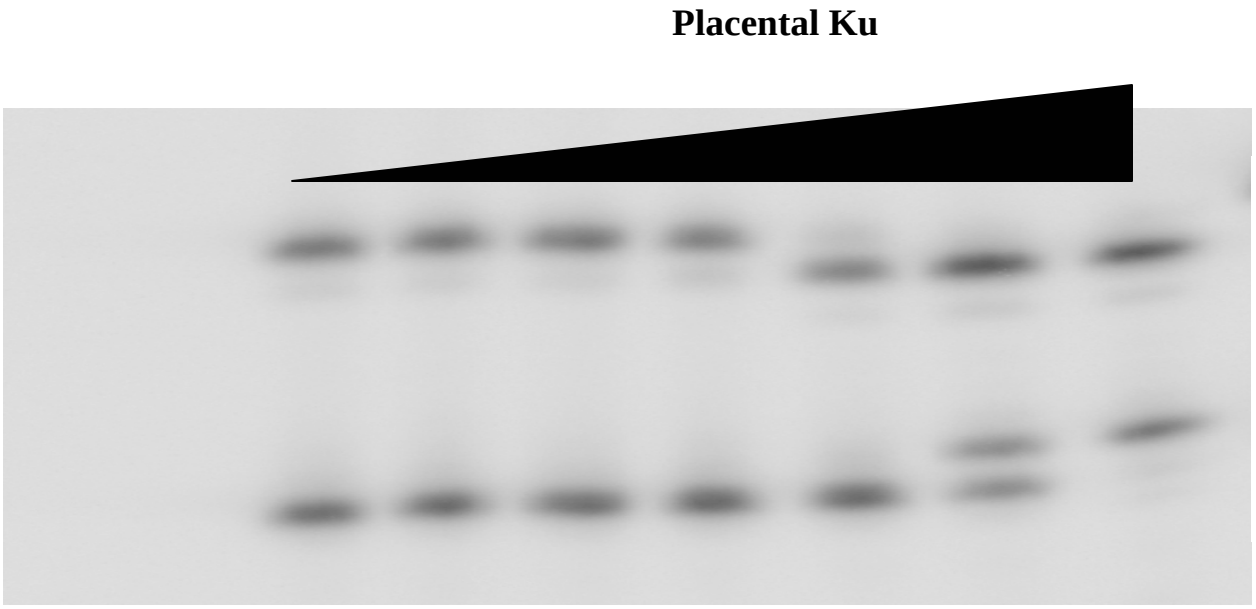

Figure 22b

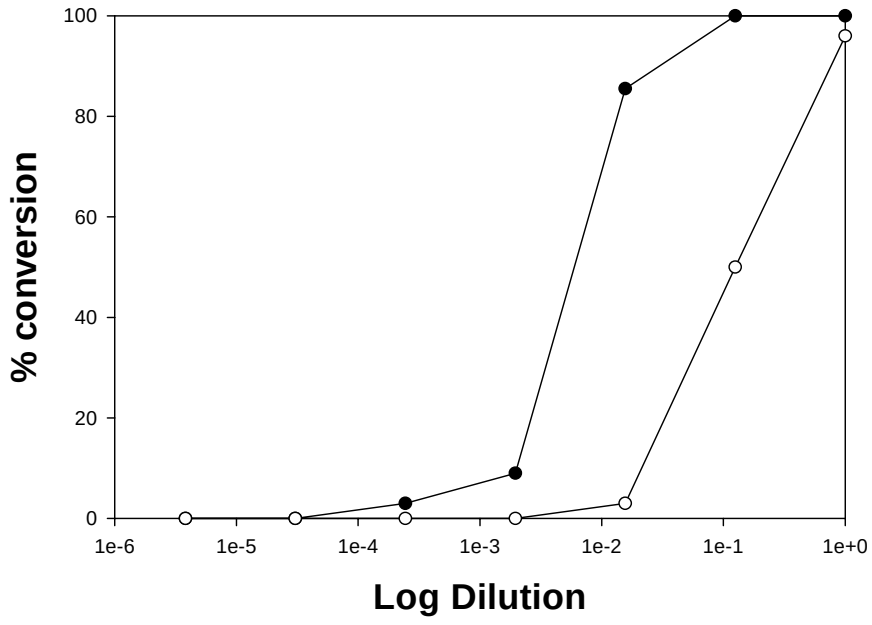

Figure 23a and b: Processing of 3'-PG and 3'-phosphotyrosine oligomers by hTdp1 in the presence of recombinant Ku

A 3'-phosphotyrosine 18-mer (●) or a 3'-PG 14-mer (○) was treated with 20 ng of recombinant Ku, commercially obtained from Trevigen, Inc., and 50, 6.25, 0.78, 0.098, 0.012, 0.0015 or 0.0002 ng of FLAG-hTdp1, purified from adenovirus infected U-87 glioma cells. The sample without Ku contained 50 ng of FLAG-hTdp1. Each 5µl reaction was incubated at 37 ºC for 15 minutes in Kedar buffer containing 5 mM EDTA. Samples were boiled for 1 minute at 90 ºC. 20 mM Mg^{2+} and 20 ng hPNKP were added. Conversion to 3'-OH was assessed by denaturing gel electrophoresis and quantified using ImageQuant software. The difference in end-processing efficiencies for the two substrates was found to be approximately 26-fold.

Figure 23a

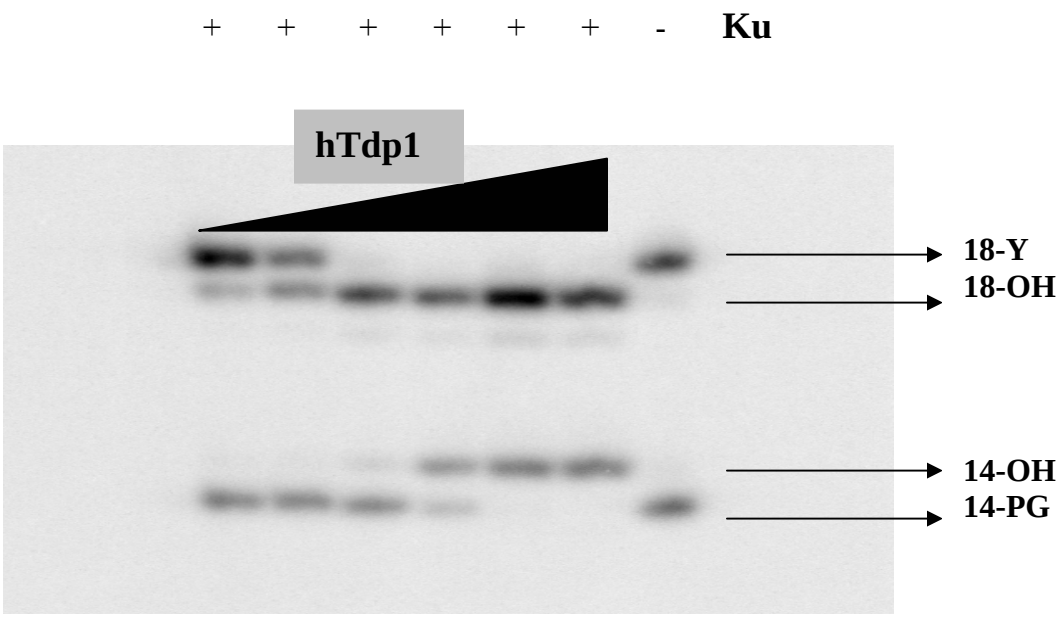

Figure 23b

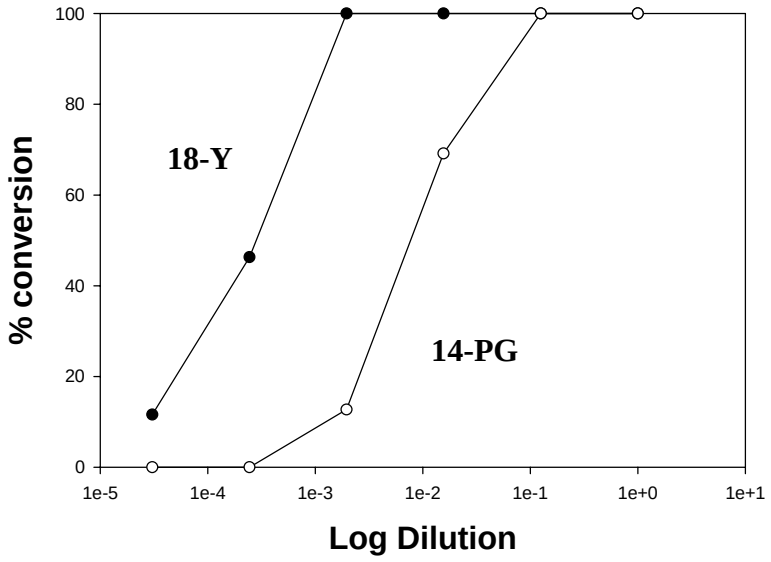

26-FOLD

PG terminus to hTdp1 when Ku is bound to the DNA end or direct interaction between hTdp1 and Ku. However, there is no evidence that Ku recruits hTdp1 to DNA ends or facilitates hTdp1-mediated end processing (Figures 24a and 24b).

Since our results showed that Ku inhibited Tdp1, we carried out similar experiments with very high concentrations of a truncated form of Ku in order to see if these high concentrations inhibited the activity of Tdp1 completely. This truncated form lacks a carboxy-terminal 19K domain known to function in DNA-PK recruitment, but which is dispensable for DNA end binding (Wlaker et al., 2001) and observed that 1 μg concentration of truncated Ku inhibited the FLAG-hTdp1 activity by nearly 80% (Figure 24c).

Processing of the double-stranded substrate with 3'-PG overhang is partially inhibited by Ku-DNA-PK and Ku-DNA-PK-XRCC4/ligase IV complexes.

On comparing the processing efficiency of samples in which both Ku and DNA-PK were incubated with the double-stranded substrate containing a 3'-PG overhang with that of samples in which DNA-PK was pre-incubated alone, we observed that the ability to process PGs by Tdp1 in samples with both Ku and DNA-PK was inhibited more than in samples with DNA-PK alone (Figures 25a and 25b). Similar results were observed when XRCC4/ligase IV was added to the complex i.e. samples containing Ku, DNA-PK and XRCC4/ligase IV inhibited Tdp1 activity more than samples containing DNA-PK and XRCC4/ligase IV only (Figures 26a and 26b). These data again suggest that once the end-joining repair complex is formed on DNA ends, end processing by Tdp1 is at least partially inhibited.

Figure 24a and b: Effect of different dilutions of Ku on FLAG-hTdp1 activity.

A double-stranded plasmid with a 3'-PG overhang was pre-incubated with 15, 30, 45, 60 or 75 ng (15 ng = 100fmoles) of recombinant Ku, obtained from Trevigen, Inc., for 5 minutes in Kedar buffer followed by incubation with 0.78 ng of FLAG-hTdp1, purified from adenovirus infected U-87 glioma cells, for 10 minutes to allow PG-processing. Following boiling of the samples at 90°C for 2 minutes, the substrate was incubated with 1000 units/ mL CIP for 1 hour at 37°C for removal of phosphate group. The samples were again heated at 90°C for 5 minutes and then incubated with *Taq*$^{\alpha}$*1* for 3 hours at 65°C to yield a 15-mer with the 3'-OH. Our results showed that increasing concentrations of Ku had an inhibitory effect on hTdp1 activity.

Figure 24a

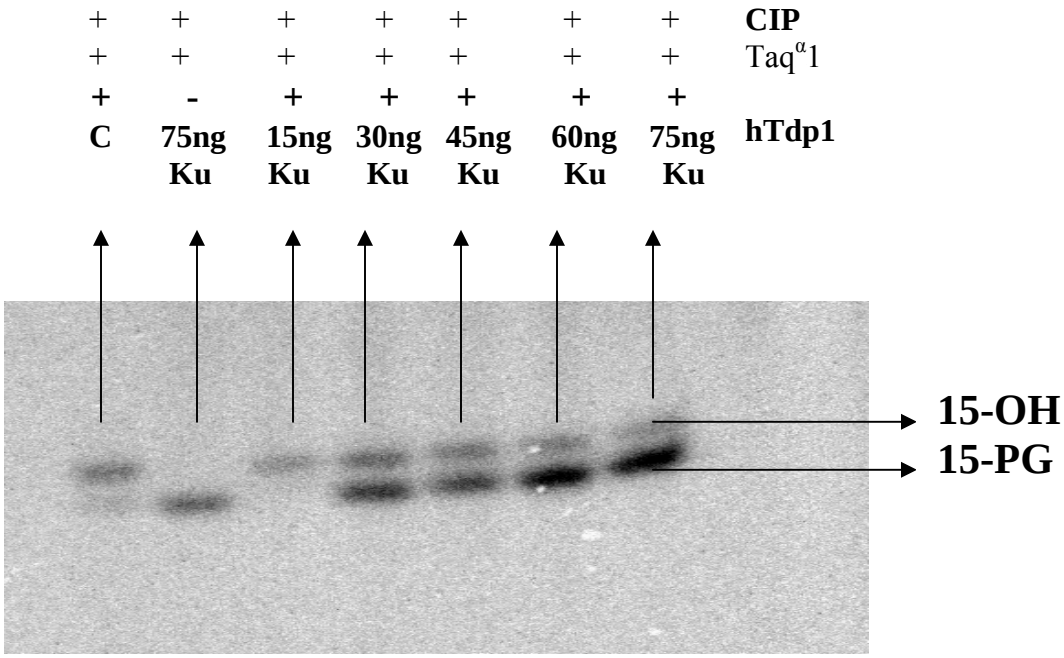

Figure 24b

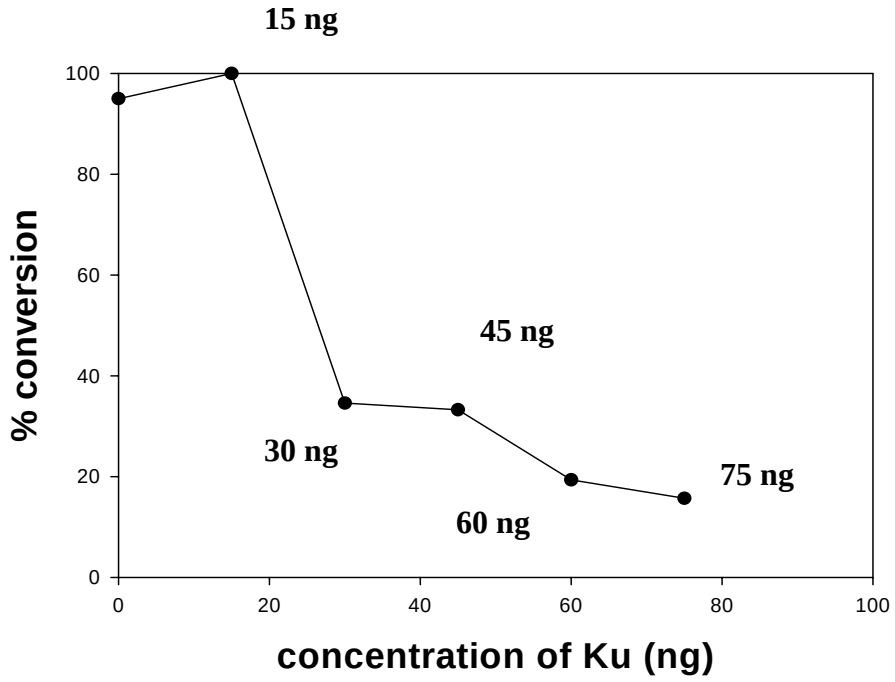

Figure 24c: Effect of different concentrations of truncated Ku on FLAG-hTdp1 activity

A double-stranded plasmid with a 3'-PG overhang was pre-incubated with 20, 50, 100, 200, 400 or 1000 ng of recombinant truncated Ku for 5 minutes followed by incubation with 0.78 ng of FLAG-hTdp1, purified from adenovirus infected U-87 glioma cells, for 10 minutes to allow PG-processing. Following boiling of the samples at 90°C for 2 minutes, the substrate was incubated with CIP for 1 hour at 37°C for removal of phosphate group. The samples were again heated at 90°C for 5 minutes and then incubated with *Taq*$^{\alpha}$*1* for 3 hours at 65°C to yield a 15-mer with the 3'-OH. Our results showed that increasing concentrations of Ku had an inhibitory effect on hTdp1 activity.

Figure 24c

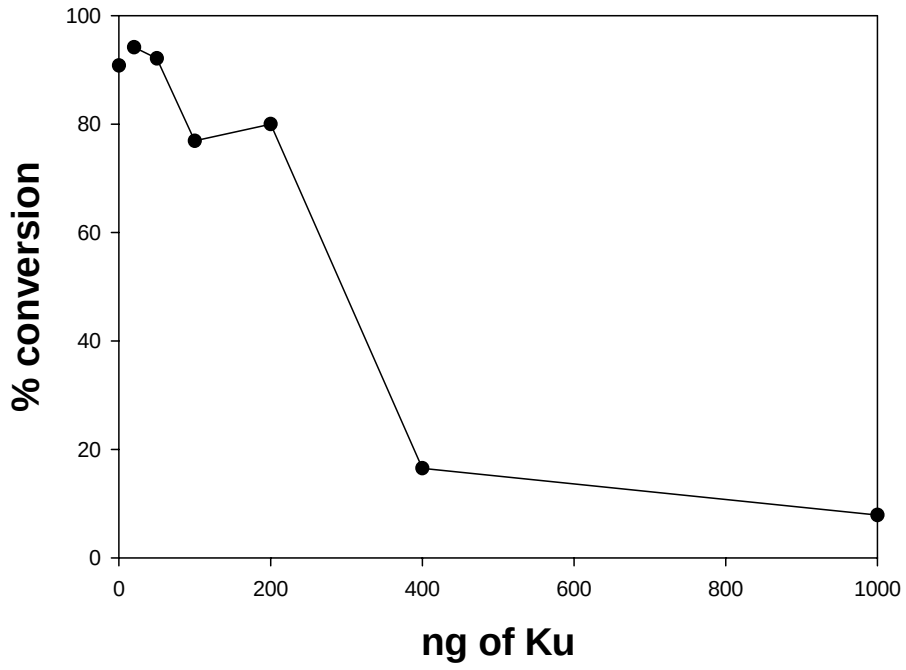

Effect of different dilutions of Ku-DNA-PK complex on FLAG-hTdp1 activity

Figure 25a- A double-stranded plasmid with a 3'-PG overhang (2 fmoles) was pre-incubated with 27 ng of recombinant Ku (180 fmoles) and 0, 4, 20, 100, 200 or 300 ng of DNA-PK for 5 minutes at 25 °C followed by incubation with 0.78 ng of FLAG-hTdp1, purified from adenovirus infected U-87 glioma cells, for 10 minutes in Ramsden buffer containing 100 μM ATP and 5 mM $MgCl_2$ to allow PG-processing. After boiling of the samples at 90°C for 2 minutes, the substrate was incubated with CIP for 1 hour at 37°C for removal of phosphate group. The samples were again heated at 90 °C for 5 minutes and then incubated with *Taq*$^{\alpha}$*1* for 3 hours at 65°C to yield a 15-mer with the 3'-OH. Our results showed that samples containing Ku and DNA-PK inhibited Tdp1 activity more than samples containing DNA-PK only.
Figure 25b: The experiment was carried out in triplicates; each showing a similar result.

Figure 25a

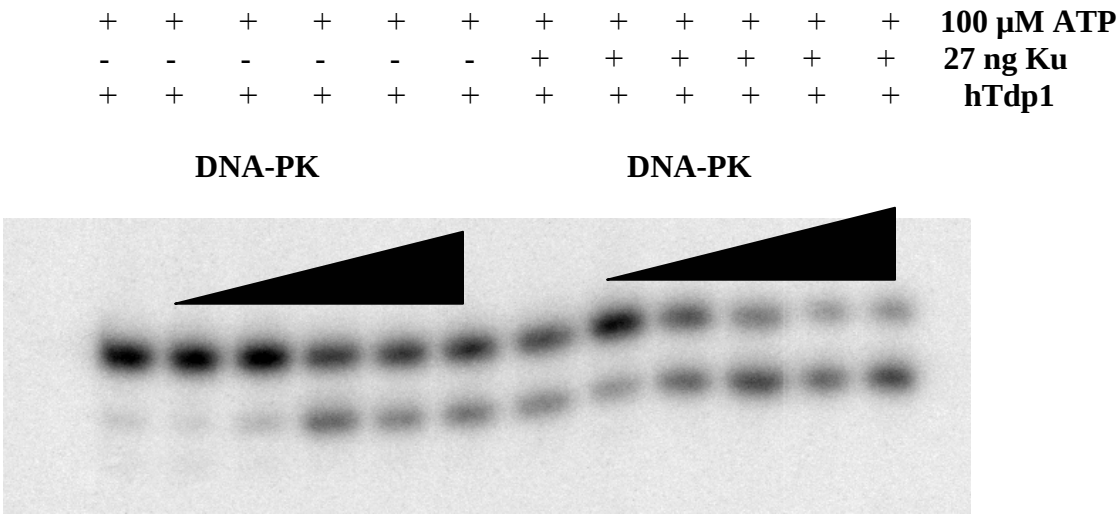

Figure 25b

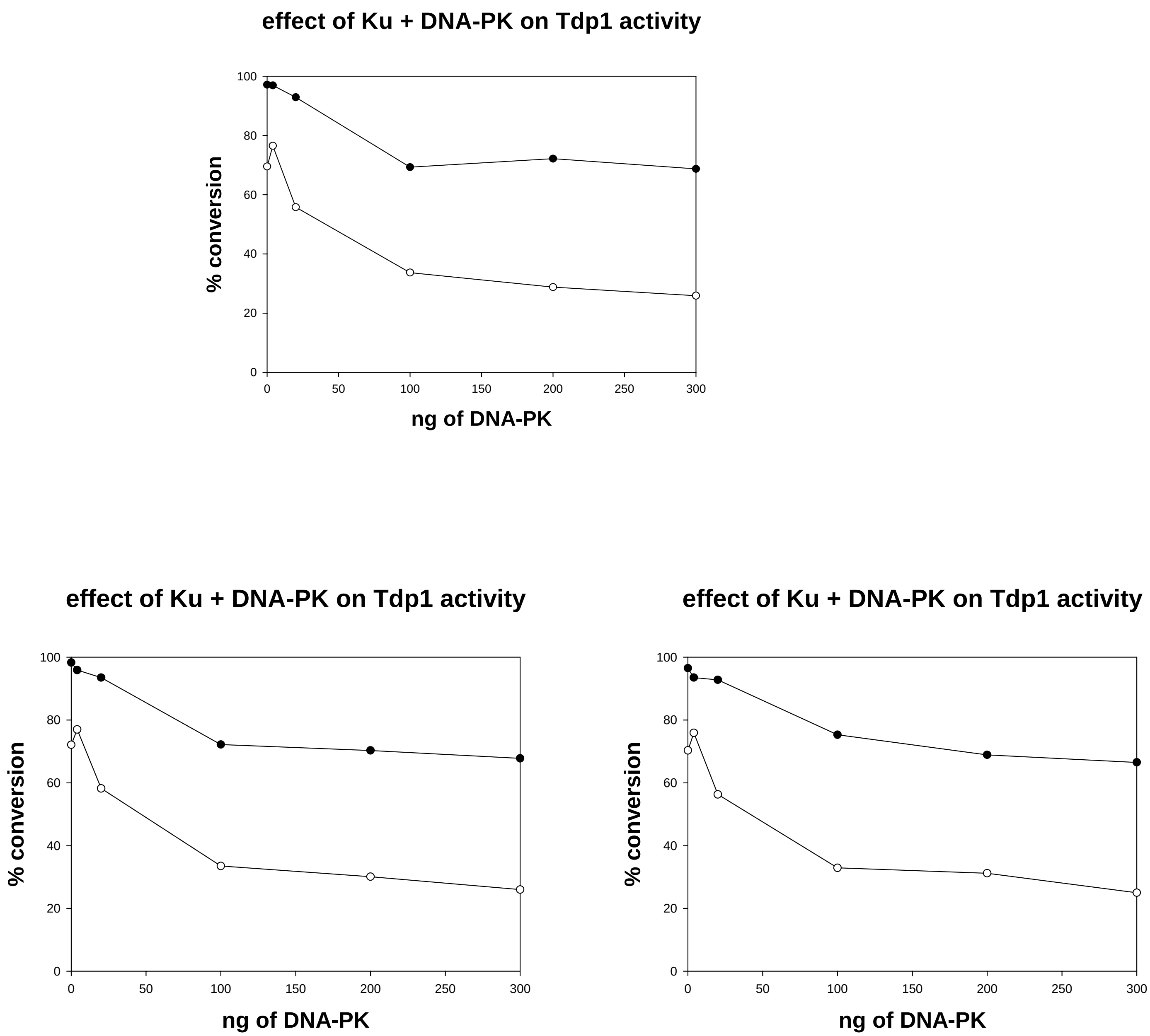

○ **DNA-PK + Ku**

● **DNA-PK alone**

Effect of different dilutions of Ku-DNA-PK-XRCC4/ligase IV complex on FLAG-hTdp1 activity

Figure 26a: A double-stranded plasmid with a 3'-PG overhang was pre-incubated with 27 ng of recombinant Ku (180 fmoles) and 0, 4, 20, 100, 200 or 300 ng of DNA-PK for 5 minutes at 25 °C followed by pre-incubation with 10 nM XRCC4/ligase IV (50 fmoles) for 5 minutes at 25 °C. reactions were carried out in Ramsden buffer containing 100 μM ATP and 5 mM $MgCl_2$. A control experiment in which the double-stranded plasmid was incubated with DNA-PK and XRCC4/ligase IV was also simultaneously carried out. 0.78 ng of FLAG-hTdp1, purified from adenovirus infected U-87 glioma cells, was added for 10 minutes to allow PG-processing. Following boiling of the samples at 90°C for 2 minutes, the substrate was incubated with CIP for 1 hour at 37°C for removal of phosphate group. The samples were again heated at 90 °C for 5 minutes and then incubated with *Taq*$^{\alpha}$*1* for 3 hours at 65°C to yield a 15-mer with the 3'-OH. Our results showed that samples containing Ku, DNA-PK and XRCC4/ligase IV inhibited Tdp1 activity more than samples containing DNA-PK and XRCC4/ligase IV only.
Figure 26b: the experiment was carried out in triplicates; each showing similar results.

Figure 26a

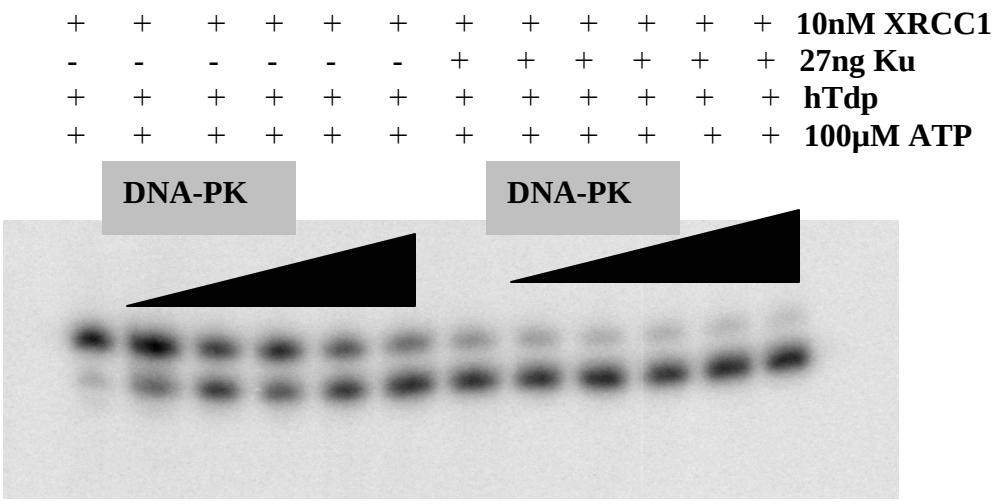

Figure 26b

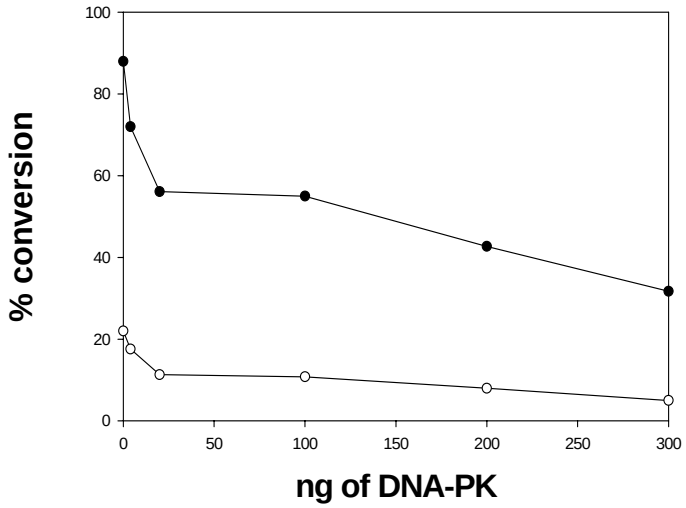

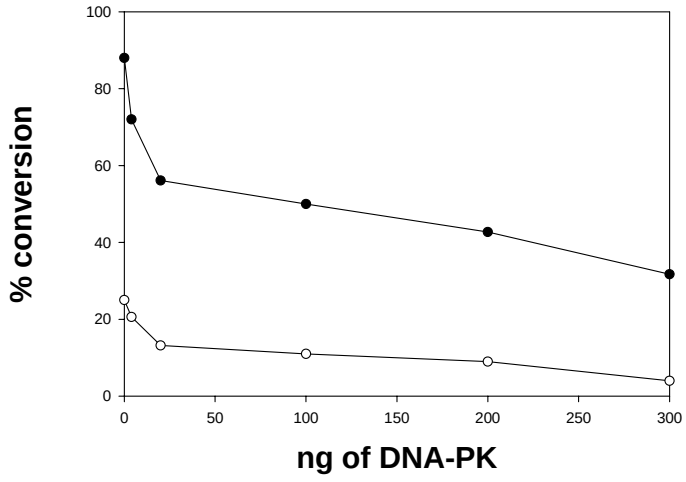

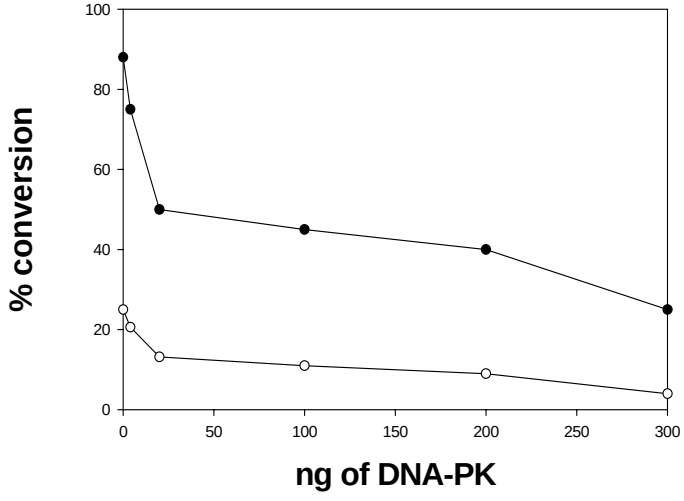

○ **XRCC1+DNA-PK + Ku**

● **DNA-PK + XRCC1**

Inhibition of DNA-PK autophosphorylation does not show a marked inhibition on Tdp1 activity.

Chan et al. (2002) and Soubeyrand et al. (2003) indicated that cellular end-joining requires DNA-PKcs to undergo autophosphorylation. They showed the presence of six autophosphorylation sites clustered within a 40-amino acid region. Later, Reddy et al. (2004) showed that autophosphorylation at these six sites uniquely makes DNA ends accessible while still allowing DNA-PKcs to persist at ends and retain XRCC4-ligase IV within a complex at the ends. Their results indicate that autophosphorylation of the six sites leads to a destabilization of DNA-PK that is critical for significant end-joining activity. Therefore, they propose that autophosphorylation within the six sites is uniquely able to direct a rearrangement of the DNA-PK complex at DNA ends that is essential for end-joining both *in vitro* as well as in cells. Based on this information, we looked at the effect of autophosphorylation of DNA-PK on Tdp1 activity. We assumed that since, according to Reddy and colleagues, autophosphorylation destabilizes DNA-PK and increases cellular end-joining, inhibition of autophosphorylation would stabilize the DNA-PK on the DNA ends, thus markedly inhibiting the Tdp1 activity. But our results showed that the presence of ATP (Figures 25a and b) resulted in only a slight reduction in the inhibition caused by presence of DNA-PK at the DNA ends. Thus based on results with purified proteins, autophosphorylation of DNA-PK does not appear to play a major role in regulating accessibility of DNA ends to hTdp1 (Figures 27a and 27b). it is possible that the putative conformational change in DNA-PK that is induced by autophosphorylation has a greater effect on the susceptibility of DNA ends to

exonucleolytic degradation (which was assayed by Reddy et al) than to simple glycolate removal by Tdp1.

Effect of inhibition of autophosphorylation of DNA-PK on hTdp1 activity.

Figure 27a: A double-stranded plasmid with a 3'-PG overhang (2 fmoles) was pre-incubated with 27 ng of recombinant Ku (180 fmoles) and 0, 4, 20, 100, 200 or 300 ng of DNA-PK for 5 minutes at 25 °C followed by incubation with 0.78 ng of FLAG-hTdp1, purified from adenovirus infected U-87 glioma cells, for 10 minutes in Ramsden buffer without ATP and Mg^{+2}. A control experiment in which the double-stranded plasmid was incubated with DNA-PK and FLAG-hTdp1 alone was also simultaneously carried out. After boiling of the samples at 90°C for 2 minutes, the substrate was incubated with CIP for 1 hour at 37°C for removal of phosphate group. The samples were again heated at 90 °C for 5 minutes and then incubated with *Taq*$^{\alpha}$*1* for 3 hours at 65°C to yield a 15-mer with the 3'-OH. Our results showed did not show a dramatic inhibition of hTdp1 activity as was expected.
Figure 27b: The experiment was carried out in triplicates; each showing a similar result.

Figure 27a

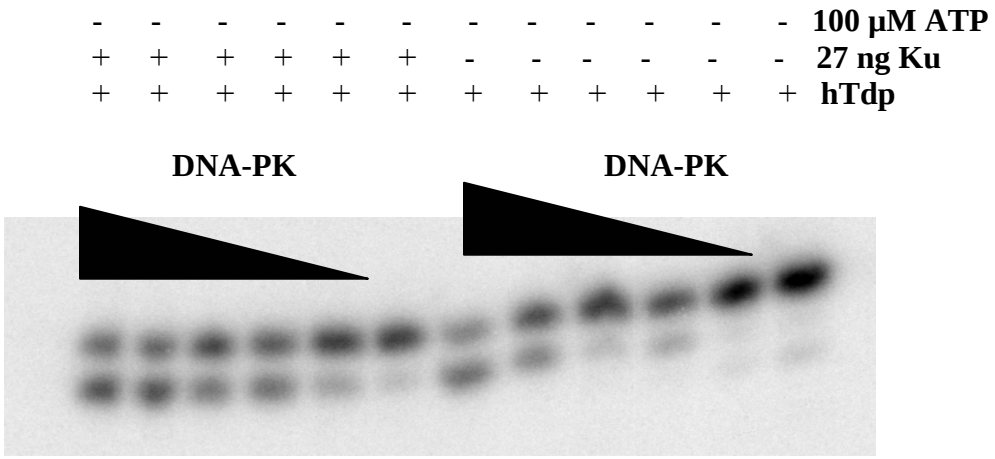

Figure 27b

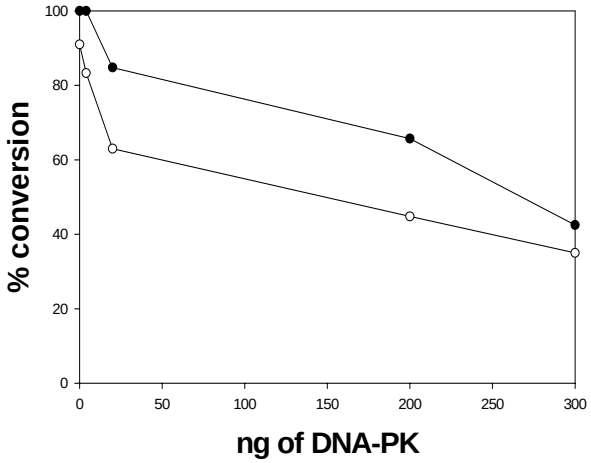

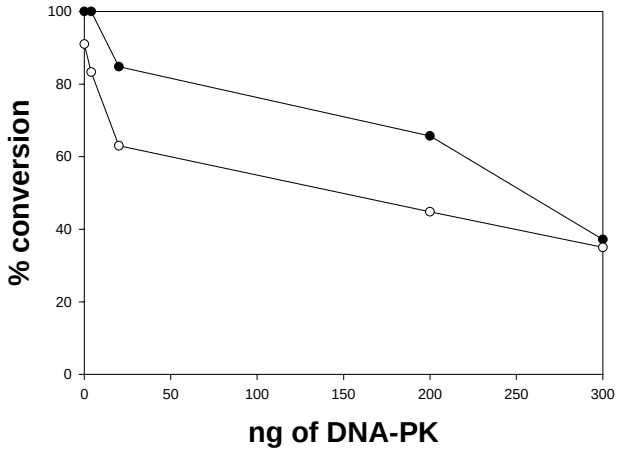

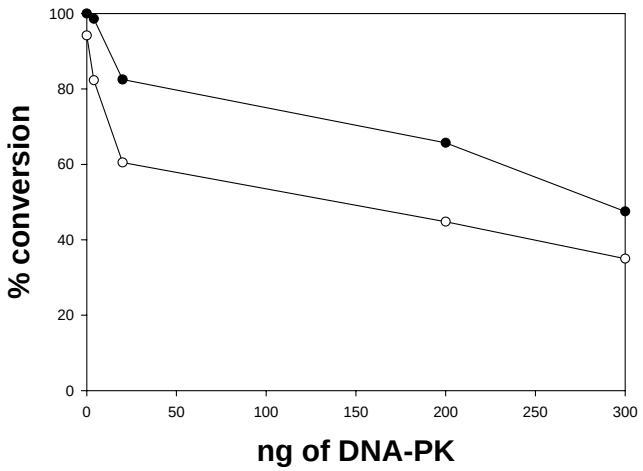

○ **DNA-PK + Ku**

● **DNA-PK alone**

Discussion

The main conclusions of this study are- 1. Altered specificity of Tdp1 in extracts *vs*. recombinant Tdp1 is due to interactions with other proteins rather than post-translational modification. 2. There was no detectable binding of NHEJ proteins with Tdp1 by western blot analysis. 3. All NHEJ proteins alone or in combination inhibited Tdp1 activity on 3‘-overhangs. 4. Mitochondria contain PG and phosphotyrosine processing activity attributable to Tdp1.

DSBs induced by radiomimetic antibiotics such as neocarzinostatin and calicheamicin typically have PG-terminated 3′ overhangs at one end of the break (Giloni et al., 1981). About half of radiation-induced strand breaks also have 3′-PG termini (Henner et al., 1983), and many of these are presumably on 3′ overhangs of DSBs. In the repair of such lesions, removal of the 3′-PG termini must necessarily precede any polymerase-mediated gap filling and/or religation of the DSB. However, while the human apurinic/apyrimidinic endonuclease Ape1 can remove PGs, albeit inefficiently, from blunt and recessed 3′ termini of DSBs, PGs on 3′ overhangs are completely refractory (Suh et al., 1997). The human polynucleotide kinase/phosphatase PNKP, which removes 3′ phosphates from single-stranded 3′ termini (Jilani et al., 1999), also had no detectable effect on 3′-PGs (Inamdar et al., 2002), just as was previously reported for rat polynucleotide kinase/phosphatase (Habraken et al., 1988). The susceptibility of 3′-PGs to *E.coli* exonuclease I (Sandigursky et al., 1993) raised the possibility that PGs on 3′ overhangs might be removed by a mammalian 3′-> 5′ exonuclease. However, DNase III,

which is the dominant 3′->5′ exonuclease in mammalian cell extracts, has no detectable effect on any 3′-PG substrates (Inamdar et al., 2002). The Wrn1 and Mre11 3′->5′ exonucleases are also unlikely candidates because both show a strong preference to recessed 3′ termini and 3′ overhangs, even if unblocked, are resistant to these enzymes (Kamath-Leob et al., 1998, Huang et al., 2002). The *Sacchromyces cerevisiae* Rad1/Rad10 endonuclease (and presumably its human ERCC1/XPF homolog) can remove a single 3′-PG (or 3′-OH) nucleotide from the 3′ end of a single-strand break in double-stranded DNA (Guzder et al., 2004), but no such activity has been reported on PG-terminated 3′ overhangs. Similarly, while Artemis, a DNA-PK activated endo/exonuclease, has been implicated in DSB repair (Moshous et al., 2001), this enzyme appears to act only on 3′-overhangs longer than 4 bases (Ma et al., 2002). Nevertheless, PGs on overhanging 3′ termini clearly are processed in *Xenopus*, human and hamster cell extracts (Ma et al., 2002).

Evidence for a 3′-phosphate intermediate in 3′-PG removal in human cell extracts (Inamdar et al., 2002) suggested possible involvement of hTdp1, and indeed, experiments carried out in our laboratory showed that both hTdp1 and scTdp1 were found to catalyze similar glycolate removal from a single-stranded oligomer as well as from a single-strand overhang of a DSB. Failure to detect this activity in previous studies could have been due to the very small difference in electrophoretic mobility between 3′-PG and 3′-phosphate oligomers and the relative inefficiency of PG processing by recombinant hTdp1 compared to its normal substrate, 3′-phosphotyrosine.

DSBs generated by ionizing radiation cannot be repaired by simple ligation because end joining is more complex due to the presence of fragmented sugars and

damaged or missing nucleotides at DNA ends. DNA treated with antibiotic bleomycin (Giloni et al., 1981) or exposed to IR (Henner et al., 1983) contains DSBs formed by sugar oxidation and fragmentation. Free radical-mediated oxidation of the C-4′ position of the deoxyribose in DNA results in sugar fragmentation and strand cleavage, releasing base propenal and leaving the two-carbon fragment-PO_4CH_2COOH, or PG, linked to the 3′-end of the break. These end groups will block the activities of DNA polymerase and DNA ligase enzymes (Noguti et al., 1975). About half of radiation-induced strand breaks have 3′-PG termini and many of these are presumably on 3′-overhangs of DSBs. In the repair of such lesions, removal of the 3′-PG termini must necessarily precede any polymerase-mediated gap filling and/or religation of the DSB. Strand breaks with modified 3-termini are two times more toxic than their 3′-OH counterparts (Kow et al., 1991).

Tyrosyl DNA phosphodiesterase (Tdp1) is the only enzyme known so far to function in DNA repair and remove blocks to leave 3′--phosphate ends. Our results showed that both yeast and human Tdp1 processed PG substrates efficiently and gave rise to 3′-phosphate product corresponding to a band that migrated between the PG and hydroxyl bands. Thus, Tdp1 is capable of selectively removing the glycolate from PG to leave behind 3′-phosphate ends that are efficiently converted to hydroxyl ends by PNKP as indicated by generation of a 3′-OH when the substrate was incubated with both the enzymes together. The crystal structure of hTdp1 (Davies et al., 2002) shows the presence of an active site in the enzyme consisting of histidine and lysine residues that are conserved in the HKD motif of phospholipase D superfamily of proteins, of which Tdp1 is a member. These residues lie close to a 40A long cleft that runs along one surface

of the protein. The active site is in the center of a 2-fold axis of symmetry between two domains in the enzyme. Based on structural and biochemical data, the conserved PLD superfamily reaction mechanism has been proposed to consist of two consecutive SN2 substitutions (Interthal et al., 2005). In the first step of the reaction, a histidine residue in the N-terminal HKD motif (His263) is proposed to carry out a nucleophilic attack on the phosphorous atom in the phosphodiester bond between the tyrosine residue and the DNA 3′ oxygen to become covalently attached to the 3′ end of the DNA via a phosphoamide bond to the Nε2 atom of the nucleophilic His263 (Davies et al., 2003 and Raymond et al., 2004). In the final step, hydrolysis of this intermediate is believed to be carried out by a water molecule that is activated by His493 from the C-terminal HKD motif acting as a general base. This Tdp1 catalysis thus produces free tyrosine and a DNA with a 3′-phosphate end. Thus, it is tempting to speculate here that a histidine residue from one domain of the active site could carry out a nucleophilic attack on the phosphorous from the PG group thus leading to the dissociation of glycolate to leave behind 3′-phosphates. The PG substrate however, required a higher concentration of the enzyme (scTdp1 as well as hTdp1) than the control phosphotyrosine substrate. The crystal structure of the enzyme as well as its mode of action on the topoisomerase I-DNA complexes may help to explain this difference in substrate specificity. The topoisomerase I-DNA phosphodiester bond is buried deep inside the covalent complex (Davies et al., 2002) and topoisomerase I needs to be degraded and the DNA unwound for easy access and efficient functioning of the enzyme. Therefore, DNA unwinding as well as the presence of a protein at the end of the DNA, both may be necessary pre-requisites for optimal functioning of the enzyme. The PG substrate lacks this protein-DNA configuration at its

end. This difference in end-structure of the substrate may account for the lower efficiency of Tdp1 on PG substrates. Since our experiments provided no evidence that the low activity of the recombinant enzyme on the PG substrates when compared to crude or fractionated cell extracts was due to lack of proper post-translational modifications, presence of the N-terminal epitope tag, or degradation or alteration of the recombinant protein during its preparation, we can speculate that the apparent increase in the inactivity of the native protein toward PG substrates may be the effect of its interactions with other repair factors in the extracts.

Although Cheng et al. in 2002 proposed that Mn^{2+} has a stimulatory effect on Tdp1 activity, our experiments showed that adding 5mM Mn^{2+} in our reaction buffer did not show any increase in PG-processing activity of hTdp1. This is in agreement with Yang et al. (1996) who proposed that Tdp1 activity is independent of any co-factor requirement. According to them, there was no stimulation of Tdp1 activity when reactions were conducted in the presence of a simple buffer that was supplemented with 10mM Mg, Ca, Co, Cd and Zn. Experiments conducted in our laboratory also showed that both crude extracts as well as purified Tdp1 (both yeast and human) processed PGs in the presence of EDTA suggesting that glycolate removal was independent of co-factor requirement.

Human mitochondria contain ~5-10 copies per mitochondrion of a covalently closed duplex DNA genome (Moraes et al., 2001). Because mitochondrial DNA molecules are closed circular and therefore topologically constrained, there must be a mechanism to relieve the DNA strain that arises during replication. Zhang et al. (2001) reported the existence of a mitochondrial topoisomerase I gene *TOP1mt*, which is

localized on human chromosome 8q24. They found a high degree of homology between top1mt and nuclear topo1 which was further demonstrated by the top1mt protein being sensitive to CPT treatment (Tua et al., 1997), thus generating DNA strand breaks by blocking the re-ligation of topo1-linked DNA breaks. The formation of the mitochondrial topo1-DNA covalent complex lead us to speculate that Tdp1 within the mitochondria may be involved in repair of DSBs with 3′-PG termini that might arise as a result of oxidative stress. Indeed our western blot analysis of mitochondrial extracts from the GM cell line showed the presence of Tdp1. Our substrate processing assays also show that both the whole-cell and mitochondrial extracts have comparable PG and tyrosine processing efficiencies suggesting that mitochondrial Tdp1 is as abundant as its cytoplasmic counterpart.

DNA DSB repair in vertebrate cells occurs mainly by the mechanism of non-homologous end-joining. This phenomenon was first demonstrated in CV1 monkey kidney cells by transfecting into them a plasmid with a polylinker inserted in the intron of SV 40 T-antigen. Prior to transfection, the polylinker was restriction digested with various enzymes to create linear DNA with mismatched ends (Roth and Wilson, 1986). Analysis of repair joints formed by the system from linearized plasmids revealed that ends with non-complementary or partially complementary 3′ and 5′-overhangs were in many cases efficiently joined via post-repair ligation without loss of any nucleotides at their termini. This ligation involved alignment of short partial complementarities from each single-stranded extensions to create gaps in both single strands to be filled in by a polymerase to create ligatable nicks. Similar experiments using Xenopus extracts (Pfeiffer et al., 1994) supported this post-repair ligation process whereby protruding

DNA ends are held in alignment during processing of mismatched 3-overhangs followed by fill-in synthesis. These experiments suggested the existence of alignment factor(s) to properly align the protruding single-strand tails in short overlaps as well as to hold abutting ends in juxtaposition. Petra Pfeiffer et al. provided a direct evidence for existence of such an alignment factor by showing that the efficiency and accuracy of NHEJ is dramatically reduced in *xrs6* extracts deficient in Ku 70/80 heterodimer and that the lack of accuracy was due to inability to align the two broken ends for DNA fill-in synthesis (Feldmann et al., 2000). These results imply that Ku plays a critical role in aligning the two broken ends together and protecting the overhangs during end-joining. Further proof came from experiments that showed that Ku actively binds the ends of DNA DSBs and promotes association of the DNA ends with each other (Pang et al., 1997). One heterodimer binds to each end and the two heterodimers interact with each other (Cary et al., 1997), thereby bridging the two DNA ends. This serves to protect the ends from processing and degradation as well as accounts for stimulation of intermolecular ligation by eukaryotic ligases (Ramsden and Gellert, 1998). DNA-PKcs associates with the Ku heterodimer and is recruited to the DNA ends by Ku which then activates its kinase function Featherstone and Jackson, 1999). A number of proteins can be phosphorylated by DNA-PK but the significance of this phosphorylation is not clear. Several observations, including its ability to associate with and phosphorylate Artemis thus, activating the latter's endonuclease activity (Ma et al., 2002), suggest a specific role for DNA-PKcs in directing end-processing events; however, DNA-PKcs deficiency affects cellular end-joining even when processing is not required (Bogue et al., 1998). A more general role for DNA-PKcs in end-joining is also consistent with *in vitro* evidence

indicating that it helps Ku recruit the XRCC4-ligase IV complex to DNA ends (Chen et al., 2000) and promotes the intermolecular synapsis of two the DNA ends (DeFazio et al., 2002). Together, these functions of DNA-PKcs may explain why XRCC4-ligase IV activity is necessary *in vitro* when using substrates that do not require processing (Hanakahi et al., 2000).

Valerie and Povirk (2003) proposed an in vitro model for the NHEJ repair pathway. According to their proposal, DNA DSBs induced by IR or bleomycin with 3′-PGs are first recognized by Ku heterodimer. Upon binding to the ends, Ku properly positions itself such that it bridges the two ends and aligns them together for repair to proceed by fill-in and ligation. Ku then recognizes the PG groups at the ends and recruits hTdp1 and PNKP, which then effectively carry out the conversion of PG to glycolate to hydroxyl ends in sequential and well-coordinated steps. The hydroxyl ends are bound and protected by Ku until it recruits DNA-PKcs, which displaces Ku ~10 base pairs to the interior of the DNA from the ends so that its can properly align itself at the end. DNA-PK then recruits and phosphorylates additional proteins such as exonucleases, Artemis and XRCC4/DNA ligase IV to the ends to form the NHEJ repair complex. DNA-PK finally undergoes autophosphorylation and removes itself from the ends to allow fill-in and re-ligation. But experiments conducted in our laboratory did not show any evidence for the above model. In our experiments, when purified Ku alone was pre-incubated with substrates followed by addition of Tdp1, Ku had an inhibitory effect on the removal of glycolate by Tdp1. If Ku did recruit Tdp1, then there should have been an increase in the latter's activity, not a marked inhibition. Ku is known to bind to the broken DNA ends and protect them from degradation by nucleases. The inhibitory effect of Ku on Tdp1 is

in agreement with this well acknowledged function of Ku. It is possible that Tdp1 actually processes the DNA ends even before Ku binds to it. It is also possible that in the presence of Ku, DNA cannot be properly threaded into the DNA binding cleft on Tdp1 protein. Cross-linking studies (Yoo and Dynan, 2000) show that when DNA-PK is recruited to the ends, Ku moves to the interior of the DNA, facilitating the binding of DNA-PK. Our Tdp1 activity assays comparing the processing of a plasmid substrate containing 3′-PG overhang by samples in which Ku-DNA-PK complex was pre-incubated versus samples in which DNA-PK was pre-incubated alone showed that when both Ku and DNA-PK are present together, there is more inhibition of Tdp1 activity than with DNA-PK alone. Therefore, though theoretically there was a possibility that once Ku moves interior, the positioning of DNA-PK on the DNA molecule may actually facilitate the access of Tdp1 to the PG groups, our results showed otherwise. One would also predict that autophosphorylation of DNA-PK, which is required for its removal from the DNA-ends, would facilitate Tdp1 activity but once again, our results from experiments conducted without addition of ATP, did not show a marked inhibition of Tdp1 activity which should have been brought about if the ends were blocked by DNA-PK. The pre-incubation of three of the NHEJ key proteins-Ku, DNA-PK and XRCC4-ligase IV also produced a high inhibition of Tdp1 activity. Because of this suppression of Tdp1 activity by DNA-PK, it is tempting to speculate here that such a suppression may require the synapsis of two DNA/DNA-PK complexes (Hammarsten et al., 2000). In intact cells, the bringing together of two broken DNA ends could be quite a slow and complex process (DiBiase et al., 2000), and thus the ability or inability of DNA-PK to protect lone DNA ends from processing could strongly affect the ultimate nature and fidelity of repair.

Takashima et al. (2002) observed that mutation of Tdp1 is associated with spinocerebellar ataxia with axonal neuropathy (SCAN1). The association of this DNA repair protein with SCAN1 is striking in that this is a disease characterized by neurodegeneration but which lacks any obvious extra neurological features such as genetic instability or cancer. Although not proven, it is generally assumed that SCAN1 pathology is a consequence of the failure of mutant Tdp1 to efficiently repair topo1-associated DNA damage (Takashima et al., 2002). This repair deficiency could indirectly confer sensitivity to oxidative damage, as certain oxidative lesions tend to promote formation of topo1 cleavable complexes (Pourquier et al., 1999), which upon replication can be converted to cytotoxic topo1-terminated DSBs (Hsiang et al., 1989). Previous experiments in our laboratory showed that in extracts of SCAN1 cells harboring mutant Tdp1, there was no detectable processing of a PG terminus on a three-base 3′-overhang formed by free radical-mediated DNA cleavage (Zhou et al., 2005). Because a substantial proportion of DNA breaks induced by ionizing radiation bear 3′-PG termini (Henner et al., 1983), cells deficient in processing of PG-terminated DSBs were expected to be profoundly radiosensitive. However, Zhou et al. (2005) showed that, in cell growth assays, only slight radiosensitivity was detected in two of three SCAN 1 cell lines, and then only for fractionated radiation in plateau phase. These results suggest that most PG-terminated DSBs are still repaired in SCAN1 cells, presumably by Tdp1-independent pathways. Blunt and recessed 3′-PG ends could be processed by Ape1, while 3′-overhangs longer than four bases could be processed by Artemis. Thus, the fraction of radiation-induced DSBs that strictly require only Tdp1 for repair may be very small, possibly less than 10%. Even for these breaks, there may be an alternative, more

complicated pathway that can substitute when simpler end-joining pathways fail, as suggested by the 'repair foci' of DSB repair factors that can be detected cytologically long after majority of DSBs have already been repaired (Bradbury et al., 2003). Whether protruding PG termini on DSBs are more persistent in SCAN1 than in normal cells *in vivo* is not known, and although a post-labeling assay for PG-formation and repair *in vivo* has been described previously (Weinfeld et al., 1991 and Bertoncini et al., 1995), this assay is relatively insensitive and does not distinguish between SSB and DSB termini. To investigate the molecular basis of SCAN1, El-Khamisy et al. (2005) carried out both quantitative γ-H2AX immunostaining and neutral comet assays. When both of these experiments failed to reveal a measurable difference between the level of DSBs in non-replicating normal and SCAN1 cells, they suggested that more than 98% of the breaks that occur accumulate in non-replicating SCAN1 cells are SSBs (El-Khamisy et al., 2005). Topoisomerase I transiently generates SSBs as a part of its normal catalytic cycle, during which it becomes covalently attached to the 3′- terminus of the break until the SSB is subsequently resealed by the topoisomerase (Wang et al., 2002). With regard to the source of SSBs in SCAN1 cells, replication-independent topo1-associated SSBs can arise by collision of cleavage complexes with RNA polymerases or by close proximity with other DNA adducts (Pommier et al., 2003). While a loss of Tdp1 function in DSB repair results in little or no observable phenotype in replicating tissues, how does loss of Tdp1 cause a dramatic phenotype in non-replicating neurons? To address this question, El-Khamisy et al. (2005) mimicked the postmitotic state of neurons by arresting mitosis in lymphoblastoid cells from SCAN1 patients and then exposed the cells to the Topo1 poison, camptothecin. Campothecin treatment caused abundant SSBs in the DNA. When

camptothecin was removed, SCAN1 cells did not repair the breaks whereas wild-type cells did so rapidly. Importantly, SSBs induced by oxidative stress, another DNA damaging agent, also were inefficiently repaired in SCAN1 cells. Additional yeast two-hybrid, co-immunoprecipitation, and reconstitution studies showed that normal human cells possess a novel Tdp1-dependent SSBR process (consisting of Tdp1, XRCC1, PNKP and Ligase IIIα) that rapidly repairs topo1-SSBs, and that this process is absent in SCAN1 cells. Consistent with this information, western blot analysis carried out by our laboratory indeed showed the presence of XRCC1 in purified Tdp1 extract (washed once with 1X TE prior to elution), adding further proof to statements made by El-Khamisy and colleagues. Our processing assays with nuclear extracts obtained from adenovirus-infected U87 cells showed that XRCC1 was found to enhance Tdp1 activity up to 4X. Keeping this information in mind, it would be interesting to check if mutated Tdp1 binds to XRCC1 at all; if there is no evidence of binding then it would be tempting to speculate that the binding site for XRCC1 is contained within the mutation.

Yet another role for Tdp1 in SCAN1 was presented by Interthal et al. (2005) who stated that, in combination with 3′-PG as a substrate, Tdp1 may also function to remove a variety of 3′ adducts including those that contain a 3′-biotin or a 3′-abasic site. Using a tryptic peptide of Tdp1 H493R (mutant form of Tdp1 in SCAN1) bound to the 3′-end of an oligonucleotide as a substrate for wild-type Tdp1, their data showed that Tdp1 is capable of hydrolyzing the phosphamide linkage between the peptide and the DNA. They observed that unlike the native topo1-DNA complex, which is not a substrate for Tdp1, Tdp1 removed a fully folded Tdp1 enzyme from the DNA. They speculated that Tdp1 somehow promotes sufficient unfolding of the Tdp1-DNA complex for its active site to

access the phosphoamide bond to be cleaved. Patients who are affected by the SCAN1 disease develop neurodegenerative symptoms during their teenage years (Takashima et al., 2002). The disease is completely recessive and heterozygous individuals remain symptom free. Based on the data provided by Interthal and colleagues, we can conclude that any H493R covalent complexes that accumulate in heterozygous individuals are repaired by wild-type Tdp1 and this likely accounts for the recessive nature of the SCAN1 defect.

But why might the pathology of SCAN1 be restricted to neurons? One possibility is that elevated oxidative stress in post-mitotic neurons creates a particularly high level of SSBs. In addition, the limited regenerative capacity of the nervous system might render this tissue particularly susceptible to cell loss, where as cell loss from tissues with greater regenerative capacity might be better tolerated. Another possibility might be that unrepaired SSBs can be processed by homologous recombination in proliferating cells, even in the absence of DNA replication, as in budding yeast. Consistent with this idea was observation by El-Khamisy et al. (2005) that HR-defective *XRCC3*$^{-/-}$ chicken DT40 cells accumulated high levels of replication-dependent strand breaks during treatement with CPT, confirming that HR repairs replication-associated DSBs in higher eukaryotes. They also observed that there was an increased frequency of spontaneous sister chromatid exchanges and an additional increase in these events in SCAN1 cells after exposure to CPT concentrations too low to trigger the exchanges in normal cells, suggesting that HR is indeed elevated in SCAN1 cells. Finally, it is possible that Tdp1 has additional, unique functions in neurons distinct from its DNA repair activities. It is also interesting to note that, based on clinical features, brain imaging and limited neuropathological studies, the

most susceptible neurons in ataxia with oculomotor apraxia (AOA1), AOA type 2, and presumably SCAN1 seem to include large, highly metabolic neurons, such as cerebellar Purkinje cells, motor neurons, and dorsal root ganglia. AOA1 cells are sensitive to hydrogen peroxide and harbor a mutation in aprataxin; a protein that interacts with XRCC1 (Mossesso et al., 2005). AOA2 is caused by mutations in senataxin; a protein that likely functions in RNA processing and transcription-coupled DNA repair (Ursic et al., 2004). RNA interference (RNAi) technology can also be harnessed to reduce Tdp1 levels in cultured neurons and *in vivo*. Viral-mediated RNAi knockdown in the cerebellum versus other brain regions could address regional susceptibility. If Tdp1-deficient neurons are shown to accumulate SSBs, it will be critically important to determine whether this genotoxic stress induces a DNA damage response or alters the neuronal transcriptome, as one might predict with these results. Another important line of inquiry will be to determine whether the AOA1 disease protein aprataxin, ties into Tdp1-dependent processes due to its link with SSBR. While the connection of the AOA2 disease protein senataxin is less well established, its predicted involvement both in RNA processing and in transcription-coupled repair further suggests intriguing links between DNA repair and transcription in neurodegeneration.

Nevertheless, a role for PG-terminated DSBs in SCAN1 pathology cannot be excluded. In cycling wild type yeast and mammalian cells, cell death induced by abortive topo1 strand breaks appears to result largely, if not entirely, from DSBs arising at replication forks (Vance et al, 2002 and Pouliot et al, 2001). In addition, mutation of genes required for homologous recombination, a process that is essential for repairing DSBs at collapsed replication forks, confers high levels of sensitivity to camptothecin in

both yeast (Vance et al., 2002) and mammalian cells (Caldecott et al., 1991). Consistent with these observations, in budding yeast Tdp1 appears to operate in concert with homologous recombination specifically at topo1-DSBs associated with replication. The neuronal apoptosis seen in knockout mice lacking critical DNA end-joining proteins, such as XRCC4 and DNA ligase IV (Gao et al., 1998 and Barnes et al., 1998), suggest that in the absence of DSB repair terminally differentiating neurons accumulate sufficient DSBs to produce significant neurological pathology. There is evidence that at least some of these 'spontaneous' DSBs reflect damage by oxygen free radicals associated with normal oxidative metabolism (Karanjawala et al., 2003). For Friedreich ataxia (FA) and other ataxias in which oxidative stress is considered to be an important pathogenic element, damage to DNA (including but not limited to SSBs) and subsequent transcriptional alterations could prove to be an important downstream consequence of oxidative stress. FA is associated with a mutant frataxin protein, which leads to increased oxidative stress due to a defect in iron homeostasis (Lodi et al., 2002 and Schulz et al., 2003). Remarkably, FA shares some of the same neuropathological hallmarks with SCAN1, including degenration of posterior columns and dorsal root ganglia. Thus, while most recent papers imply a role of SSBR in SCAN1 cells, several lines of circumstantial evidence also suggest a possible linkage among Tdp1 deficiency, oxidative damage, DSBs and cerebellar ataxia. Even though lymphoblastoid cell lines derived from SCAN1 patients show at most only mild radiosensitivity (Zhou et al., 2005), it is possible that endogenous tissues of SCAN1 patients are more sensitive to free radical damage than the cell lines. Because cultured cells are subjected to higher oxygen tensions than would

occur *in vivo*, they may be more likely to adapt to Tdp1 deficiency, for example, by upregulating alternative pathways for repair of DSBs and other oxidative damage.

Clinical significance

Elucidating the mechanism of NHEJ is integral to understanding how normal cells can avoid oncogenic transformation when challenged with the DNA DSB lesions, but also for exploiting this pathway for cancer therapeutics. With the advent of gene therapy, it may be possible to prevent carcinogenesis and hypersensitivity to radiation in patients who have been diagnosed with any of the NHEJ gene deficiency. It is a well-known fact that many tumors that are amenable to treatment by either chemotherapy or radiotherapy become resistant to treatment after a period of time. Recurrence of the tumor after going into remission is also a major challenge faced today in the treatment protocols of certaincancers. Majority of the drugs or other modalities of treatment concentrate on causing DNA damage to an extent that renders cells incapable of survival. However, very few drugs target proteins involved in the repair of these DNA breaks. NHEJ is now a well-established mode of DSB repair in vertebrate cells that involves Ku, DNA-PK and XRCC4/DNA ligase IV as the key players in addition to others like Artemis and DNA polymerase. Also, a role for Tdp1 in NHEJ repair cannot be completely excluded at this point. What is the contribution of the NHEJ process and the proteins involved in this process in the development of resistance by a tumor or recurrence of a tumor? It is possible that a cancerous cell has elevated levels of these repair factors that enable the cell to survive in spite of treatment and also contribute to recurrence. A robust repair system can attenuate response to treatment. Knowing what proteins play a crucial role in such repair systems and their structure and function will aid in the development of

specific and potent inhibitors of these proteins. For example, LY294002, IC87361 and wortmanin are well known inhibitors of DNA-PK and completely abolish end-joining. Sodium ortho-vanadate is the only known inhibitor of Tdp1 (Davies et al., 2002). Such specific inhibitors can be combined with conventional chemotherapeutic agents to enhance the latter's effectiveness as cytotoxic agents. This can be of an added advantage in that it can also help in reducing the toxic effects associated with high doses of chemotherapy. While inhibition of Tdp1 may not confer radiosensitivity, it would likely confer sensitivity to topoI-mediated agents such as camptothecin. However, it will be first necessary to develop inhibitors that are more specific to these proteins, before the feasibility of this approach can be tested.

Molecular diagnostics is a rapidly advancing field in which insights into disease mechanisms are being elucidated by use of new gene-based biomarkers. Until recently, diagnostic and prognostic assessment of diseased tissues and tumors relied heavily on indirect indicators that permitted only general classifications into broad histologic or morphologic subtypes and did not take into account the alterations in individual gene expression. Global expression analysis using microarrays now allows for simultaneous interrogation of the expression of thousands of genes in a high-throughput fashion and offers unprecedented opportunities to obtain molecular signatures of the state of activity of diseased cells and patient samples. Microarray analysis may provide invaluable information on disease pathology, progression, resistance to treatment, and response to cellular microenvironments and ultimately may lead to improved early diagnosis and innovative therapeutic approaches for cancer. Development of new molecular markers as diagnostic probes has revolutionized the detection methods for certain cancers in their

very early stages. For example, p63, a homologue of the tumor suppressor gene p53, is now known to be a useful marker for clinically undetectable but ultrasound suspected prostate cancers. The discovery of SCAN1 gives rise to the important question as to what cancers, if any, may have increased or decreased levels of this protein. If the level of Tdp1 is found to be significantly altered in any of the cancers, then it can serve as a useful tool in their detection. This technology also has many potential commercial uses including: a method for screening camptothecin analogues or other compounds for their resistance to repair by Tdp1 or to prescreen patients for their sensitivity to topisomerase inhibitors which could identify patients most likely to respond to camptothecin therapy. Further, it also provides for a vector comprising of the nucleic acid molecule for TDP1 as well as the method of altering the level of TDP1 in a cell, a tissue, an organ or an organism. Another possibility is that cells, particularly neurons wuth lower than normal levels of Tdp1 may be more susceptible to oxidative DNA damage. Molecular diagnostics may identify individuals with such partial Tdp1 deficiency as candidates for anti-oxidant preventive therapies.

In conclusion, the identification of Tdp1 adds a new level of complexity to the field of DNA DSB repair. Though our data conclusively shows that Tdp1 is capable of removing PGs from DNA DSBs, we could not find any proof of its interaction with any of the protein machinery of NHEJ repair pathway. Studying the gentypic and phenotypic characteristics of *tdp1-/-* knockout mice in comparison with wild-type mice will unveil important information as to the exact role of Tdp1 in repair of free radical mediated DNA DSBs. If such a role were determined, it would contribute significantly towards making it a prime target for chemotherapy, radiotherapy or a combination of both.

List of References

Abraham RT. Cell cycle checkpoint signaling through the ATM and ATR kinases. *Genes Dev.*, **15**, 2177-2196 (2001)

Anderson CW and Lees-Miller SP. The nuclear serine/threonine protein kinase DNA-PK. *Crit. Rev. Eukaryot. Gene Expr.*, **2**, 283-314 (1992)

Bannister AJ, Gottlieb TM, Kouzarides T, Jackson SP. c-Jun is phosphorylated by the DNA-dependent protein kinase in vitro; definition of the minimal kinase recognition motif. *Nucleic Acids Res.* **21**:1289-95 (1993)

Bai Y, Symington LS. A Rad52 homolog is required for RAD51-independent mitotic recombination in Saccharomyces cerevisiae. *Genes Dev.* **10,** 2025-37 (1996)

Barthelmes HU, Habermeyer M, Christensen MO, Mielke C, Interthal H, Pouliot JJ, Boege F, Marko D. TDP1 overexpression in human cells counteracts DNA damage mediated by topoisomerases I and II. *J Biol Chem.* **279**, 55618-25 (2004)

Baumann P, West SC. DNA end-joining catalyzed by human cell-free extracts. Proc Natl Acad Sci U S A. **95**, 14066-70 (1998)

Bernstein C, Bernstein H, Payne CM and Garewal H. DNA repair/pro-apoptotic dual-role proteins in five major DNA repair pathways: fail-safe protection against carcinogenesis. *Mutat. Res.*, **511**, 145-178 (2002)

Blier PR, Griffith AJ, Craft J, Hardin JA. Binding of Ku protein to DNA. Measurement of affinity for ends and demonstration of binding to nicks. *J Biol Chem.* **268**, 7594-601 (1993)

Bryant PE. Enzymatic restriction of mammalian cell DNA: evidence for double-strand breaks as potentially lethal lesions. *Int J Radiat Biol Relat Stud Phys Chem Med.* **45**:55-60 (1985)

Burma S, Chen BP, Murphy M, Kurimasa A, Chen DJ. ATM phosphorylates histone H2AX in response to DNA double-strand breaks. *J Biol Chem.* **276**:42462-7 (2001)

Caldecott KWProtein-protein interactions during mammalian DNA single-strand break repair. *Biochem Soc Trans.* **31**, 247-51 (2003)

Caldecott KW. DNA single-strand break repair and spinocerebellar ataxia. *Cell.* **112**, 7-10 (2003)

Callebaut I, Mornon JP. From BRCA1 to RAP1: a widespread BRCT module closely associated with DNA repair. *FEBS Lett.* **400**, 25-30 (1997)

Carter T, Vancurova I, Sun I, Lou W, DeLeon S. A DNA-activated protein kinase from HeLa cell nuclei. *Mol Cell Biol.* **10**, 6460-71 (1990)

Cary RB, Peterson SR, Wang J, Bear DG, Bradbury EM, Chen DJ. DNA looping by Ku and the DNA-dependent protein kinase. *Proc Natl Acad Sci U S A.* **94**:4267-72 (1997)

Cao QP, Pitt S, Leszyk J, Baril EF. DNA-dependent ATPase from HeLa cells is related to human Ku autoantigen. *Biochemistry.* **33**, 8548-57 (1994)

Chan DW and Lees-Miller SP. The DNA-dependent protein kinase is inactivated by autophosphorylation of the catalytic subunit. *J. Biol. Chem.*, **271**, 8936-8941 (1996)

Chaudhry, M. A., Dedon, P. C., Wilson, D. M., Demple, B., and Weinfeld, M. Removal by human apurinic/apyrimidinic endonuclease 1 (Ape 1) and Escherichia coli exonuclease III of 3'-phosphoglycolates from DNA treated with neocarzinostatin, calicheamicin, and gamma-radiation. *Biochem. Pharmacol.* **57**, 531-538 (1999)

Chen X, Kinoshita K, Honjo T. Variable deletion and duplication at recombination junction ends: implication for staggered double-strand cleavage in class-switch recombination. *Proc Natl Acad Sci U S A.* **98**, 13860-5 (2001)

Cheng TJ, Rey PG, Poon T, Kan CC. Kinetic studies of human tyrosyl-DNA phosphodiesterase, an enzyme in the topoisomerase I DNA repair pathway. *Eur J Biochem.* **269**, 3697-704 (2002)

Connelly JC, Leach DR. Repair of DNA covalently linked to protein. *Mol Cell.* **13**, 307-16 (2004)

Critchlow SE, Jackson SP. DNA end-joining: from yeast to man. *Trends Biochem Sci.* **23**, 394-8 (1998)

Dasika GK, Lin SC, Zhao S, Sung P, Tomkinson A and Lee EY. DNA damage-induced cell cycle checkpoints and DNA strand break repair in development and tumorigenesis.*Oncogene*, **18**, 7883-7899 (1999)

Davies DR, Interthal H, Champoux JJ, Hol WG. Explorations of peptide and oligonucleotide binding sites of tyrosyl-DNA phosphodiesterase using vanadate complexes. *Med Chem.* **47**, 829-37 (2004)

Davies DR, Interthal H, Champoux JJ, Hol WG. The crystal structure of human tyrosyl-DNA phosphodiesterase, Tdp1. *Structure.* **10**, 237-48 (2002)

Dunlop J, Morin X, Corominas M, Serras F, Tear G. glaikit is essential for the formation of epithelial polarity and neuronal development. *Curr Biol.* **14**, 2039-45 (2004)

DiBiase SJ, Zeng ZC, Chen R, Hyslop T, Curran WJ Jr, Iliakis G. DNA-dependent protein kinase stimulates an independently active, nonhomologous, end-joining apparatus. *Cancer Res.* **60**, 1245-53 (2000)

Dizdaroglu M, Bergtold DS. Characterization of free radical-induced base damage in DNA at biologically relevant levels. *Anal Biochem.* **156**:182-8 (1986)

Downs JA, Lowndes NF, Jackson SP. A role for Saccharomyces cerevisiae histone H2A in DNA repair. *Nature.* **408**:1001-4 (2000)

Durocher D and Jackson SP. DNA-PK, ATM and ATR as sensors of DNA damage: variations on a theme? *Curr. Opin. Cell Biol.*, **13**, 225-231 (2001)

Dvir A, Peterson SR, Knuth MW, Lu H, Dynan WS. Ku autoantigen is the regulatory component of a template-associated protein kinase that phosphorylates RNA polymerase II. *Proc Natl Acad Sci U S A.* **89**, 11920-4 (1992)

Elliott B and Jasin M. Double-strand breaks and translocations in cancer. *Cell. Mol. Life Sci.*, **59**, 373-385 (2002)

El-Khamisy SF, Saifi GM, Weinfeld M, Johansson F, Helleday T, Lupski JR, Caldecott KW. Defective DNA single-strand break repair in spinocerebellar ataxia with axonal neuropathy-1. *Nature.* **434**, 108-13 (2005)

Essers J, Hendriks RW, Swagemakers SM, Troelstra C, de Wit J, Bootsma D, Hoeijmakers JH, Kanaar R. Disruption of mouse RAD54 reduces ionizing radiation resistance and homologous recombination. *Cell.* 1997 **89**, 195-204 (1997)

Essers J, van Steeg H, de Wit J, Swagemakers SM, Vermeij M, Hoeijmakers JH, Kanaar R. Homologous and non-homologous recombination differentially affect DNA damage repair in mice. *EMBO J.* 19, 1703-10 (2000)

Erixon K, Cedervall B. Linear induction of DNA double-strand breakage with X-ray dose, as determined from DNA fragment size distribution. *Radiat Res.* **142,** 153-62 (1995)

F. Liang, M. Han, P.J. Romaniekno and M. Jasin, Homology-directed repair is a major double-strand break repair pathway in mammalian cells. *Proc. Natl. Acad. Sci. U.S.A.* **95**, 5172–5177 (1998)

Falck J, Mailand N, Syljuasen RG, Bartek J, Lukas J. The ATM-Chk2-Cdc25A checkpoint pathway guards against radioresistant DNA synthesis. *Nature.* **410**, 842-7 (2001)

Falzon M, Fewell JW, Kuff EL. EBP-80, a transcription factor closely resembling the human autoantigen Ku, recognizes single- to double-strand transitions in DNA. *J Biol Chem.* **268**, 10546-52 (1993)

Feldmann E, Schmiemann V, Goedecke W, Reichenberger S, Pfeiffer P. DNA double-strand break repair in cell-free extracts from Ku80-deficient cells: implications for Ku serving as an alignment factor in non-homologous DNA end joining. *Nucleic Acids Res.*, **28**, 2585-96 (2000)

Fisher TL, Terhorst T, Cao X, Wagner RW. Intracellular disposition and metabolism of fluorescently-labeled unmodified and modified oligonucleotides microinjected into mammalian cells. *Nucleic Acids Res.*, **21**, 3857-65 (1993)

Game JC. DNA double-strand breaks and the RAD50-RAD57 genes in Saccharomyces. *Semin Cancer Biol.* **4**, 73-83 (1993)

Giloni L, Takeshita M, Johnson F, Iden C, Grollman AP. Bleomycin-induced strand-scission of DNA. Mechanism of deoxyribose cleavage. *J Biol Chem.* **256**, 8608-15 (1981)

Goto S, Watanabe M, Yatagai F. Delayed cell cycle progression in human lymphoblastoid cells after exposure to high-LET radiation correlates with extremely localized DNA damage. *Radiat Res.* **158**, 678-86 (2002)

Gottlieb TM, Jackson SP. The DNA-dependent protein kinase: requirement for DNA ends and association with Ku antigen. *Cell.* **72,** 131-42 (1993)

Gradzka I, Buraczewska I, Kuduk-Jaworska J, Romaniewska A, Szumiel I. Radiosensitizing properties of novel hydroxydicarboxylatoplatinum(II) complexes with high or low reactivity with thiols: two modes of action. *Chem Biol Interact.* **146**, 165-77 (2003)

Haber JE. Partners and pathways repairing a double-strand break. T*rends Genet.*, **16**, 259-264 (2000)

Hammarsten O, DeFazio LG, Chu G. Activation of DNA-dependent protein kinase by single-stranded DNA ends. *J Biol Chem*, **275**, 1541-50 (2000)

Hartley KO, Gell D, Smith GC, Zhang H, Divecha N, Connelly MA, Admon A, Lees-Miller SP, Anderson CW, Jackson SP. DNA-dependent protein kinase catalytic subunit: a relative of phosphatidylinositol 3-kinase and the ataxia telangiectasia gene product. *Cell.* **82**, 849-56 (1995)

Henrie MS, Kurimasa A, Burma S, Menissier-de Murcia J, de Murcia G, Li GC, Chen DJ. Lethality in PARP-1/Ku80 double mutant mice reveals physiological synergy during early embryogenesis. *DNA Repair (Amst).* **2**, 151-8 (2003)

Hoeijmakers JH. From xeroderma pigmentosum to the biological clock contributions of Dirk Bootsma to human genetics. *Mutat Res.* **485**, 43-59 (2001)

Hughes WE, Elgundi Z, Huang P, Frohman MA, Biden TJ. Phospholipase D1 regulates secretagogue-stimulated insulin release in pancreatic beta-cells. *J Biol Chem.* **279**, 27534-41 (2004)

Humeau Y, Vitale N, Chasserot-Golaz S, Dupont JL, Du G, Frohman MA, Bader MF, Poulain B. A role for phospholipase D1 in neurotransmitter release. *Proc Natl Acad Sci U S A.* **98**, 15300-5 (2001)

Hutchinson F. Chemical changes induced in DNA by ionizing radiation. *Prog Nucleic Acid Res Mol Biol.* **32**,115-54 (1985)

Inamdar KV, Pouliot JJ, Zhou T, Lees-Miller SP, Rasouli-Nia A, Povirk LF. Conversion of phosphoglycolate to phosphate termini on 3' overhangs of DNA double strand breaks by the human tyrosyl-DNA phosphodiesterase hTdp1. *J Biol Chem.* **277**, 27162-8 (2002)

Interthal H, Pouliot JJ, Champoux JJ. The tyrosyl-DNA phosphodiesterase Tdp1 is a member of the phospholipase D superfamily. *Proc Natl Acad Sci U S A.* **98**, 12009-14 (2001)

Ivanov EL, Sugawara N, Fishman-Lobell J, Haber JE. Genetic requirements for the single-strand annealing pathway of double-strand break repair in Saccharomyces cerevisiae. *Genetics.* **142**, 693-704 (1996)

Izzard RA, Jackson SP, Smith GC. Competitive and noncompetitive inhibition of the DNA-dependent protein kinase. *Cancer Res.* **59**, 2581-6 (1999)

J.E. Haber, Partners and pathways repairing a double-strand break. *Trends Genet.* **16**, 259–264(2000)

Jackson SP. Detecting, signalling and repairing DNA double-strand breaks. *Biochem. Soc. Trans.*, **29**, 655-661 (2001)

Jackson SP and Jeggo PA. DNA double-strand break repair and V(D)J recombination: involvement of DNA-PK. *Trends Biochem. Sci.*, **20**, 412-415 (1995)

Jilani A, Ramotar D, Slack C, Ong C, Yang XM, Scherer SW, Lasko DD. Molecular cloning of the human gene, PNKP, encoding a polynucleotide kinase 3'-phosphatase and evidence for its role in repair of DNA strand breaks caused by oxidative damage. *J Biol Chem.* **274**, 24176-86 (1999)

Johnson RD and Jasin M. Sister chromatid gene conversion is a prominent double-strand break repair pathway in mammalian cells. *EMBO J.*, **19**, 3398-3407 (2000)

Kanaar R, Hoeijmakers JH and van Gent DC. Molecular mechanisms of DNA double strand break repair. *Trends Cell Biol.*, **8**, 483-489 (1998)

Karimi-Busheri F, Daly G, Robins P, Canas B, Pappin DJ, Sgouros J, Miller GG, Fakhrai H, Davis EM, Le Beau MM, Weinfeld M. Molecular characterization of a human DNA kinase. *J Biol Chem.* **274**, 24187-94 (1999)

Kim ST, Lim DS, Canman CE and Kastan MB. Substrate specificities and identification of putative substrates of ATM kinase family members. *J. Biol. Chem.*, **274**, 37538-37543 (1999)

Labhart P. Nonhomologous DNA end joining in cell-free systems. *Eur J Biochem.* **265**, 849-61 (1999)

Laskey RA, Earnshaw WC. Nucleosome assembly. *Nature.* 286, 763-7 (1980)

Lee JW, Inamdar KV, Hannah MF, Lees-Miller SP, Povirk LF. DNA end sequestration by DNA-dependent protein kinase and end joining of sterically constrained substrates in whole-cell extracts. *Environ Mol Mutagen.* **42**, 279-87 (2004)

Lees-Miller SP, Chen YR and Anderson CW. Human cells contain a DNA-activated protein kinase that phosphorylates simian virus 40 T antigen, mouse p53, and the human Ku autoantigen. *Mol. Cell. Biol.*, **10**; 6472-6481 (1990)

Leber R, Wise TW, Mizuta R, Meek K. The XRCC4 gene product is a target for and interacts with the DNA-dependent protein kinase. *J Biol Chem.* **273**, 1794-801 (1998)

Lengauer C, Kinzler KW, Vogelstein B. Genetic instabilities in human cancers. *Nature.* **396**, 643-9 (1998)

Li Z, Otevrel T, Gao Y, Cheng HL, Seed B, Stamato TD, Taccioli GE, Alt FW. The XRCC4 gene encodes a novel protein involved in DNA double-strand break repair and V(D)J recombination. *Cell.* **83**, 1079-89 (1995)

Lindahl T. Instability and decay of the primary structure of DNA. *Nature.* **362**, 709-15 (1993)

Lindahl T. Antimutagenesis/anticarcinogenesis 2001: screening, methods and biomarkers. *Mutat Res.* **496**, 1-4 (2001)

Liu C, Pouliot JJ, Nash HA. Repair of topoisomerase I covalent complexes in the absence of the tyrosyl-DNA phosphodiesterase Tdp1. *Proc Natl Acad Sci U S A.* **99**, 14970-5 (2002)

Liu C, Pouliot JJ, Nash HA. The role of TDP1 from budding yeast in the repair of DNA damage. *DNA Repair (Amst).* **3**, 593-601 (2004)

Lu T, Pan Y, Kao SY, Li C, Kohane I, Chan J, Yankner BA. Gene regulation and DNA damage in the ageing human brain. *Nature.* **429**, 883-91 (2004)

Mannironi C, Bonner WM, Hatch CL. H2A.X. a histone isoprotein with a conserved C-terminal sequence, is encoded by a novel mRNA with both DNA replication type and polyA 3' processing signals. *Nucleic Acids Res.* **17**, 9113-26 (1989)

Marintchev,A., Mullen,M.A., Maciejewski,M.W., Pan,B., Gryk,M. and Mullen,G.P. Solution structure of the single-strand break repair protein XRCC1 N-terminal domain. *Nature Struct. Biol.*, **6**, 884–893 (1999)

Martensson S, Hammarsten O. DNA-dependent protein kinase catalytic subunit. Structural requirements for kinase activation by DNA ends. *J Biol Chem.* **277**, 3020-9 (2002)

McIlwraith MJ, Van Dyck E, Masson JY, Stasiak AZ, Stasiak A, West SC. Reconstitution of the strand invasion step of double-strand break repair using human Rad51 Rad52 and RPA proteins. *J Mol Biol.* **304**, 151-64 (2000)

Mimori T, Akizuki M, Yamagata H, Inada S, Yoshida S, Homma M. Characterization of a high molecular weight acidic nuclear protein recognized by autoantibodies in sera from patients with polymyositis-scleroderma overlap. *J Clin Invest.* 68, 611-20 (1981)

Morrison C, Sonoda E, Takao N, Shinohara A, Yamamoto K and Takeda S. The controlling role of ATM in homologous recombinational repair of DNA damage. *EMBO J.*, **19**, 463-471 (2000)

Norbury CJ and Hickson ID. Cellular responses to DNA damage. *Annu. Rev. Pharmacol. Toxicol.*, **41**, 367-401 (2001)

Obe G, Johannes C, Schulte-Frohlinde D. DNA double-strand breaks induced by sparsely ionizing radiation and endonucleases as critical lesions for cell death, chromosomal aberrations, mutations and oncogenic transformation. *Mutagenesis.* **7**, 3-12 (1992)

Ochem AE, Skopac D, Costa M, Rabilloud T, Vuillard L, Simoncsits A, Giacca M, Falaschi A. Functional properties of the separate subunits of human DNA helicase II/Ku autoantigen. *J Biol Chem.* **272**, 29919-26 (1997)

Ohya T, Kawasaki Y, Hiraga S, Kanbara S, Nakajo K, Nakashima N, Suzuki A, Sugino A. The DNA polymerase domain of pol(epsilon) is required for rapid, efficient, and highly accurate chromosomal DNA replication, telomere length maintenance, and normal cell senescence in Saccharomyces cerevisiae. *J Biol Chem.* **27**, 728099-108 (2002)

Patel KJ, Yu VP, Lee H, Corcoran A, Thistlethwaite FC, Evans MJ, Colledge WH, Friedman LS, Ponder BA, Venkitaraman AR. Involvement of Brca2 in DNA repair. *Mol Cell.* **1**, 347-57 (1998)

Pastink A, Eeken JC, Lohman PH. Genomic integrity and the repair of double-strand DNA breaks. *Mutat Res.* **480-481**, 37-50 (2001)

P. Wang, R.H. Zhou, Y. Zou, C.K. Jackson-Cook and L.F. Povirk, Highly conservative reciprocal translocations formed by apparent joining of exchanged DNA double-strand break ends. *Proc. Natl. Acad. Sci. U.S.A.* **94**, 12018–12023 (1997)

Pastwa E, Blasiak J. Non-homologous DNA end joining. *Acta Biochim Pol.*; **50**, 891-908 (2003)

Paull TT and Gellert M. The 3' to 5' exonuclease activity of Mre 11 facilitates repair of DNA double-strand breaks. *Mol. Cell*, **1**, 969-979 (1998)

Pfeiffer P, Goedecke W, Obe G. Mechanisms of DNA double-strand break repair and their potential to induce chromosomal aberrations. *Mutagenesis.* **15**, 289-302 (2000)

Pierce AJ, Stark JM, Araujo FD, Moynahan ME, Berwick M, Jasin M. Double-strand breaks and tumorigenesis. *Trends Cell Biol.* **11**, S52-9 (2001)

Plo I, Liao ZY, Barcelo JM, Kohlhagen G, Caldecott KW, Weinfeld M, Pommier Y. Association of XRCC1 and tyrosyl DNA phosphodiesterase (Tdp1) for the repair of topoisomerase I-mediated DNA lesions. *DNA Repair (Amst).* **2**, 1087-100 (2003)

Pommier Y. Camptothecins and topoisomerase I: a foot in the door. Targeting the genome beyond topoisomerase I with camptothecins and novel anticancer drugs: importance of DNA replication, repair and cell cycle checkpoints. *Curr Med Chem Anticancer Agents.* **4**, 429-34 (2004)

Pouliot JJ, Robertson CA, Nash HA. Pathways for repair of topoisomerase I covalent complexes in Saccharomyces cerevisiae. *Genes Cells.* **6**, 677-87 (2001)

Pouliot JJ, Yao KC, Robertson CA, Nash HA. Yeast gene for a Tyr-DNA phosphodiesterase that repairs topoisomerase I complexes. *Science.* **286**, 552-5 (1999)

Povirk LF. DNA damage and mutagenesis by radiomimetic DNA-cleaving agents: bleomycin, neocarzinostatin and other enediynes. *Mutat Res.* **355**, 71-89 (1996)

Powis G, Bonjouklian R, Berggren MM, Gallegos A, Abraham R, Ashendel C, Zalkow L, Matter WF, Dodge J, Grindey G. Wortmannin as a unique probe for an intracellular signalling protein, phosphoinositide 3-kinase. *Cancer Res.* **54**, 2419-23 (1994)

Raymond AC, Rideout MC, Staker B, Hjerrild K, Burgin AB Jr. Analysis of human tyrosyl-DNA phosphodiesterase I catalytic residues. *J Mol Biol.* 338, 895-906 (2004)

Raymond WE, Kleckner N. Expression of the Saccharomyces cerevisiae RAD50 gene during meiosis: steady-state transcript levels rise and fall while steady-state protein levels remain constant. *Mol Gen Genet.* **238**, 390-400 (1993)

Rideout MC, Raymond AC, Burgin AB Jr. Design and synthesis of fluorescent substrates for human tyrosyl-DNA phosphodiesterase I. *Nucleic Acids Res.* **32**, 4657-64 (2004)

Rogakou EP, Pilch DR, Orr AH, Ivanova VS, Bonner WM. DNA double-stranded breaks induce histone H2AX phosphorylation on serine 139. *J Biol Chem.* 273, 5858-68 (1998)

Roth DB, Porter TN, Wilson JH. Mechanisms of nonhomologous recombination in mammalian cells. *Mol Cell Biol.* **5**, 2599-607 (1985)

Rosenzweig KE, Youmell MB, Palayoor ST, Price BD. Radiosensitization of human tumor cells by the phosphatidylinositol3-kinase inhibitors wortmannin and LY294002 correlates with inhibition of DNA-dependent protein kinase and prolonged G2-M delay. *Clin Cancer Res.* **3**, 1149-56 (1997)

Santoro MM, Gaudino G, Villa-Moruzzi E. Protein phosphatase 1 binds to phospho-Ser-1394 of the macrophage-stimulating protein receptor. *Biochem J.*, **376**, 587-94 (2003)

Scully R, Chen J, Ochs RL, Keegan K, Hoekstra M, Feunteun J, Livingston DM. Dynamic changes of BRCA1 subnuclear location and phosphorylation state are initiated by DNA damage. *Cell.* **90**, 425-35 (1997)

Shinohara A, Ogawa H, Ogawa T. Rad51 protein involved in repair and recombination in S. cerevisiae is a RecA-like protein. *Cell.* **69**, 457-70 (1992)

Sibanda BL, Critchlow SE, Begun J, Pei XY, Jackson SP, Blundell TL, Pellegrini L. Crystal structure of an Xrcc4-DNA ligase IV complex. *Nat Struct Biol.* **8**, 1015-9 (2001)

Smith GC, Jackson SP. The DNA-dependent protein kinase. *Genes Dev.*, **13**, 916-34 (1999)

Steighner RJ, Povirk LF. Bleomycin-induced DNA lesions at mutational hot spots: implications for the mechanism of double-strand cleavage. *Proc Natl Acad Sci U S* A.; **87**,8350-4 (1990)

Sugiyama T, Zaitseva EM, Kowalczykowski SC. A single-stranded DNA-binding protein is needed for efficient presynaptic complex formation by the Saccharomyces cerevisiae Rad51 protein. *J Biol Chem.* **272**, 7940-5 (1997)

Suh, D., Wilson III, D. M., and Povirk, L. F. 3'-phosphodiesterase activity of human apurinic/apyrimidinic endonuclease at DNA double-strand break ends. *Nucleic Acids Res.* **25**, 2495-2500 (1997)

Sung P. Catalysis of ATP-dependent homologous DNA pairing and strand exchange by yeast RAD51 protein. *Science.* **265**, 1241-3 (1994)

Takashima H, Boerkoel CF, John J, Saifi GM, Salih MA, Armstrong D, Mao Y, Quiocho FA, Roa BB, Nakagawa M, Stockton DW, Lupski JR. Mutation of TDP1, encoding a topoisomerase I-dependent DNA damage repair enzyme, in spinocerebellar ataxia with axonal neuropathy. *Nat Genet.* **32**, 267-72 (2002)

Takata M, Sasaki MS, Sonoda E, Morrison C, Hashimoto M, Utsumi H, Yamaguchi-Iwai Y, Shinohara A and Takeda S. Homologous recombination and non-homologous end-joining pathways of DNA double-strand break repair have overlapping roles in the maintenance of chromosomal integrity in vertebrate cells. *EMBO J.*, **17**, 5497-5508(1998)

Taylor,R.M., Moore,D.J., Whitehouse,J., Johnson,P. and Caldecott,K.W. A cell cycle-specific requirement for the XRCC1 BRCT II domain during mammalian DNA strand break repair. *Mol. Cell. Biol.*, **20**, 735–740 (2000)

Thompson,L.H., Brookman,K.W., Jones,N.J., Allen,S.A. and Carrano,A.V. Molecular cloning of the human *XRCC1* gene, which corrects defective DNA strand break repair and sister chromatid exchange. *Mol. Cell. Biol.*, **10**, 6160–6171 (1990)

Thompson LH and Schild D. Recombinational DNA repair and human disease. *Mutat. Res.*, **509**, 49-78 (2002)

Thompson,L.H. and West,M.G. XRCC1 keeps DNA from getting stranded. *Mutat. Res.*, **459**, 1–18 (2000)

Tuteja N, Tuteja R, Ochem A, Taneja P, Huang NW, Simoncsits A, Susic S, Rahman K, Marusic L, Chen J. Human DNA helicase II: a novel DNA unwinding enzyme identified as the Ku autoantigen. *EMBO J.* **13**, 4991-5001 (1994)

Ui M, Okada T, Hazeki K, Hazeki O. Wortmannin as a unique probe for an intracellular signalling protein, phosphoinositide 3-kinase. *Trends Biochem Sci.* **20**, 303-7 (1995)

Vance JR, Wilson TE. Yeast Tdp1 and Rad1-Rad10 function as redundant pathways for repairing Top1 replicative damage. *Proc Natl Acad Sci U S A.* 99, 13669-74 (2002)

Varon R, Vissinga C, Platzer M, Cerosaletti KM, Chrzanowska KH, Saar K, Beckmann G, Seemanova E, Cooper PR, Nowak NJ, Stumm M, Weemaes CM, Gatti RA, Wilson RK, Digweed M, Rosenthal A, Sperling K, Concannon P, Reis A. Nibrin, a novel DNA double-strand break repair protein, is mutated in Nijmegen breakage syndrome. *Cell.* **93**, 467-76 (1998)

Vogelstein B, Kinzler KW. The multistep nature of cancer. *Trends Genet.*, **9,** 138-41 (1993).

Waldmann TA, Misiti J, Nelson DL, Kraemer KH. Ataxia-telangiectasis: a multisystem hereditary disease with immunodeficiency, impaired organ maturation, x-ray hypersensitivity, and a high incidence of neoplasia. *Ann Intern Med.* **99**, 367-79 (1983)

Walker JR, Corpina RA, Goldberg J. Structure of the Ku heterodimer bound to DNA and its implications for double-strand break repair. *Nature.* **412**, 607-14 (2001)

Wang P, Zhou RH, Zou Y, Jackson-Cook CK, Povirk LF. Highly conservative reciprocal translocations formed by apparent joining of exchanged DNA double-strand break ends. *Proc Natl Acad Sci U S A.* **94**, 12018-23 (1997)

Wang S, Guo M, Ouyang H, Li X, Cordon-Cardo C, Kurimasa A, Chen DJ, Fuks Z, Ling CC, Li GC. The catalytic subunit of DNA-dependent protein kinase selectively regulates p53-dependent apoptosis but not cell-cycle arrest. *Proc Natl Acad Sci U S A.*, **97**, 1584-8 (2000)

Weinfeld M, Chaudhry MA, D'Amours D, Pelletier JD, Poirier GG, Povirk LF, Lees-Miller SP. Interaction of DNA-dependent protein kinase and poly(ADP-ribose) polymerase with radiation-induced DNA strand breaks. *Radiat Res.* **148**, 22-8 (1997)

Williams CJ, Grandal I, Vesprini DJ, Wojtyra U, Danska JS, Guidos CJ. Irradiation promotes V(D)J joining and RAG-dependent neoplastic transformation in SCID T-cell precursors. : *Mol Cell Biol*; **21**, 400-13 (2001)

Wu X, Lieber MR. Protein-protein and protein-DNA interaction regions within the DNA end-binding protein Ku70-Ku86. *Mol Cell Biol.* **16**, 5186-93 (1996)

Yaneva M, Kowalewski T, Lieber MR. Interaction of DNA-dependent protein kinase with DNA and with Ku: biochemical and atomic-force microscopy studies. *EMBO J.* **16**, 5098-112 (1997)

Yang, S. W., Burgin, A. B., Jr., Huizenga, B. N., Robertson, C. A., Yao, K. C., and Nash, H. A. A eukaryotic enzyme that can disjoin dead-end covalent complexes between DNA and type I topoisomerases. *Proc. Natl. Acad. Sci. U. S. A.* **93**, 11534-11539 (1996)

Yannone SM, Roy S, Chan DW, Murphy MB, Huang S, Campisi J, Chen DJ. Werner syndrome protein is regulated and phosphorylated by DNA-dependent protein kinase. *J Biol Chem.* **276**, 38242-8 (2001)

Yoo S, Dynan WS. Characterization of the RNA binding properties of Ku protein. Biochemistry. 37, 1336-43 (1998)

Haritha Tatavarthi was born on April 8th, 1978 in Visakhapatnam, INDIA. She received her undergraduate degree in Pharmacy from M.S. Ramaiah College of Pharmacy, INDIA in 2000.

1. Presented a poster (Action of Tdp1 on 3'-PG terminated Double strand breaks) at the 23rd Annual Graduate Research Association of Students in Pharmacy (GRASP) meeting held in Richmond in May, 2003
2. Presented a poster (Action of Tdp1 on 3'-PG terminated Double strand breaks) at the 19th Annual Watt's Day presentations held at the Medical College of Virginia, Richmond in October, 2004
3. Presented a poster (Action of Tdp1 on 3'-PG terminated Double strand breaks) at the 2005 Annual American Association for Cancer Research held in Anaheim, California
4. Zhou T, Lee JW, Tatavarthi H, Lupski JR, Valerie K, Povirk LF. Deficiency in 3'-phosphoglycolate processing in human cells with a hereditary mutation in tyrosyl-DNA phosphodiesterase (TDP1). Nucleic Acids Res. **33**, 289-97 (2005)